Identification and characterization of novel targets in Papillary Thyroid Cancer (PTC)

DISSERTATION

ZUR ERLANGUNG DES GRADES

DOKTOR DER NATURWISSENSCHAFTEN

AM FACHBEREICH BIOLOGIE

DER JOHANNES GUTENBERG-UNIVERSITÄT MAINZ

VON

ASWINI KRISHNAN

(AUS PAYYOLI, INDIA)

MAINZ, 2019

Dekan:

1. Berichterstatter:

2. Berichterstatter:

Tag der mündlichen Prüfung: 06-09-2019

TABLE OF CONTENTS

Abbreviations

°C	Degree Celsius
^{131}I	Radioactive iodine
Akt	Protein Kinase B
ALK	Anaplastic lymphoma kinase
AML	Acute myeloid leukemia
ARAF	RAF kinase A isoform
ATC	Anaplastic thyroid cancer
ATP	Adenosine triphosphate
BCL-3	B-cell lymphoma 3 protein
BCL-6	B-cell lymphoma 6 protein
BRAF	RAF kinase B isoform
BSA	Bovine serum albumin
C-cells	Parafollicular cells
c-Kit	Mast/stem cell growth factor receptor Kit
C-terminal	Carboxy-terminal
CBFB	Core-binding factor subunit beta
CBL	Casitas B-lineage lymphoma
CC domain	Coiled-coil domain
CCD6	Cell division control protein Ccd6
CDC25A	M-phase inducer phosphatase 1
cDNA	Complementary DNA
CHX	Cycloheximide
cIAP2	Cellular IAP2
cm	Centimeter
CML	Chronic Myeloid Leukemia
CMV	Cucumber mosaic virus
CO_2	Carbon dioxide
CRAF	RAF kinase C isoform
ctrl	Control

CYLD	Ubiquitin carboxyl-terminal hydrolase CYLD
DFG	Asp-Phe-Gly
DMEM	Dulbecco's modified Eagle's medium
DMSO	Dimethylsulfoxide
DNA	Deoxyribonucleic acid
DSS	Disease specific survival
DTC	Differentiated thyroid cancer
DTME	Dithiobismaleimidoethane
DTT	Dithiothreitol
DUBs	Deubiquitinating enzymes
E1	Ubiquitin activating enzyme
E2	Ubiquitin conjugating enzymes
E3	Ubiquitin ligating enzyme
EGFR	Epidermal growth factor receptor
ER	Endoplasmic Reticulum
ERG	ETS –related gene
ERK1/2	Extracellular-regulated kinase 1/2
ETS	E-twenty-six
EV	Empty Vector
FBS	Fetal bovine serum
FDA	The Food and Drug Administration
FLT3	Receptor-type tyrosine-protein kinase FLT3
FNA	Fine needle aspiration
FNAB	Fine needle aspiration biopsy
FOXO1	Forkhead box protein O1
FOXO4	Forkhead box protein O4
FRS2	Fibroblast growth factor receptor substrate 2
FTC	Follicular thyroid cancer
FVPTC	Follicular-variant of PTC
GAP	GTPase activating protein
GDNF	Glial cell line-derived neurotrophic factor
GDP	Guanosine diphosphate
GEF	Guanine nucleotide exchange factor
GFP	Green fluorescent protein

GTP	Guanosine triphosphate
h	Hours
H&E	Haemotoxylin and Eosin
HAUSP	Herpesvirus-associated ubiquitin-specific protease
HECT	Homologous to the E6-AP Carboxyl Terminus
HIF-1 α	Hypoxia-inducible factor 1-alpha
His	Histidine
HRAS	Rat sarcoma protein, H isoform
HUWE1	HECT, UBA And WWE Domain Containing 1, E3 Ubiquitin Protein Ligase
IAP	Inhibitor of apoptosis
IgG	Immunoglobulin G
IP	Immunoprecipitation
JM	Juxtamembrane
JUN	Transcription factor AP-1
K^+	Potassium ion
kb	Kilobase pairs
kDa	Kilodalton
Ki-67	Proliferation marker protein Ki-67
KLF5	Krueppel-like factor 5
KRAS	Rat sarcoma protein, K isoform
LC-MS	Liquid chromatography-mass spectrometric
Lck	Tyrosine-protein kinase Lck (Leukocyte C-terminal Src kinase)
M2PK	Pyruvate kinase isoenzyme type M2
MALT	Mucosa-associated lymphoid tissue
MAP2K	MAPK kinase
MAPK	Mitogen-activated protein kinase
MAST1	Microtubule-associated serine/threonine-protein kinase 1
MAST2	Microtubule-associated serine/threonine-protein kinase 2
MBP	Myelin-binding protein
MCL1	MCL1, BCL2 family apoptosis regulator
MDM2	MDM2 proto-oncogene
MEK1	MAPK/ERK kinase 1
MEK2	MAPK/ERK kinase 2

MEK5	Dual specificity mitogen-activated protein kinase kinase 5
MEKK2	Mitogen-activated protein kinase kinase kinase 2
MEKK3	Mitogen-activated protein kinase kinase kinase 3
MEN2A	Multiple Endocrine Neoplasia type 2A
MEN2B	Multiple Endocrine Neoplasia type 2B
MET	Hepatocyte growth factor receptor
Mg-ATP	Magnesium ATP
Min	Minutes
mIU/L	Milli-international units per liter
MIZ1	Myc-interacting zinc finger
MKI	Multi kinase inhibitor
mm	Millimeter
mRNA	Messenger RNA
MTC	Medullary thyroid cancer
mTOR	Mammalian target of rapamycin
MTT	3-(4,5-dimethylthiazol-2-yl)-2,5-diphenyltetrazolium bromide
MYC	Myc proto-oncogene protein
MYH1	Myosin-1
N-terminal	Amino-terminal
N-terminus	Amino terminus
Na-K ATPase	Sodium Potassium ATPase
Na^+	Sodium ion
NBR1	Next to BRCA1 gene 1 protein
NCI	National Cancer Institute
NcoA4	Nuclear receptor coactivator 4
NEMO	Mitogen-activated protein kinase
NF-κB	Nuclear factor kappa light chain enhancer of activated B cells
NGF	Nerve growth factor
NGS	Next generation sequencing
NIS	Sodium/iodide symporter
Notch1	Neurogenic locus notch homolog protein 1
NRAS	Rat sarcoma protein, N isoform
NSCLC	Non-small-cell lung carcinoma
NTRK	Neurotrophic tyrosine receptor kinase

p	phosphorylated
P-loop	phosphate-binding loop
PAX8	Paired box protein Pax-8
PB1	Phox and Bem1p
PBS	Phosphate buffered saline
PBST	Phosphate buffered saline with tween
PCR	Polymerase chain reaction
PDGFR	Platelet-derived growth factor receptor
PDTC	Poorly differentiated thyroid cancer
PEI	Polyethylenimine
PI3K	Phosphatidylinositol 3-kinase
PIK3CA	Phosphatidylinositol 4,5-bisphosphate 3-kinase catalytic subunit alpha isoform
PML	Promyelocytic leukemia protein
PPAR γ	Peroxisome proliferator-activated receptor gamma
PTC	Papillary thyroid cancer
PTEN	Phosphatidylinositol 3,4,5-trisphosphate 3-phosphatase and dual-specificity protein phosphatase PTEN
RAF	Rapidly accelerated fibrosarcoma
RAI	Radioiodine treatment
RARA	Retinoic Acid Receptor Alpha
RAS	Rat sarcoma
RASGAP	RAS GTPase activating proteins
RASGEF	RAS guanine nucleotide exchange factors
RET	Proto-oncogene tyrosine-protein kinase receptor Ret
RET	Proto-oncogene tyrosine-protein kinase receptor Ret
RFG	Nuclear receptor coactivator 4
RFS	recurrence-free survival
RING	Really Interesting New Gene
RIP1	Receptor-interacting serine/threonine-protein kinase 1
RIP2	Receptor-interacting serine/threonine-protein kinase 2
RITA	reactivation of p53 and induction of tumor cell apoptosis
RNA	Ribonucleic acid
ROS	Proto-oncogene tyrosine-protein kinase ROS

RPKM	Reads Per Kilobase Million
RPM	Revolutions per minute
RPMI	Roswell Park Memorial Institute medium
RT-PCR	real time PCR
RTK	receptor tyrosine kinases
SCF	Stem cell factor
SDS	Sodium dodecyl sulphate
SDS-PAGE	SDS-Polyacrylamide gel electrophoresis
sec	Seconds
SEER	Surveillance, Epidemiology and End Results Program
SHC	SHC-transforming protein 1
SHP1	UBX domain-containing protein 1
Src	Proto-oncogene tyrosine-protein kinase Src
STAT1	Signal transducer and activator of transcription 1-alpha/beta
STAT3	Signal transducer and activator of transcription
T-ALL	T-cell acute lymphoblastic leukaemia
T3	Triiodothyronine
T4	Tetraiodothyronine or thyroxine
TANK	TANK protein
TBSRTC	The Bethesda System for Reporting Thyroid Cytopathology
TCGA	The Cancer Genome Atlas
TERT	Telomerase reverse transcriptase
TFG	TRK-fused gene protein
TGIF1	Homeobox protein TGIF1
TK	tyrosine kinase
TM	Transmembrane
TMPRSS2	Transmembrane protease serine 2
TNM	tumor, node, metastasis
TP53	Cellular tumor antigen p53
TPM3	Tropomyosin alpha-3 chain
TPR	Nucleoprotein TPR
TRAF2	TNF receptor-associated factor 2
TRAF6	TNF receptor-associated factor 6
TRH	Thyroptin releasing hormone

TSH	Thyroid stimulating hormone
Ub	Ubiquitin
UBA	Ubiquitin-associated domain
UBCH5	Ubiquitin-conjugating enzyme E2 D1
UBP7	Ubiquitin carboxyl-terminal hydrolase 7
US	United States
USP10	Ubiquitin carboxyl-terminal hydrolase 10
USP28	Ubiquitin carboxyl-terminal hydrolase 28
USP9X	Probable ubiquitin carboxyl-terminal hydrolase FAF-X
VEGFR	Vascular endothelial growth factor receptor
viz	videlicet
WHO	World Health Organisation
WT	Wild Type
XIAP	X-linked apoptosis protein (BIRC4)

Summary

Papillary thyroid cancer (PTC) is the most common type of endocrine cancer. Partial or complete removal of the thyroid lobe, followed by radioactive iodine treatment (^{131}I) (RAI) is the standard treatment strategy for the treatment of thyroid cancer. But the management of tumors that cannot undergo resection, mostly due to distant metastasis and/or development of resistance to RAI is challenging. Identifying and understanding the molecular pathogenesis underlying thyroid cancer is important for the development of better diagnosis and treatment. The main aim of the project is the identification and validation of novel molecular alterations in PTC patient samples by employing genomic and proteomic approaches.

From a set of patients whose PTC did not harbour any BRAF or RAS mutations (the most common mutations in PTC), a 35 years old male patient's normal, primary tumor and metastatic tissues were selected for both genomic and proteomic analysis. We identified a novel RET gene fusion in this patient and the oncogenic ability of this novel gene fusion was tested in transformation assays. Stable expression of the novel RET fusion gene activated several oncogenic signalling pathways and transformed immortalized human thyroid cells. The novel RET fusion exhibited high kinase activity and formed dimers and oligomers partially in a PB1 domain dependent manner. Quantitative proteomic analysis of normal vs tumour vs metastasis of the same patient revealed the upregulation of proteins involved in the ubiquitination machinery including HECT carrying E3 ligase HUWE1 and Deubiquitinating enzymes (DUBs) like USP9X and UBP7 in the tumour and metastatic lesions. Inhibition of RET, HUWE1 and DUBs by small molecule inhibitors significantly reduced RET-mediated oncogenesis. Apart from unveiling a novel oncogenic RET fusion in PTCs, our data opens a novel avenue of targeting ubiquitin signalling machinery in human PTCs.

Zusammenfassung

Das papilläre Schilddrüsenkarzinom (= papillary thyroid carcinoma, PTC) ist die häufigste endokrine Krebserkrankung. Zur Behandlung wird den betroffenen Patienten zunächst teilweise oder vollständig die Schilddrüse entfernt und im Anschluss erhalten sie eine Radiojodtherapie (RAI). Eine Behandlung von Tumoren, die z. B. auf Grund von Metastasierung nicht mehr operativ entfernt werden können oder Resistenzen gegen die RAI Therapie entwickelt haben, ist jedoch eine Herausforderung. Das Erkennen und Verstehen der molekularen Pathogenese, die dem Schilddrüsenkrebs zu Grunde liegt, ist wichtig für die Entwicklung besserer Behandlungsmöglichkeiten sowie diagnostischer Strategien. Durch genomische und proteomische Analysen von primärem PTC Material war ein Hauptziel dieser Arbeit die Identifizierung und nachfolgende Validierung neuartiger molekularer Veränderungen bei dieser Krebserkrankung.

Aus einer Gruppe von Patienten, deren Schilddrüsentumore keine BRAF- oder RAS-Mutationen aufwies (die häufigsten Mutationen bei PTC), wurden normales sowie primäres Tumorgewebe und Gewebe von Metastasen eines 35-jährigen männlichen Patienten genauer analysiert. In weiterführenden Genom- und Proteomanalysen konnten wir eine neue RET-Genfusion bei diesem Patient identifizierten. Die onkogene Funktion wurde durch in vitro Transformationsassays getestet: Die stabile Expression des neuen RET-Fusionsgens aktivierte mehrere onkogene Signalwege und transformierte immortalisierte, humane Schilddrüsenzellen. Die neue RET-Fusion zeigte eine hohe Kinaseaktivität und bildete, teilweise in Abhängigkeit von der PB1-Domäne, Dimere und Oligomere. Die quantitative proteomische Analyse von normalem vs. Tumorgewebe vs. Gewebe isolierter Metastasen desselben Patienten ergab, dass Proteine, die an der Ubiquitinierungsmaschinerie beteiligt sind, einschließlich der HECT Domäne tragenden E3-Ligase HUWE1 und DUBs wie USP9X und UBP7 im Tumor und Metastasen hochreguliert sind. Die Hemmung von RET, HUWE1 und Deubiquitinasen (DUBs) durch niedermolekulare Inhibitoren reduzierte die RET-vermittelte Onkogenese signifikant. In dieser Arbeit konnten wir eine neuartige onkogene RET-Fusion in primärem Tumormaterial eines PTC-Patienten nachweisen. Darüberhinaus weisen unsere Daten daraufhin, dass die Inhibierung der

Ubiquitinmaschinerie eine Möglichkeit bietet, neue therapeutische Ansätze für die Behandlung von Schilddrüsenkarzinomen zu entwickeln.

1 Introduction

1.1 The Thyroid

The thyroid (Latin: glandula thyreoidea) is an endocrine gland that synthesises, stores and secretes vital hormones that are involved in the proper development of brain in infants, regulation of metabolism and growth rate of the body throughout the lifespan. During development, the thyroid gland is the first endocrine gland to develop and is located in the back of the tongue, which then migrates to the front of the neck before birth. It has a butterfly shaped structure – the right and the left lobe, which lies around the trachea and are connected by a narrow strip of tissue called the isthmus (Figure 1.1). The thyroid comprises of - i) the follicular cells that form thyroid follicles, which enclose colloids containing lumen and ii) the parafollicular C cells. The thyroid gland produces three hormones - Triiodothyronine (T3) and Tetraiodothyronine (thyroxine or T4), which are produced by the follicular cells - collectively called the thyroid hormones, and calcitonin which is secreted by the C cells [2, 3]. The levels of thyroid hormones in the plasma are maintained within a narrow normal range by the thyroid stimulating hormone (TSH) secreted by the pituitary gland which is in turn regulated by the thyroptin releasing hormone (TRH) secreted by the hypothalamus [2] (Figure 1.2). Iodine is essential for the synthesis of thyroid hormones. The sodium/iodide symporter (NIS) protein present on the basolateral plasma membrane of the epithelial follicular cells of the thyroid mediates the uptake of iodide from the plasma in a Na^+-K^+-ATPase dependent manner [4]. The iodide is concentrated and oxidised at the follicular cell-colloidal interface to form iodine, which then iodinates the tyrosine residues of a protein called thyroglobulin to form mono- or di-iodinated tyrosine residues. These iodinated tyrosine residues couple to form the thyroglobulin bound T3 (one mono- and one di-) and T4 (2 di-) hormones and are stored in the lumen. A normal thyroid gland stores enough hormones that the body requires for a month. Before being released into the plasma, the thyroglobulin bound T3 and T4 hormones are taken up by the follicular cells and are subjected to protease activity, hence releasing the T3 and T4 hormones

from the thyroglobulin before its secretion into the bloodstream. The secreted T3 and T4 hormones negatively regulate the secretion of TRH, hence when there are enough thyroid hormones in the body, the thyroid hormones inhibits the secretion of TRH from the hypothalamus [4]. Besides the thyroid hormones, the thyroid gland also produces the hormone called calcitonin. The parafollicular C cells of the thyroid secrete calcitonin when the serum calcium level increases, protecting against hypercalcemia [3].

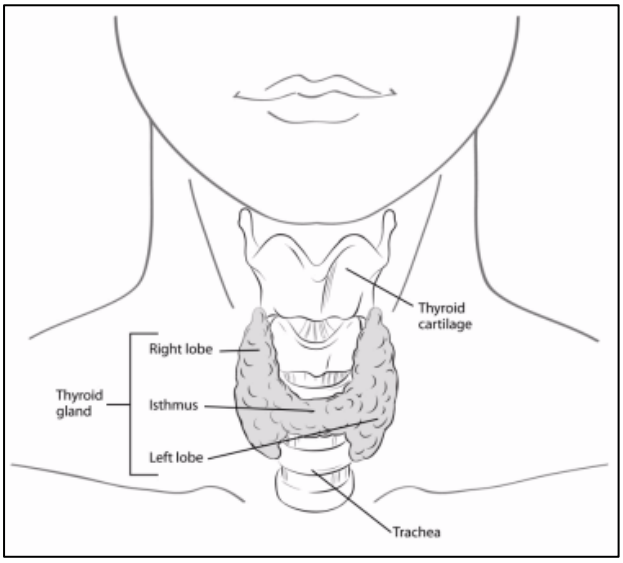

Figure 1.1: The structure of thyroid (from[5]).

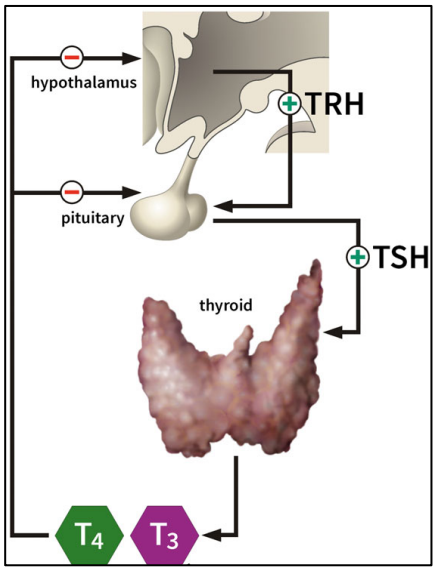

Figure 1.2: Thyroid hormone regulation (from [6]).

1.2 Thyroid Disorders

1.2.1 Benign alterations of the thyroid

Thyroid associated diseases are amongst the most common endocrine disorders and can be broadly classified as thyroid dysfunction disorders – hypothyroidism (insufficient levels of thyroid hormone) and hyperthyroidism (excessive amounts of thyroid hormones), as well as structural diseases – goitre, nodules and cancer [7]. Various studies reveal that thyroid disorders exhibit a clear preponderance in females, though the exact reasons underlying this is unclear [8, 9].

Iodine deficiency is a major cause of hypothyroidism. There is a vast disparity in the global epidemiology of hypothyroidism - geographically, areas in the mountain regions, and economically, the diet regime of poorer countries may not contain enough iodine. In iodine-replete regions, Hashimoto thyroiditis – a chronic auto immune response where there is a progressive destruction of the thyroid is a leading cause of hypothyroidism. Symptoms of hypothyroidism include fatigue, weight gain and cold intolerance. Thyroid hormone replacement is the treatment of choice for hypothyroidism. Hyperthyroidism is less common than hypothyroidism and can be caused by auto immune responses where the auto reactive TSH receptor antibodies abnormally stimulate the TSH receptor resulting in increased thyroid activity (Graves disease). Symptoms of hyperthyroidism include weight loss, anxiety, breathlessness and palpitation [7]. Treatment for hyperthyroidism includes anti-thyroid drugs, radioactive iodine treatment and surgery. Determining thyroid dysfunction is performed by testing serum TSH levels.

Goitre is a condition where there is an asymmetrical enlargement of the thyroid as a consequence of impaired thyroid hormone synthesis and may cause hyperplasia and hypertrophy of thyroid cells. Dietary iodine deficiency is the leading cause of goitre. Goitre may develop as a solitary thyroid nodule or as multiple nodules on both sides of the thyroid resulting in an overall enlargement of the thyroid gland. Goitre is a benign neoplasia and, thus, is not cancerous [7].

1.2.2 Thyroid cancer

Thyroid cancer is the most common type of endocrine cancer and there has been a world wide increase in thyroid cancer in the past decades [10]. It is the most rapidly increasing cancer in the US, with an estimated annual increase in incidence by 3.6% per year from 1974 to 2013, as well as a significant increase in the thyroid cancer related mortality [11, 12]. A study by Rahib et al. predicted that, by 2030, thyroid cancer would be the fourth leading cancer to be diagnosed following breast, prostate and lung cancer [13]. However, there are varied notions regarding the increase in thyroid cancer. A 2014 study by Davies et al. suggested that the increased incidence of thyroid cancer is an epidemic of diagnosis rather than an epidemic of disease because of advancement and

increased use of diagnostic techniques resulting in increased diagnosis of indolent localised tumor and/or small cancers [14]. But a more recent study by Lim et al. concluded that the increase is true, demonstrated by a significant increase in the incidence and mortality associated with larger and advanced-stage thyroid cancer patients [12]. The estimated new cases of thyroid cancer in the US for the year 2018 is 53,990 which would account for 3.1% of all the cancer cases reported in 2018 and caused 2060 deaths [15]. The relative 5-year survival of thyroid cancer ranges from 98-99% for localised cancer to only about 55.5% in cases with distant metastasis.

Thyroid cancer is the fifth common cancer in women [16]. Many studies, including the data from National Cancer Institute's Surveillance, Epidemiology and End Results Program (SEER 9) shows not only that the incidence of thyroid cancer is higher in women (occurs about 3 times more in women when compared to men), but also that the relative increase in the incidence rate of thyroid cancer has been larger in women than in men (about 4 times greater in women) [14]. The study also showed that this difference in the rate of incidence between the genders did not reflect in the mortality, as there seemed to be not much difference in mortality rate between men and women. The possible reason for this could be that the incidence of aggressive cancer is more prevalent or equal in men when compared to women and/or that men are usually older at diagnosis, though the exact reasons for higher incidence in women remain largely unclear. Thyroid cancer seems to be more prevalent in young adults, though all age groups can be affected. Exposure to ionizing radiation, especially in childhood, is the only known cause of thyroid cancer [17]. Two large geographical cohorts that demonstrate ionizing radiation induced thyroid cancer are the Japanese atomic-bomb survivors and the victims of the 1986 Chernobyl nuclear fall out [18, 19]. Various studies including the study by Imaizumi et al. show that young individuals when exposed to atomic bomb radiations were at higher risk of thyroid cancer and that there was a dose-dependent increase in prevalence [18]. In 1992, a report suggested that there was a marked increase in frequency of thyroid cancer in children from 1990 onwards in Belarus and associates this rise with the Chernobyl tragedy [19]. Patients exposed to radioactive iodine ^{131}I and are given external radiotherapy are also susceptible to thyroid cancer [17]. Gender, age, size of tumor, presence of lymph node and distant metastasis are factors that are often considered in the risk assessment of thyroid cancer, though not all of these factors have reached a consensus. Other risk factors that may contribute to the increase in incidence of thyroid cancer include familial history, exposure to fertility

drugs [20], overweight in post menopausal women [21], menstrual and reproductive factors [22], at least in certain ethnic populations.

1.3 Management of thyroid cancer

Abnormal growth of the thyroid cells that forms a lump within the thyroid gland are referred to as thyroid nodules. Defining the nature of a thyroid nodule, accurate stratification of the lesions and deciding on the optimal treatment strategy are the challenges in the management of thyroid cancer. Thyroid nodules are a common clinical finding and are detected in 5% of the population by physical examination of the neck. Ultrasound examinations reveal a much higher occurrence of thyroid nodules (between 20-70%) [23]. Though most of the cases presented with thyroid nodules are non-malignant in nature, studies indicate that patients with multiple thyroid nodules are at a higher risk to develop thyroid cancer. A study by Smith JJ et al. [24] implied that nearly 1 in 5 patients presented with multiple thyroid nodules had thyroid cancer. It is very important to diagnose if the nodules are only benign or actually malignant in order to ensure that the patient is not overtreated or undertreated. Surgical removal of the thyroid, which is the standard treatment for thyroid cancer, can result in undesired consequences including hormone imbalance, hypoparathyroidism, laryngeal nerve injury or infections. Hence, it is important to limit unnecessary thyroidectomy of non-malignant lesions. If the nodules are diagnosed to be benign, they would be subjected to serial ultra sound examinations in order to further monitor the nodules, sparing the cost and complications of surgery. Techniques and advancements in methods for the management of thyroid cancer are discussed below.

1.3.1 Ultra sonography and TSH levels

Thyroid nodules are usually detected by thyroid or neck sonography and less frequently by palpation. Ultrasound can reveal certain features of the nodules like hypoechogenecity, microcalcifications and extrathyroidal extensions that can be indicative of its malignancy status. It is also very useful in the determination of the size and monitoring the growth of thyroid nodules. But it is often not completely reliable to

distinguish benign from malignant lesions. Many studies have tried to investigate any correlation between the size of thyroid nodules and risk of malignancies, and the findings were not very conclusive. While some studies recommended surgical treatment for larger nodules following their evaluation that larger size was associated with higher risk of malignancy, other studies ruled out the correlation of nodule size with the risk of malignancy [25, 26]. A study by Kamran et al. concluded that though 15% of nodules >2 cm in size were cancerous as opposed to only 10.5% cancerous cases in nodules with sizes 1.0-1.9 cm, they saw that above 2 cm diameter, increasing thyroid nodule size (nodule diameter 2.0-2.9 cm, 3.0-3.9 cm and >4 cm) had a nonlinear impact on the risk of cancer respective percentage of cancerous cases 14%, 16% and 15% [26]. Studies were also conducted to investigate TSH levels as predictors of malignancy. Most of the patients with thyroid cancer are euthyroid and do not present with abnormalities in their TSH levels. Haymart et al. for the first time in a retrospective study showed an increased risk of malignancy with higher TSH levels [27]. While patients with TSH levels less than 0.06 mIU/litre had 11% likelihood of malignancy, patients with TSH levels greater than or equal to 5 mIU/litre had a 46% likelihood of malignancy. Even when the patients are presented within the accepted normal TSH ranges (0.4–4.99 mIU/liter), there was a significantly higher likelihood of thyroid cancer when the TSH level was above the population mean [27].

1.3.2 Fine needle aspiration biopsy (FNAB)

Introduction of FNAB in clinical practice has played an important role in improving the diagnostic prediction, reducing the number of diagnostic and unnecessary therapeutic surgeries associated with thyroid nodules. Owing to reduced inadequate sampling, ultra sound guided fine needle aspiration had higher sensitivity, specificity, accuracy and predictive values than palpation guided FNA [28]. FNA is quick, accurate, cost-effective, causes less morbidity in the patients and can be used in sampling smaller thyroid nodules. The recent years saw a 50% reduction in the number of thyroidectomies and improved predictions of malignant cases (from 14% to 30-50% surgical cases) [29]. Despite how FNA has improved diagnosis of thyroid nodules, there are few problems that are of major concern in the FNA mediated diagnostics. Cytological evaluation followed by FNA categorises about 25% cases as indeterminate

after FNAB, hence requiring a diagnostic surgery or more FNAB samples for appropriate diagnosis. False negative FNA cytology as high as 8%, resulting in delayed treatment can have a major negative impact on the prognosis and outcome of the patients [30]. Studies suggest that false negative FNAs are higher in nodules larger than 3-4 cm and this could be attributed to eccentric malignant foci present in the nodules, but could not be sampled, hence not exactly representing the true cytology of the nodules [30, 31]. Also, a study by Mazzaferri et al. noted that FNA of thyroid nodules smaller than 5 mm yielded very high rates of non-diagnostic FNA [32]. Even in larger thyroid nodules FNA may yield indeterminate diagnostics. Additional to the ambiguities associated with FNA, cytological evaluation also comes with its complexities like overlap of cytological patterns between neoplastic and non-neoplastic lesions and between different neoplasms and existence of multiple malignancies in the same gland. Despite improvement in diagnostic methods and several studies investigating risk factors and better predictors of malignancy, precise classification of the cancer and determination of appropriate management protocols has been a challenge in the field of thyroid cancer. Tremendous efforts have been put into compiling available information and methods used for evaluation and interpretation of thyroid nodules, with the aim of developing evidence-based guidelines for accurate diagnosis, stratification and management of thyroid cancer. 'The NCI Thyroid FNA State of the Science Conference' organized by the National Cancer Institute in Bethesda in 2007 was one such initiative that brought together many pathologists, endocrinologists, surgeons and radiologists and came up with a 6-tiered classification system (The Bethesda System for Reporting Thyroid Cytopathology (TBSRTC) with malignancy risk associated with each category, hence hoping to have a uniform FNA reporting and management system. The TBSRTC was revised in 2017 where the malignancy risks associated with each category and recommendations for management of each category have been updated based on patient data post 2010 [33]. While most of the categories are very well defined by the Bethesda classification, it still has the drawback of having indeterminate FNA categories comprising of non-diagnostic or unsatisfactory diagnosis, atypia or follicular lesion of unknown significance and suspicious follicular neoplasms.

1.3.3 Surgical management

Surgery is the standard treatment for thyroid cancer, though the extent of thyroidectomy is a matter of debate in the field. Reasons that support total thyroidectomy include higher chances of adequate removal of the disease, prevention of recurrence, and avoidance of further surgery in cases of progression to malignancy. Though treatment guidelines recommend that only thyroid lobectomy would be enough for the management of indeterminate thyroid nodules, small (<1 cm), unifocal low-risk thyroid cancers, such cancers are also extensively managed with total thyroidectomy [34]. This is a matter of concern as it can have severe consequences due to complications in surgery and the patient is subjected to life long thyroid hormone therapy as well as higher treatment and treatment related expenses. Though surgical skill and experience play an important role the extent of success and good outcome of the surgery, studies also suggest that the type of surgery also has an influence on morbidity [34]. In a study that aimed at reviewing the impact of thyroid lobectomy versus total thyroidectomy with tumors ranging 1-4 cm in size on tumor recurrence and survival, it was implied that lobectomy and total thyroidectomy yield comparable oncologic outcomes [35]. Hence, it is very important to avoid any unnecessary surgical intervention, especially in the management of benign and small tumors.

1.3.4 Radioiodine treatment (RAI)

Owing to the ability of thyroid cells to uptake iodine, when radioactive iodine (^{131}I) is administered in liquid or capsule form, it is taken up only by the thyroid cells of the body, which are consequently ablated. Thyroidectomy is usually followed by RAI for the removal of residual thyroid tissue post surgery as well as for the treatment of metastasized thyroid cancer. Appropriate levels of TSH stimulation and absence of iodine contamination are key prerequisites for successful RAI uptake and effective treatment. About two-thirds of patients with metastatic cancer demonstrate significant RAI uptake, but despite successful RAI uptake the treatment might become ineffective. There could be several reasons for this including lower radiation dose in tumor tissue and shorter effective half-life of ^{131}I as well as heterogeneity in ^{131}I uptake within a given metastasis [36]. Tumors responding to ^{131}I treatment display decrease in tumor

volume on anatomical imaging. Better responses are achieved in younger patients and patients with small pulmonary metastasis, while patients with bone metastasis tend to have poorer prognosis, likely owing to larger size of the lesions. Older patients and patients with advanced stages of thyroid cancer are refractory to ^{131}I treatment [36] [37]. Loss of ability of the tumors to uptake iodine is also a major reason for ^{131}I refractiveness. One approach that has been investigated in the treatment of ^{131}I refractory patients is the restoration of the ability of tumor cells to uptake iodine. A study by Ho et al. showed that treatment with MEK1/2 inhibitor selumetinib 4 weeks prior to ^{131}I therapy reversed the RAI refractiveness of tumour in patients with advanced thyroid cancer [38]. Similarly, another group showed that Dabrafenib (a BRAF inhibitor) administration to patients with unresectable or metastatic iodine-refractory PTC harbouring BRAFV600E mutation could stimulate RAI uptake in 60% of the patients in the study [39].

Patients refractive to ^{131}I are also considered for chemotherapy. Various new agents including doxorubicin, gemcitabine, oxaliplatin and combinatorial therapies are being investigated for the treatment of RAI refractory thyroid cancer. Further, with the increasing understanding of the molecular mechanisms underlying thyroid cancer, various molecular targeted therapies are also being extensively investigated for the treatment of RAI refractory thyroid cancer, which are discussed in the later sections.

1.4 Types of thyroid cancer

Thyroid cancer has been categorised into various types and subtypes, primarily based on histocytology, cell of origin and stage. Histologically, there are 4 main types of thyroid cancer – differentiated, anaplastic, poorly differentiated and medullary thyroid cancer (figure 1.3) [40].

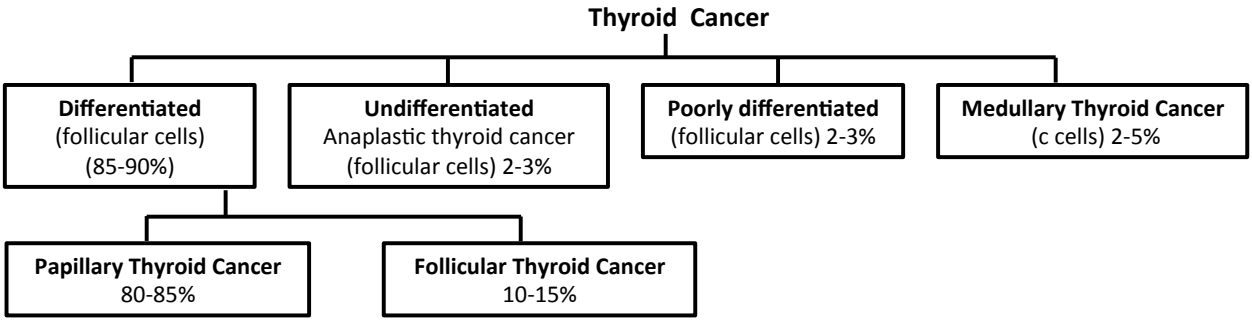

Figure 1.3: Main types of thyroid cancer. The broad classification, cellular origin and prevalence of the thyroid cancer are shown above.

1.4.1 Differentiated thyroid cancer (DTC)

DTC includes both papillary thyroid cancer (PTC) and follicular thyroid cancer (FTC), which are very well differentiated cancers. Both originate from the follicular cells of the thyroid. Increase in the occurrence of thyroid cancer has been almost exclusively attributed to the increase in PTC [10]. Histopathology of PTC includes well recognisable papillar projections of the cells, calcified cellular clumps probably originating from the necrosed papillas and large, clear nuclei often referred to as 'Orphan Annie eyed' nuclei, whereas FTC exhibits abnormal extracapsular and intravascular spread of thyroid follicles. PTC accounts for 80-85% of thyroid cancer [40]. Morphological variants of PTC include conventional PTC (CPTC), follicular-variant of PTC (FVPTC) and tall-cell PTC. FTC accounts for only about 10-15% of total thyroid cancers, though they have high propensity for metastasis and poor prognosis. Hürthle cell carcinoma, though was earlier considered an oxyphilic variant of FTC, it is now widely being considered as a distinct clinicopathological entity and accounts for 3% of all thyroid carcinomas [40]. Presence of oncocytes - large polygonal cells with hyperchromatic nuclei and an eosinophilic granular cytoplasm as a result of abundant mitochondria, is a characteristic feature of Hürthle cell carcinoma [41]. Metastasis of DTC usually occurs in the lymph nodes, lungs and bone. The standard treatment for differentiated thyroid cancer is partial or complete thyroidectomy. In cases presented with aggressive disease or metastasis, surgery is followed by TSH suppression and radioactive iodine (RAI) ablation. Patients can be or develop ^{131}I

refractiveness, in such cases they are subjected to levothyroxine treatment or focal treatment of metastasis is performed (surgery), if possible.

1.4.2 Anaplastic thyroid cancer (ATC)

ATC is an undifferentiated cancer that arises from the thyroid follicular cells. Aggressiveness and poor prognosis of thyroid cancer is inversely related to the degree of differentiation of the constituting cells, thus making ATC a very lethal type of thyroid cancer. They usually possess heavy mutational burden. An analytical validation study of hybridisation capture-based assay targeting all coding regions of 341 tumor associated genes by Cheng et al. detected a median mutation burden of 6 per tumor in ATC, which is much higher than the median mutation burden detected in PTC (1 per tumor), a relatively indolent type of thyroid cancer [42]. Many of the genetic alterations in ATC are also seen in the less aggressive DTC, thus indicating that ATC may derive de novo from DTC. This is also supported by histological studies that show that DTC exists in about 30-50% of ATC [43]. Though it is an uncommon (2-3%) form of thyroid cancer, it has been categorised as a stage IV disease by the American Joint Committee on Cancer Staging as it is a rapidly growing, highly aggressive cancer with mortality rate as high as almost 100% and has a median survival of only 5 months [44, 45]. Partly owing to the rarity of the disease, there is no defined treatment protocol for ATC. Treatment is usually multimodal and surgery is performed whenever possible – like when the cancer is only intra and/or extrathyroidal and has not invaded the aerodigestive tract. Less than 10% of patients presented with ATC have the tumor confined to the thyroid, while most patients also show local or distant metastasis [46]. So, surgery is followed by radiotherapy or chemotherapy and such multimodal treatment approaches seem to improve the overall survival of ATC patients [43]. Chemotherapeutics like docetaxel, paclitaxel and cisplatin have been used post surgically or in combination with radiation therapy in order to improve the overall survival of ATC patients. Owing to the improvement in understanding the biology and molecular basis of ATC, various drugs are being considered for targeted therapeutics. In May 2018, the FDA has approved a combinatorial chemotherapeutic treatment with dabrafenib (BRAF inhibitor) and trametinib (MEK1/2 inhibitor) for cases of local and distant metastasised ATC, which are diagnosed with a BRAFV600E mutation [47].

1.4.3 Poorly differentiated thyroid cancer (PDTC)

PDTC was considered as a variant of DTC until the World Health Organisation (WHO) classified it as a distinct pathological entity in 2004. The WHO define PDTC as follicular neoplasms that show limited evidence of structural follicular cell differentiation and occupy both morphologically and behaviorally an intermediate position between differentiated (follicular and papillary carcinomas) and undifferentiated (anaplastic) carcinomas. PDTC is not a commonly occurring type of thyroid cancer, studies imply its occurrence in 2-3% of thyroid cancer patients in North America [48]. Since it is a rare disease, there is not a lot of data available about the growth pattern, histological subtypes or prognostic markers of PDTC. In an attempt to report the treatment outcomes of 91 patients with a median follow up of 50 months, who were treated for PDTC with or without adjuvant therapy, it was observed that with appropriate surgical and adjuvant therapy, excellent locoregional control could be achieved and disease specific deaths mostly occurred due to distant metastases [49].

1.4.4 Medullary thyroid cancer (MTC)

MTC is a relatively rare form of thyroid cancer (2-5% of all thyroid cancers), which arises from the parafollicular C cells of the thyroid. Elevated calcitonin levels are a characteristic feature of this tumor [50]. Nests of round or ovoid cells with fibrovascular stroma are the histopathological signatures of MTC. Majority cases (75-80%) of MTC are sporadic in occurrence, while others are associated with familial inheritance due to multiple endocrine neoplasia (MEN2A and MEN2B) or familial medullary thyroid cancer (FMTC). As the C cells reside on the upper poles of the thyroid gland, MTC patients often have nodules on the upper portions of the thyroid. While sporadic MTC is usually seen only in one of the two thyroid lobes, MEN associated MTC tend to occur bilaterally and are multicentric [50]. Indeed patients presented with distant metastasis have poorer prognosis (about 20% 10-years survival) when compared to the 95.6% 10-years survival rate in patients with non-metastatic MTC [51]. Distant metastasis in MTC usually occurs in liver, lung and bone. Surgery is the primary line of treatment for

MTC, while it is non-responsive to conventional chemotherapy. Unlike cancers arising from the follicular cells, owing to its parafollicular origin, cells of the MTC cannot take up ^{131}I and hence, the residual cells cannot be managed using RAI treatment. External beam radio therapy also has shown to be beneficial in the treatment of MTC including cases with unresectable metastasis [52]. A study by Berber et al. demonstrated that laparoscopic radiofrequency thermal ablation treatment in a group of patients with neuroendocrine liver metastasis prevented cancer progression in 41% of patients and 65% patients showed a partial or significant reduction in tumor markers during follow-up [53]. Assessment of serum calcitonin levels and also carcinoembryonic antigen post therapy monitors the prognosis of the patient, as absence both these markers in serum is an indication of disease free condition. MTC carries relatively lesser types of mutations and RET mutation is the predominant genetic alteration found. This has been exploited in the development of targeted therapy of MTC. In a randomised Phase III trial, vandetanib (multi kinase inhibitor against RET, VEGFR and EGFR) treatment in patients with locally advanced or metastatic hereditary MTC demonstrated a prolongation of progression free survival [54]. Another phase III study investigating the effect of cabozantinib (pantyrosine kinase inhibitor) in patients with progressive MTC showed that the drug benefitted the patients with improved response rates and progression free survival [55]. The US Food and Drug Administration (FDA) approved vandetanib and cabozantinib for the treatment of patients with progressive systemic disease [56-58].

1.5 Genetic alterations in thyroid cancer

1.5.1 Gene mutations

Undisputedly, the advent of better diagnostic tools, particularly FNAB evaluation has improved the management of thyroid cancer. Yet, precise stratification and consequently the right therapeutic intervention and prediction of prognosis are major issues in the management of thyroid cancer. Clearly, understanding the molecular events underlying its pathogenesis can be a powerful tool in the refinement of stratification, staging and risk evaluation of thyroid cancers. So far, with the advances in molecular biology and genetic screening techniques, the field has managed to

remarkably expand the knowledge and understanding about the disease. Some major discoveries at the level of molecular mechanisms and pathogenesis of thyroid cancer are discussed below.

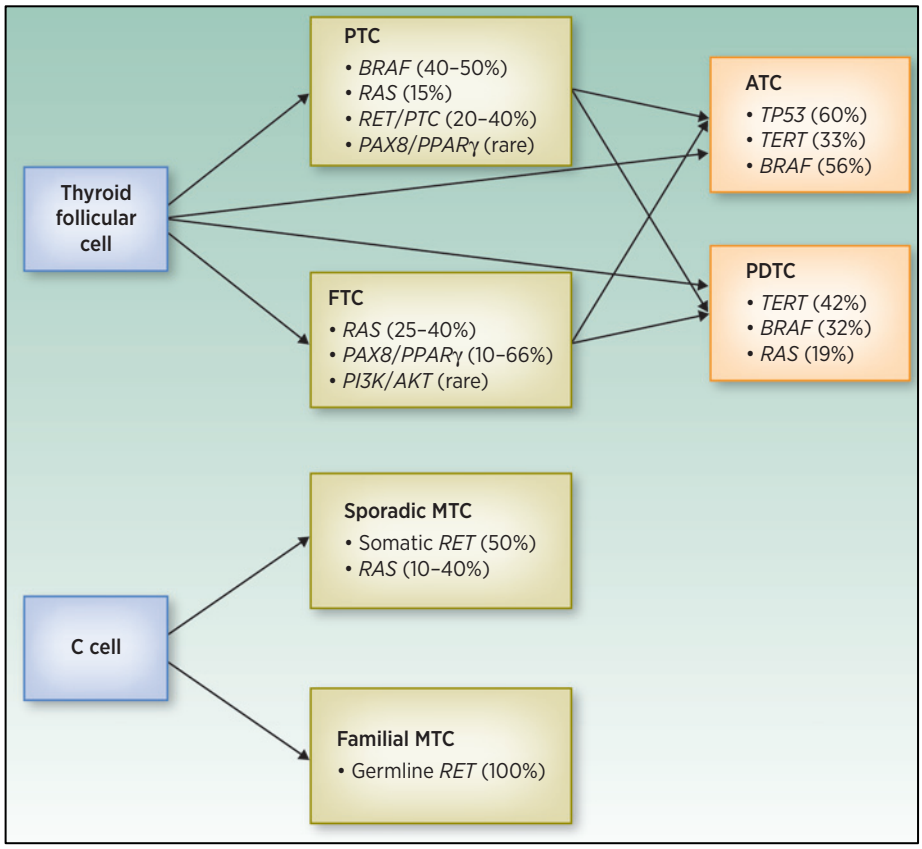

Figure 1.4: Main subtypes of thyroid cancer and associated genetic alterations (from [59])

1.5.1.1 BRAF mutation

RAF kinases (ARAF, BRAF and CRAF) are serine-threonine kinases and play a central role in the mitogen-activated protein kinase (MAPK) pathway which comprises of the RAS-RAF-MEK1/2-ERK1/2 signal transduction network. This pathway plays an important role in the regulation of a variety of cellular processes including cell proliferation, differentiation, apoptosis and oncogenic transformation. Binding of GTP-bound RAS, along with other regulatory events including phosphorylation, dephosphorylation and dimerisation results in the membrane recruitment and activation of RAF proteins, which in turn phosphorylate MEK1/2 at residues S217 and S221 leading to the subsequent phosphorylation and activation of ERK1/2, which then

translocate to the nucleus and phosphorylates transcription factors, thereby regulating the expression of various genes [60]. Owing to its constitutive phosphorylation at S445 and the presence of negatively charged amino acid in the N-region, BRAF seems to be more primed for activation in comparison with ARAF and CRAF [61]. Among the RAF kinases, BRAF exhibits the highest basal kinase activity and has the strongest activity as well as binding affinity towards MEK [62]. Mutations in BRAF are among the most common molecular events in human cancer including melanoma, colorectal cancer and non-small cell lung (NSCLC) cancer. About 30 single site missense mutations associated with BRAF in human cancers have been identified, mostly within the glycine-rich ATP-phosphate-binding P-loop or the activation segment within or adjacent to the DFG motif, both of which are located in the protein kinase domain proximal to the C-terminus, and majority of these mutations leads to increased BRAF kinase activity [63]. 90% of BRAF mutations are attributed to the point mutation caused by the substitution of Valine for Glutamic acid at residue 600 in the activation segment of BRAF (BRAFV600E). BRAFV600E has elevated kinase activity and has the ability to stimulate ERK1/2 activity independent of RAS activation [64]. A study by Paul T.C.Wan et al. showed that substitution of the medium sized, hydrophobic valine side chain with a larger, charged residue like glutamic acid would confer an active conformation to BRAF by destabilizing the interactions that maintains the DFG motif in an inactive state [63].

BRAFV600E is the most frequent genetic alteration seen in PTC, occurring in about 36-83% cases [65]. It is also prevalent in up to 25% of ATC cases, but does not seem to occur in neither FTC nor MTC [40]. A rarer form of BRAF mutation is the BRAFK601E resulting also in the activation of the MAPK pathway, which was detected in about only 5% of the follicular variant of PTC [66]. A comprehensive meta-analysis examining the association of BRAFV600E with clinicopathological outcomes demonstrated that patients carrying this mutation are closely related to high-risk clinicopathological factors like extrathyroidal invasion and advanced TNM (tumor, node, metastasis) stage across different study populations [67]. A retrospective multicentre study investigating the relationship between BRAFV600E mutation and recurrence of PTC demonstrated that in patients with the mutation, recurrence rates were significantly higher than in patients without the mutation, even in patients diagnosed with low risk stage I and II disease [68]. However, these observations seem

to be contradictory. In a study by Trovissco et al. it was observed that BRAFV600E mutation was exclusively detected in PTC with a papillary or mixed follicular/papillary architecture, although did not correlate with tumor aggressiveness, hence implying a predictable phenotype associated with BRAFV600E genotype [66]. The study also indicated that PTC harbouring BRAFV600E mutation did not correlate with higher aggressiveness in terms of vascular invasion, extra-thyroid extension and nodal metastasis and were less often multicentric than PTC without BRAFV600E mutation. In another extensive study, Henke L.E et al. analysed the relationship between BRAF mutation status and recurrence-free survival (RFS) and disease specific survival (DSS) [69]. While the multivariate analysis correlated the presence of BRAFV600E mutation with capsular invasion, cervical node involvement and classic papillary histology, it did not find any significant correlation with recurrence-free survival and disease specific survival. Similar findings were reported in a study which compared the clinicopathological features of PTC patients with and without BRAF mutation which concluded that there was no significant association between BRAF mutation and features suggestive of disease aggressiveness like tumor multicentricity, lymphovascular invasion, extranodal extension, central neck involvement, advanced stage, and distant metastasis [70]. All these studies suggest that BRAF is minimally prognostic in PTC.

Despite the uncertainties regarding BRAFV600E as a significant prognostic predictor, efforts were put into exploiting BRAFV600E as a candidate for targeted therapy in ATC, as differentiated thyroid cancer with BRAFV600E mutation with late-event mutations is thought to lead to progressive dedifferentiation to ATC. McFadden et al. demonstrated that though treatment of ATC-bearing BRAFV600E with only BRAF inhibitor (PLX4720) did not lead to tumor regression, the combination of (PLX4720) and MEK inhibitor (PD0325901) suppressed the MAPK signalling in mouse and human ATC cell lines and improved the survival of the mouse models [71]. Subsequently, a Phase II trail in ATC patients with BRAFV600E mutation showed that combination therapy targeting both BRAF (dabrafenib) and MEK1/2 (trametinib) demonstrated a high overall response rate, prolonged duration of survival and survival with manageable toxicity [72]. Currently, the FDA has approved combination therapy with dabrafenib and trametinib for the treatment of patients positive for BRAFV600E with unresectable ATC [47]. A phase I study wherein patients with BRAFV600E positive metastatic PTC

were treated with the oncogenic BRAF kinase inhibitor Vemurafenib showed that the treatment resulted in partial response and prolonged stabilisation of locoregional and distant disease, thus suggesting potential clinical benefits of targeted therapy with Vemurafenib in BRAFV600E PTC patients [73]. This was further demonstrated by antitumor activity of Vemurafenib in a phase II trial including patients with recurrent or metastatic BRAFV600E positive PTC refractory to ^{131}I treatment [74].

1.5.1.2 Rat sarcoma (RAS) mutations

Ras genes are proto-oncogenes originally identified in the genome of rodents. By introducing them into human cells in vitro, cells were transformed [75]. In normal cells, RAS is ubiquitously present and RAS signals via various downstream effector pathways including RAF-MEK-ERK and PI3K-Akt pathways. These pathways are important in the regulation of various cellular processes including growth, differentiation, apoptosis and membrane trafficking. RAS is a guanine nucleotide binding protein – RAS in the GTP bound state is active, while GDP bound RAS is inactive. Upon growth factor stimulation, the RAS guanine nucleotide exchange factors (RASGEFS) activates RASGDP to RASGTP by the release of GDP and transient formation of RASGTP, subsequently activating the downstream signalling pathways. RAS GTPase activating proteins (RASGAPs) hydrolyses the RAS bound GTP to return RAS to its inactive state. When RAS is mutated, RAS lacks any intrinsic or RASGAP mediated hydrolysis activity, thus RAS is stabilized in its active GTP bound state [76]. About 30% of all human cancer including lung, colon and pancreatic cancer which are listed as 3 of the top 4 cancer killers, carry activating RAS mutations [77]. RAS genes encode four mammalian protein isoforms – KRAS 4A, KRAS 4B, HRAS and NRAS. KRAS is the most frequently mutated isoform (86%), followed by NRAS (11%) and HRAS (3%) [78]. Up to 99% of mutations occur at the residues G12 and G13 located in exon 1 or Q61 located in exon 2 [78]. Although RAS signalling has been extensively studied and various approaches including targeting mutant RAS, GTP-competitive inhibition of RAS or inhibition of RAS isoprenylation mediated membrane association of RAS, which is a key step in the activation of RAS, RAS proteins still remain as undruggable targets. Up to date there are no inhibitors of RAS approved for use in clinic.

Mutations in all three RAS genes have been reported in various types of thyroid cancer though studies suggest that mutation in NRAS (67-88%) is the most prevalent RAS mutation in thyroid cancer [79]. RAS mutations occur more in FTC (40-50%) when compared to PTC (10-20%) most of which are FVPTC, as well as in PDTC and ATC. They are also present in about 20-40% of non malignant follicular adenomas [40]. Its prevalence in FTC makes it utilizable as a diagnostic marker, but since RAS mutations are present in both benign and malignant thyroid tumors, its role as a prognostic predictor is controversial [79]. When the occurrence of RAS mutations across the full differentiation spectrum of thyroid cancer was examined, its presence was detected in all stages of differentiation from early anapalsia to late anaplastic stages [80]. Existence of RAS mutations in the more evolved PDTC and ATC along with other mutations might be indicative of the possibility of earlier acquired RAS mutations predisposing the differentiated cancer to further molecular alterations resulting in the dedifferentiation and aggressiveness of cancer [79]. There are few studies that relates RAS mutation with distant metastasis, recurrence and death, hence associated the mutation with poor prognosis/outcome [79]. A study in which the regions of RAS codons 12,13 and 61 were sequenced indicated that NRASQ61 mutation was prevalent in follicular adenoma and FTC [81]. This was also suggested in other studies, while Hurthle cell carcinomas lacked this mutation and exhibited mutation of HRAS and KRAS conferring a histotypic association [82].

1.5.1.3 TERT Activation and mutations

Telomeres are special chromatin structures, comprising of repetitive chromosomal regions that play an important role in the maintenance of the structural integrity and stability of the chromosomes. In humans, the telomeres contain tandem repeats of TTAGGG sequence and as a consequence of the inability of DNA polymerase to completely replicate the linear chromosomes at the end, these repeats are lost progressively during the course of continuous cell division, resulting in the shortening of telomeres and leading to chromosomal instability and loss of cell viability [83]. The mammalian telomeres consist of various components including telomerase, various telomere binding proteins, chromatin regulators and DNA repair proteins [84]. The most extensively studied and a very important component of the telomere complex is

telomerase. This enzyme is involved in the maintenance of telomere length by adding tandem repeat sequences to the 3'end of the telomeres. The telomerase is comprised of the reverse transcriptase catalytic subunit (TERT), which adds tandem repeat sequences to the 3' end of the telomeres and the RNA subunit that serves as the template for DNA addition by TERT. Expression and activity of telomerase is tightly regulated, it is highly expressed in cells that have high proliferative potential and is, thus, considered as a hallmark of cancer [85]. A study by Kim et al. demonstrated that in cells cultured from different human tissues, 98 of the 100 immortal cell types were positive for telomerase activity while, all the mortal cell types were negative for telomerase. Hence, a link between telomerase activity and cell immortality is implied [86]. Further, a comparison of telomerase activity between human primary tumor material and normal somatic tissues revealed the presence of telomerase in 89% of biopsies representing 12 different types of tumor, while it was absent in all the normal and benign tissues tested [86]. Various other studies have also investigated and strengthened the idea of the link between telomerase activity and cell proliferation, immortalization and tumor growth [87]. TERT is expressed in up to 90% of all human cancers and has been shown to have a dominant role in the reactivation of telomerase leading to the malignant transformation of cells [88]. Many studies also demonstrate the role of other mechanisms than just telomere elongation that accounts for the role of reactivated telomerase in cancer. Telomerase has been shown to directly regulate NF-κB-dependent gene expression [89], modulate EGFR regulated growth promotion [90] and stabilise MYC levels thereby regulating MYC driven oncogenesis [91].

Apart from the 'solid cell nests' of the thyroid, which are thought to be a pool of stem cells in the adult thyroid that are positive for telomerase activity, the rest of the cells in the thyroid are negative for telomerase activity [92]. While up to 80-90% of various human cancer types exhibit telomerase activation, an analysis of results from many studies that examined telomerase activity suggested that only about 66% of thyroid cancer had telomerase activation [93]. This study also showed that telomerase activation was more associated with ATC, the more advanced form of thyroid cancer (up to 78%). Activation was also present in both PTC and FTC but with a lesser frequency. Apart from the increased telomerase activity, mutations in the promoter region of TERT have also emerged as a carcinogenic event in thyroid cancer. Mutations at residues 228 (C228T) and 250 (C250T) of TERT, of which the C228T is far more common but occur

mutually exclusively with C250T, are known to be associated with thyroid cancer arising from the follicular cells - PTC, FTC, PDTC and ATC, though is more prevalent in the more aggressive PTDC and ATC, while no mutations were found in the parafollicular C cells derived MTC [94]. Mechanistically, both mutations contain a 11 base pair nucleotide which serves as a consensus binding site for E-twenty-six (ETS) transcription factors resulting in the augmentation of TERT mediated transcriptional activity [95]. TERT mutations coexist with BRAF as well as RAS mutation carrying thyroid cancers [96]. Studies associate TERT promoter mutations with aggressive clinicopathological parameters like distant metastasis, advanced disease stage, cancer recurrence and patient mortality [96].

1.5.1.4 TP53 mutations

Mutations in the tumor suppressor gene TP53 leading to either dominant negative expression of the mutated P53 or complete absence of the protein have been associated with various human cancers including colon, lung, brain and breast cancer. TP53 inactivation was thought to be mostly absent in well-differentiated types of thyroid cancer, while it was associated with ATC (seen in up to 59%), hence has been considered as a hallmark of ATC [97]. Though a more recent study that employed next generation sequencing (NGS) to analyse DNA from 228 thyroid neoplastic and non-neoplastic samples revealed the presence of TP53 mutations concurrent with BRAFV600E bearing PTC in 2 of the 19 samples in which mutations were identified [98]. While one of these cases presented with lung metastasis, the other presented with local reccurrence. This study also could detect TP53 mutation in about 20% of Hürthle cell carcinoma, hence implying the mutation as an indicator of tumors with a tendency for dedifferentiation. The detection was attributed to the high allelic frequency of these mutations, rather than the sensitivity of the NGS approach.

1.5.1.5 PI3K, AKT and PTEN alterations

The phosphoinositide 3-kinase (PI3K)/Akt signalling pathways can be activated by both receptor tyrosine kinases (RTKs) and G-protein-coupled receptors and is important in the regulation of various cellular processes including cell growth, proliferation and survival. The p110 catalytic subunit of PI3K can be activated by the binding of RAS to its RAS binding site or by the activation of RTKs like epidermal growth factor receptor (EGFR), vascular epithelial growth factor receptor (VEGFR), platelet-derived growth factor receptor (PDGFR) in response to growth factor stimulation. In turn this results in the membrane localisation and activation of AKT, which triggers the mammalian target of rapamycin (mTOR signalling) leading to cellular consequences including increased cell survival, cell migration and inhibition of apoptosis [99]. Activating mutations in PIK3CA, the gene encoding for the α-type p110 catalytic subunit of the PI3K heteromer (PIK3CA) is prevalent in many human cancers including ovarian, breast and colorectal cancers [100]. In a study that investigated PIK3CA mutations in DTC and ATC, non-synonymous mutations were identified in 23% of ATC, 8% of FTC and 2% of PTC and activation of AKT was seen in most of the ATC with PIK3CA mutations [101]. Also, in PIK3CA mutation positive cases where ATC coexisted with differentiated cancer, the mutations were restricted to the ATC component within the kinase domain. Hence, these observations imply an oncogenic role of PIK3CA rather in ATC than in well-differentiated thyroid carcinoma. Another major genetic alteration involving the PIK3CA gene is copy number gain, which is seen in FTC (24%) and more prominently in ATC (42%) [102, 103]. PTEN is a phosphatase protein that antagonizes the PI3K/AKT pathway and acts as a major tumor suppressor protein and is inactivated in many cancers by gene mutations or epigenetic gene silencing. A study by Halachmi N et al. demonstrated that 27% of follicular carcinomas and 7% of follicular adenomas exhibited loss of PTEN heterozygosity implying the inactivation of PTEN in follicular thyroid cancer [104]. A more recent study demonstrated PTEN inactivation in up to 24.5% of PTC samples, especially the follicular variant of PTC [105]. However, in the presented immunohistochemical studies no association between loss of protein expression and gene deletion were found. Thus, other mechanisms like promoter methylation-mediated gene silencing might lead to the inactivation of PTEN.

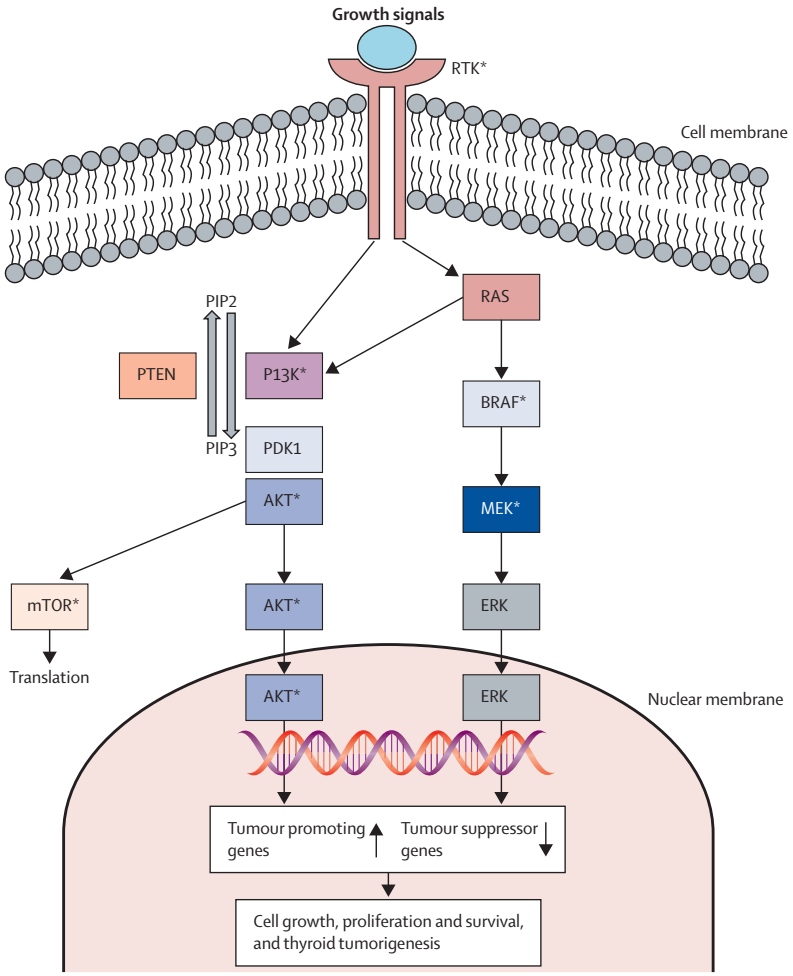

Figure 1.5: Major oncogenic alterations in the MAPK and PI3K-AKT-MTOR pathways occurring in thyroid cancer (from [106]). (Gain of function mutations indicated by *)

1.5.2 Gene Fusions

Chromosomal translocations between genes belonging to the same or different chromosomes can give rise to different patterns of chimeric transcripts. The expression of these chimeric transcripts may result in fusion proteins having altered functions and thus may have pathological consequences. Figure 1.6 shows a schematic representation of the various patterns of chromosomal rearrangements.

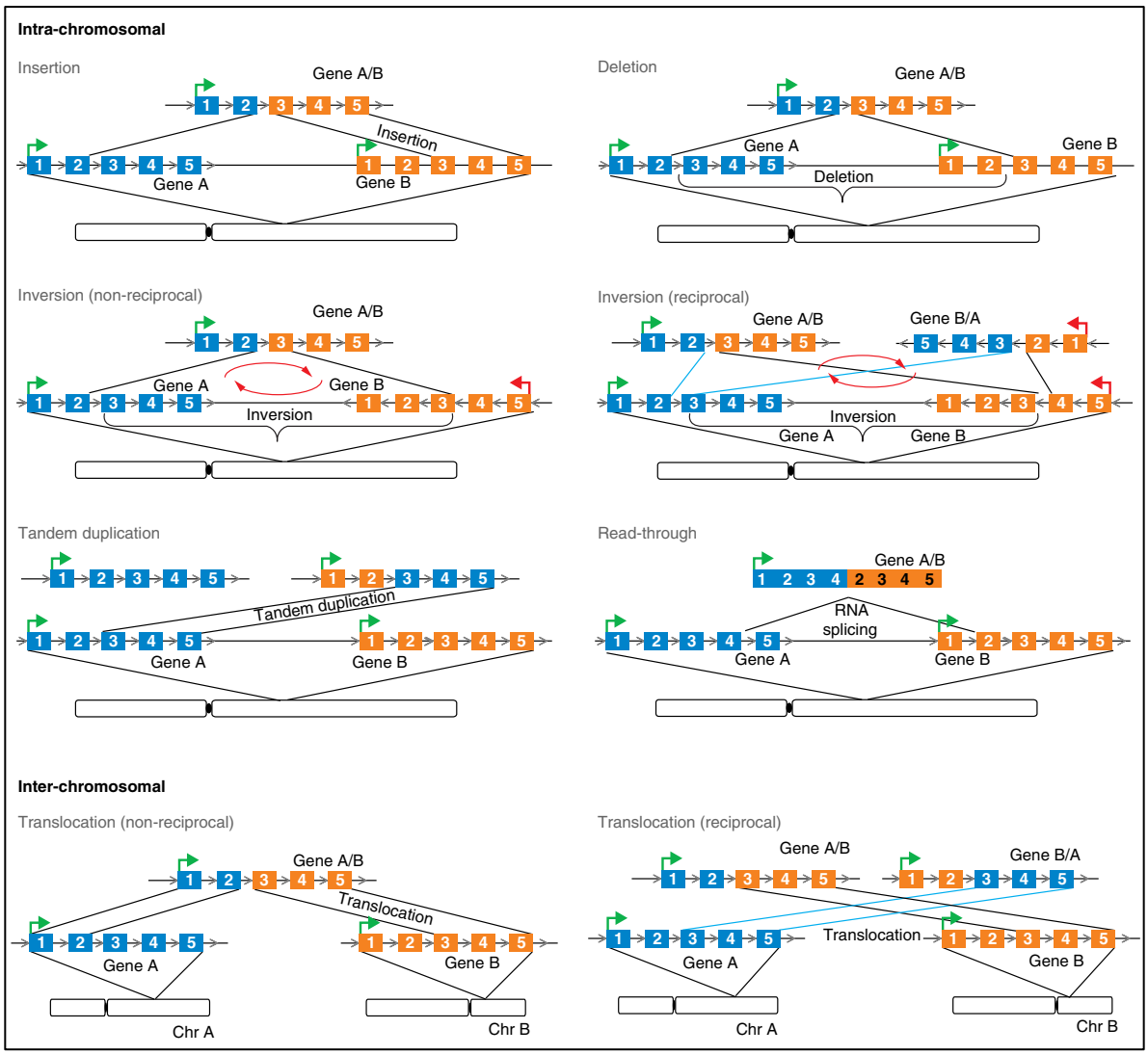

Figure 1.6: Schematic representation of the various patterns of chromosomal rearrangements (from [107]).

Kinase fusions, particularly tyrosine kinase (TK) fusions seem to occur at higher rates in thyroid cancers. The major oncogenic fusions that are known to occur in thyroid cancer are discussed below.

1.5.2.1 RET fusions

In 1985, Takahashi M et al. identified a novel-transforming gene present in NIH3T3 cells that were transfected with human lymphoma DNA [108]. The transforming gene consisted of two segments of DNA that were unlinked in normal human and primary

lymphoma DNAs but were co-transcribed in transformed NIH3T3 cells. This transforming gene was activated by rearrangement of normal human DNAs during the transfection process and was called REarranged during Transfection (RET). Following its initial discovery in transforming NIH3T3 cells, the RET transforming gene was characterised as a recombination between the RET proto-oncogene, encoding a putative kinase receptor, and the rfp gene, encoding for a putative zinc finger protein [109, 110]. The RET protein is a single-pass transmembrane, tyrosine kinase protein which has three splice isoforms – RET9, RET43 and RET51, of which RET9 and RET51 are the most abundant isoforms [111]. RET is expressed in the precursor cells of the neuronal crest and urogenital tract and is known to play an important role in the development of several subpopulations of cells derived from the neuronal crest, including enteric, sensory and sympathetic neurons, kidney and spermatogenesis [112, 113]. RET signalling involves its activation triggered by the binding of ligands belonging to the GDNF family to the glycosylphophatidylinositol-anchored GDNF-family receptors to form a ligand-receptor complex which then interacts with RET leading to the subsequent autophosphorylation and activation of RET [113]. RET signalling regulates various pathways involved in cell survival, differentiation, proliferation and migration. Different signalling pathways are triggered by phosphorylation of the different sites of RET kinases – up to 18 different phosphorylation sites have been identified in RET 43 and 51, while RET 9 has 16 phosphorylation sites of which at least 12 are autophosphorylation sites [114]. The RET signal transduction is involved in the activation of various proteins and associated pathways including Src, Protein Kinase C enzymes, PI3K/AKT pathway, MAPK pathway and JNK pathway [113].

The clinical significance of RET rearrangements or fusions was first demonstrated in PTC and now we know that these fusions are a common event in PTC, and occur in up to 40% of PTC patients [113]. These chromosomal aberrations occur as a consequence of DNA damage occurring after exposure to external radiation. It was reported that 60% cases of post Chernobyl PTCs were positive for RET fusions and it was also prevalent in patients who underwent external irradiation for the treatment of benign or malignant disease [115, 116]. Gene fusions involving RET are such that the kinase domain containing C terminus of the RET gene, which in most cases is not normally expressed in the thyroid follicular cells, is fused with the promoter containing N terminus of an unrelated gene which is ubiquitously expressed in these cells. A study by Nikiforova et

al. implied that spatial contiguity of the genes involved in the fusion during interphase may be the structural basis for radiation induced gene fusions [117]. 11 in 12 autophosphorylation sites are preserved in the fusion protein. The phosphorylation of 3 sites - Y905, Y1015 and Y1062, which is important for promoting cell survival and clonal propagation, recruitment of various signal transduction proteins are required for the oncogenic signalling of RET fusions [113, 114]. In almost all cases the breakpoint in the *ret* gene involved in the fusions occurred at sites distributed across intron 11 of the gene, which resulted in the loss of transmembrane domain as well as the deletion of negative regulatory domains of the protein, hence promoting the cytoplasmic localisation, constitutive and ligand-independent activation of the fusion protein [118, 119]. Further, almost all the fusion partners of RET protein are predicted to possess a coiled-coiled domain which are protein-protein interaction domains able to mediate dimerisation of proteins. As dimerisation is an important event in the oncogenic activation of RET fusions, these domains play an important role in RET fusion-mediated oncogenesis. Figure 1.7 summarises the crucial events involved in the activation of RET fusion proteins [119]. As a consequence of RET fusions, various oncogenic signalling pathways are hyperactivated including ERK1/2 signalling [120], PI3K/AKT signalling [121], NFkB signalling [122] as well as activation of signal transducer and activator of transcription (STAT1) [121, 123]. RET/PTCs are known to exist mutually exclusively with activating RAS and BRAF mutations [124].

So far, 12 different RET fusion partner genes have been identified and some of them have different breakpoints hence giving rise to 17 different RET fusion oncogenes. Figure 1.8 (bottom panel) schematically illustrates many of the RET fusion genes reported so far. RET fusions account for up to 13-25% of PTCs and for up to 13% of PDTCs [125]. Of these RET/PTC1 and RET/PTC3 are the most commonly occurring RET fusions accounting for up to 60-70% and 20-30%, respectively [113]. CCDC6 and NcoA4 are the respective fusion partners of RET/PTC1 and RET/PTC3, and both these partners are located on the same chromosome as RET (chromosome 10). It has also been reported that other fusion partners are present in different chromosomes, hence implying paracentric inversion and chromosomal translocation as the mechanism of DNA rearrangement underlying RET fusions [119].

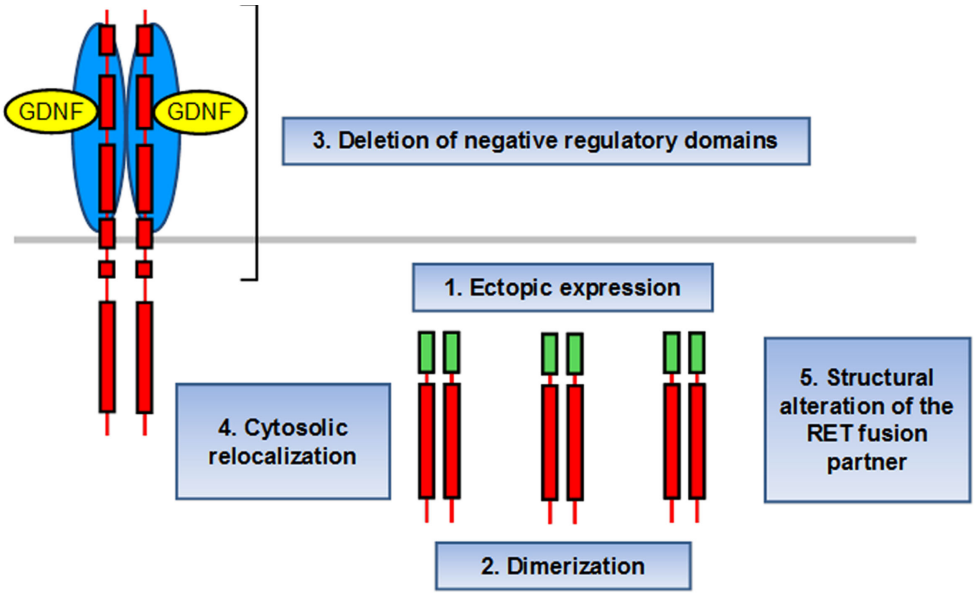

Figure 1.7: Important events in the activation of RET fusions (from [126]).

Some groups successfully established transgenic mouse models expressing RET/PTCS: In these models animals develop slowly progressive thyroid carcinomas, which exhibited nuclear cytogenic features, developed thyroid hyperplasia and local invasion similar to human PTC [127-129]. A study by Santoro et al. showed that injection of RET/PTC into a differentiated rat thyroid epithelial cell line resulted in the complete loss of their thyroid differentiation markers as well as their ability to trap iodine, although RET/PTC expression was not enough to transform these cells in vitro (soft agar colonies) or induce tumors in nude mice. But with the introduction of additional KRAS mutations, these cells could achieve a malignant phenotype, hence implying the possible involvement of other genetic alterations in RET/PTC harboring tumors [130]. The prognostic relevance of these fusions are still not very clear though some studies could associate particular fusions with certain types of thyroid cancer. The RET/PTC3 fusion was found to be highly enriched in children who were victims of the Chernobyl tragedy and patients suffering from a more aggressive solid variant of PTC [131]. RET/PTC has also been associated with Hürthle cell carcinoma. Apart from PTCs, recent studies reported the detection of RET fusions including RET/PTC1, RET/PTC3 in NSCLC, colon adenocarcinoma as well as breast cancer [132-134].

Targeted next generation sequencing studies that aimed at studying the genomic landscape of RET aberrations in human cancers implied that RET aberrations occurred

in up to 1.8% of the 4,871 cancers analysed and mutations in RET were the most common aberrations accounting for up to 38.6% RET aberrations [135]. Activating somatic mutations of RET has also been reported in thyroid cancer and they are found in about 40-50% of sporadic MTCs, though they are not known to occur in follicular cell derived DTC [136]. M918T mutation is the most commonly occurring RET mutation in MTC [137]. Other RET mutations associated with MTC include mutations in codon 634, 883, 630 and 611 [136]. Germ line mutations of RET are hallmarks of Multiple Endocrine Neoplasia (MEN2) that include MEN2A, MEN2B and familial MTC [136]. A study by Shumei Kato et al. wherein 4,871 patients were screened for RET aberrations in various cancers reported that RET mutations were also detected in 16.7% of ATC as well as paraganglioma and urothelial carcinoma [135]. As far as targeted therapy of RET altered cancers are concerned, only multikinase inhibitors (MKIs), which nonselectively inhibit RET are used in the clinics. Vandetanib is a MKI capable of blocking the tyrosine kinase activity of vascular endothelial growth factor receptor 2 (VEGFR2), epidermal growth factor receptor (EGFR) as well as RET kinases. A double-blind phase III trial involving 331 patients with advanced MTC demonstrated therapeutic efficiency of this drug and currently vandetanib is an FDA approved drug for MTC [54]. Cabozantinib (XL184), yet another inhibitor that inhibits multiple tyrosine kinases in a phase III clinical trial demonstrated an improvement in the progression free survival of MTC patients across all subgroups including by age, prior tyrosine kinase inhibitor (TKI) treatment and RET mutations associated with both hereditary and sporadic MTCs [55]. FDA approved cabozantinib for the treatment of MTC in 2012. As both these drugs and many other MKIs are non-specific inhibitors, they are quite obviously associated with off target side effects, and not very successful in the potent reduction of RET pathway.

Hence, there are a lot of efforts being made in search of inhibitors, which are more specific to RET. A recent study by Subbiah et al. tested the ability of LOXO-292, a highly selective ATP-competitive small molecule RET inhibitor in the inhibition of diverse RET fusions, activating mutations and acquired resistance mutations [138]. They demonstrated that LOXO-292 was effective as a RET specific inhibitor in cell lines harboring RET alterations and patient-derived xenografts. Further, they could show that LOXO-293 treatment in a patient with metastatic M918T MTC, who also possessed an acquired RET V804M gatekeeper resistance mutation, following treatment with six MKI regimens showed a tumor response demonstrated by rapid reductions in

tumor calcitonin, cell-free DNA, resolution of painful hepatomegaly and tumor-related diarrhea.

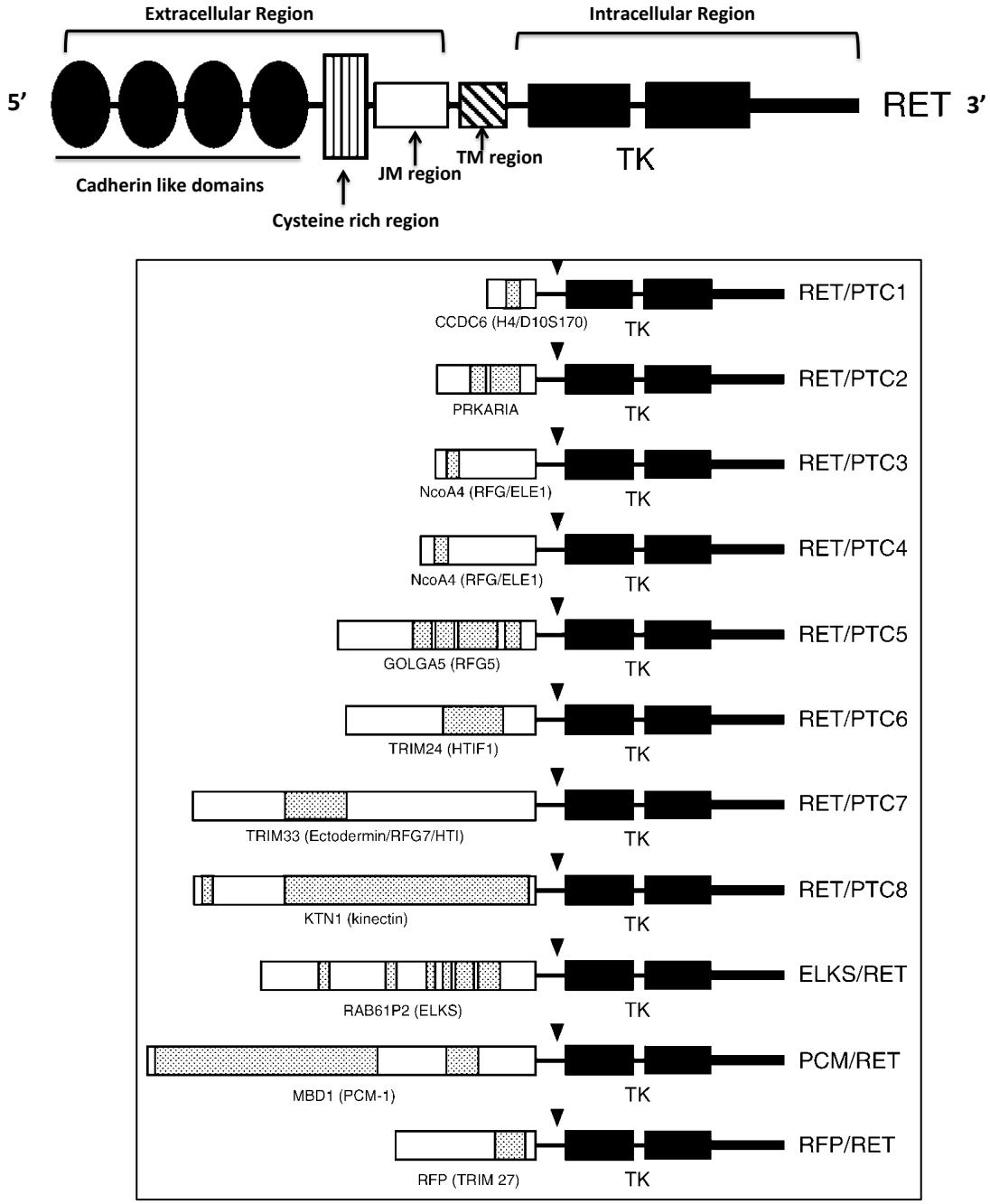

Figure 1.8: Top panel: Schematic drawing of RET protein (JM-juxtramembrane domain, TM – transmembrane domain, TK-tyrosine kinase domain). Bottom panel: Schematic drawing of RET fusions (arrows indicate breakpoints).(from[119]).

Yet another study demonstrated the potency of BLU-667 as a RET inhibitor which could selectively inhibit thyroid xenografts driven by RET mutant and fusion proteins, without inhibiting VEGFR-2. Its potential as a treatment option for RET altered MTC was demonstrated by durable clinical responses in patients without notable off target toxicity [139].

1.5.2.2 NTRK fusions

Neurotrophic tyrosine receptor kinase (NTRK) proteins are encoded by the genes NTRK1, NTRK2 and NTRK3, and they function as high affinity receptors for nerve growth factors (NGFs). Upon activation by NGF, they can promote various signalling events including activation of RAS, MAPK and PI3K signalling resulting in the regulation of proliferation, differentiation and apoptosis. All the NTRK isoforms have been reported to form oncogenic fusions in various cancers including PTC, NSCLC, glioblastoma and sarcoma, although they have only a very low frequency [134, 140]. NGS analysis revealed the existence of both NTRK1 and NTRK2 fusions in thyroid cancer [134]. NTRKI fusions include genomic rearrangement with TPM3, TPR and TFG. Frequency of somatic NTRK1 rearrangements is reported to be much lesser than RET fusions in PTC and an association of these mutations with radiation is not yet documented [134]. Larotrectinib is a TRK inhibitor that has been very recently approved by FDA for solid tumors with NTRK gene fusions [141].

1.5.2.3 Other fusions in thyroid cancer

Other less common gene fusions reported in thyroid cancer include PAX8/PPARG which are seen in FTC and FVPTC [131].With the tremendous advancement in NGS techniques, it is now possible to conduct large screening for genetic alterations in cancer and this has obviously lead to a growing list of fusion proteins that are being reported. In a search of the landscape of recurrent kinase fusions in solid tumors, fusions involving CRAF, BRAF, MET, and ALK were identified in thyroid cancer [134].

1.6 Ubiquitination associated proteins in cancer

Ubiquitination is a multi-step, reversible post-translational modification that involves the covalent conjugation of mono-ubiquitin or poly-ubiquitin chains to target proteins. Although initially ubiquitination was thought to be a mechanism that marks misfolded and desuete proteins for proteasomal degradation, we now know that ubiquitination plays an important role in the mediation of several cellular processes like gene transcription, subcellular localisation, DNA repair, endocytosis, antigen processing and apoptosis [142]. Ubiquitination involves the attachment of ubiquitin on lysine residues of target proteins in an ATP-dependent manner, through a sequential three-step mechanism that involves three classes of enzymes namely, the E1 activating enzyme, E2 conjugating enzyme and the E3 ligases (Figure 1.9). The initial step in the ubiquitination pathway involves the ATP-dependent activation of the C terminus of ubiquitin and its conjugation to the active site of the E1 enzyme via a thiol-ester bond, following which ubiquitin is transferred to the active site of the E2 enzyme by trans-thiolation. In the third step, which is catalyzed by the E3 ligase, ubiquitin is transferred from the E2 enzyme to the amino group of the lysine in the target enzyme. Further, the deubiquitinases (DUBs) cleaves ubiquitin from the substrate proteins which is important for maintaining ubiquitin homeostasis as well as regulating ubiquitin mediated cellular processes [143]. Based on the structural composition of their E2 binding domain and mechanism of action, E3 ligases are classified into three categories namely the homologous to E6-AP carboxyl terminus (HECT) domain containing, the really interesting new gene (RING) finger domain containing and the U box E3 ligases. There are different types of ubiquitination that in turn lead to a wide range cellular processes [144]. Target proteins can be monoubiquitinated, that is, ubiquitinated by a single ubiquitin molecule at a single lysine residue of the substrate or multi-ubiquitinated, where many single ubiquitin molecules are conjugated at different lysine residues of the substrate (Figure 1.9). Since ubiquitin itself contains 7 lysine residues (Lys 6, Lys 11, Lys 27, Lys 29, Lys 33, Lys 48 and Lys 63), consecutive conjugation of ubiquitin molecules to these residues results in formation of ubiquitin chains of varying/various lengths leading to polyubiquitination. Further, polyubiquitination can be homotypic where sequential ubiquitination occurs at the same lysine residue of all the ubiquitin

molecules in the polyubiquitin chain or mixed linkage chains where different lysines of ubiquitin are used for sequential conjugation [145].

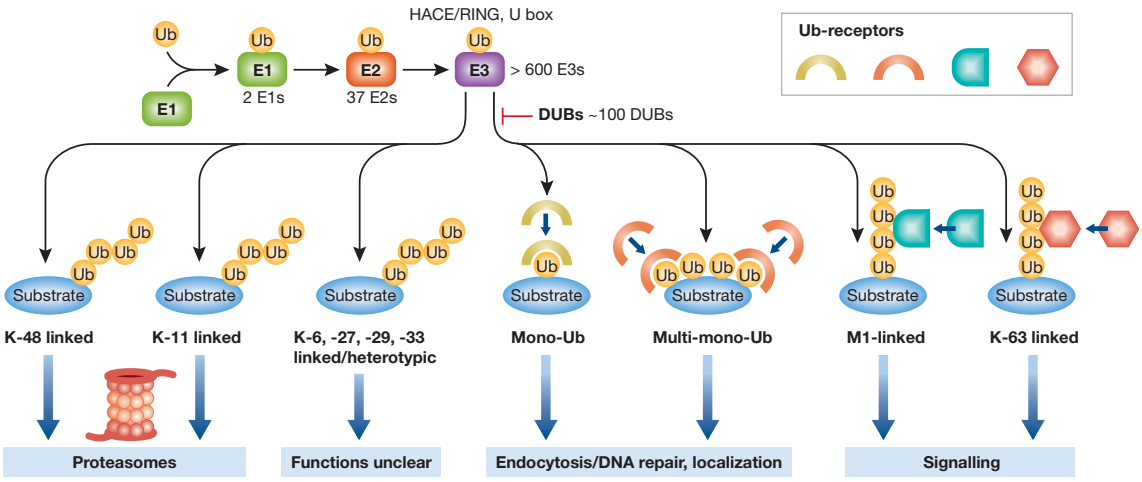

Figure 1.9: The Ubiquitination pathway. The figure illustrates the major steps involved in ubiquitination of proteins, the different types of ubiquitination and the known consequences of ubiquitination (from [1]).

Given their role in the regulation of cellular processes like gene transcription, cell-cycle and apoptosis which are very relevant mechanisms in the context of tumorigenesis, quiet expectedly, the ubiquitination pathway is deregulated in various human cancers [1]. A remarkable achievement in cancer therapy that came out from understanding the ubiquitin mediated proteasomal degradation of proteins is the use of bortezomib to target the proteasome itself in the treatment of multiple myeloma and mantle cell lymphoma [146]. Bortezomib mediated inhibition of the proteasome complex has been shown to induce various pro-apoptotic pathways, inhibit the NF-kB pathway, which in turn down regulates of various growth and survival factors [146, 147]. With respect to the players in the ubiquitination pathway, of particular importance are the E3 ligases and DUBs, as they impart target specificity to the ubiquitination mechanism. E3 ligases can be exploited therapeutically by either inhibiting the E3 ligases that target tumor-suppressor proteins for degradation or by promoting the activity of E3 ligases that targets oncoproteins for degradation, the latter being a more challenging approach. Deregulation of several E3 ligases and DUBs has been reported in various cancers, which has created platforms for novel therapeutic interventions (table 1.1, table 1.2). Ubiquitination mediated regulation of the tumor supressor p53 has been studied to a good extent: the RING type E3 ligase MDM2 is involved in the polyubiquitination and degradation of the tumor suppressor p53 [148]. Reports indicate the overexpression of MDM2 in cancers including non-small cell lung cancer, osteosarcoma and

glioblastoma, and associate high MDM2 expression to poor prognosis, increased likelihood of distant metastasis and dampened responses to therapeutic intervention [149-152]. Studies attribute MDM2 mediated oncogenicity to its role in p53 degradation. Activation of p53 by the inhibition of MDM2, which can in turn induce apoptosis and growth arrest, is a possible therapeutic strategy that can be employed for cancer treatment [153]. Small molecule inhibitors that either target the E3 ligase activity of MDM2 (HLI98) or disrupt the interaction of MDM2 with p53 have demonstrated promising anti-tumor activity in cancer cells [1, 154]. Further, in terms of role of DUBs in p53 regulation, it has been shown that downregulation of Herpes virus-associated ubiquitin-specific protease (HAUSP)/USP7, a DUB protein that directly stabilises p53, is associated with the reduced expression of p53 in NSCLC [155]. A study by Li et al. showed that although partial reduction of HAUSP indeed reduced p53 levels, a nearly complete ablation of HAUSP resulted in p53 stabilisation. This might be explained by the fact that HAUSP also stabilises MDM2 in a p53-dependent manner, hence playing a dynamic role in the regulation of functional p53 levels [156]. USP10 is another DUB protein that has been demonstrated to be stabilised upon DNA damage, which in turn regulates the nuclear translocation and activation of p53 [157]. Casitas B-lineage lymphoma (CBL), inhibitors of apoptosis (IAPs) and the stem cell factor (SCF) complex, a multi-subunit ubiquitin ligase complex are other well studied E3 ligases that have implications in cancer [158]. Many drugs that target these machineries are already in different phases of clinical trials [1].

Other studies reveal the role of DUBs in cancer. For example USP28 shows high expression in colon and breast carcinoma and has been demonstrated to deubiquitinate and stabilise the proto-oncogene c-MYC [159]. Therefore, inhibition of USP28 might be a potential approach in tumors where downregulation of MYC expression is a potential therapeutic strategy. Inactivation of A20, a negative regulator of NF-KB, has been implicated in the pathogenesis of B-cell lymphomas [160]. The list of E3 ligases and DUBs that may play a role in cancer has been increasing and with further understanding of their mechanism of fine-tuning the cellular processes, they hold potential as targets for therapeutic intervention (table 1.1).

Enzymes	Targets	Cancer association
E3 ligases		
MDM2 (HDM2)	p53	Over-expressed in multiple cancers including soft tissue sarcoma and lung cancer (Anderson et al, 1999; Lind et al, 2006; Menin et al, 2006)
CBL	RTKs, *e.g.* FLT3, c-Kit	c-Cbl point mutation (Cbl-R420Q) was detected in AML and myoproliferative disorders (Grand et al, 2009)
FBW7	Myc, Jun, cyclin E, KLF5, Notch1 and TGIF1, Mcl-1	Deleted or mutated in various cancers including T-ALL (Inuzuka et al, 2011; Wertz et al, 2011)
FBX011	Bcl-6	Deleted or inactivated in diffuse large B-cell lymphoma (Duan et al, 2011)
IAPs	Various substrates	Over-expressed in various cancers. C-IAP2 is associated with MALT-lymphoma (Dierlamm et al, 1999; Fulda & Vucic, 2011)
Deubiquitinases		
CYLD	Various substrates including RIP1 and Bcl3	Mutated in familial cylindromatosis, inactivated in skin cancers, hepatocellular and cervical carcinoma (Bignell et al, 2000; Massoumi et al, 2006; Strobel et al, 2002)
USP7	MDM2, PTEN, FOXO4 and others	Downregulation reported in non-small cell lung cancer (Masuya et al, 2006)
A20	RIP1, RIP2, TRAF2, TRAF6, UBCH5, NEMO and others	Frequent inactivation in B-cell lymphomas (Kato et al, 2009)
Usp9x	Mcl-1, β-catenin and others	Over-expressed in follicular lymphomas and diffuse large B-cell lymphomas, multiple myeloma (Schwickart et al, 2010)
Usp10	P53	Downregulated in renal cell carcinomas (Yuan et al, 2010)
DUB3	Cdc25A	Overexpression in breast cancers (Pereg et al, 2010)
Others		
PTEN	Promoted ubiquitylation of EGFR through formation of EGFR–CBL complex	Inactivated in various cancers (Trotman et al, 2007)

Table 1.1: E3 ligases and DUBs associated with cancer (from [1]

Drugs	Properties	Source	Stage of clinical development
Bortezomib	20S proteasome inhibitor	Millennium Pharmaceuticals	Approved for multiple myeloma, mantle cell lymphoma
MLN9708	Oral proteasome inhibitor	Millennium Pharmaceuticals	Phase I
Carfilzomib/PR-171	Proteasome inhibitor derived from epoxomycin	Onyx Pharmaceuticals	Phase I/II
NPI-0052	Irreversible 20S proteasome inhibitor	Nereus Pharmaceuticals	Phase I
ONYX 0912	Oral proteasome inhibitor	Onyx Pharmaceuticals	Phase I
RO5503781, RO5045337	Small molecule MDM2 antagonist	Hoffmann-La Roche	Phase I
MLN4924	NEDD8 inhibitor	Millenium Pharmaceuticals	Phase I
JNJ-26854165	MDM2 inhibitor	Johnson & Johnson Pharmaceutical Research & Development, LLC	Phase I
AT-406	IAP inhibitor	Ascenta Therapeutics	Phase I
LCL-161	IAP antagonist	Novartis Pharmaceuticals	Phase I

Table 1.2: Ubiquitin machinery targeting anti cancer drugs in clinical trials (adapted from [1]); Source: www.clinicaltrials.gov.

1.7 Aims of the project

The occurrence of thyroid cancer and associated mortality has been increasing over the past decades. PTC is the most common type of endocrine malignancy and accounts for about 80-85% cases of thyroid cancer [40]. The development of diagnostic tools like sonography and molecular analysis of the tumor has tremendously contributed to the treatment and prognosis of PTC. Surgery followed by RAI usually leads to good prognosis of PTC. But disease recurrences leading to distant metastasis, tumors that cannot be surgically removed and/or become resistant to RAI treatment are still major challenges in the treatment of PTC patients. Another important factor in the management of thyroid cancer is the appropriate risk stratification of the thyroid lesions. Precise risk stratification of the thyroid lesions is important, not only for the optimisation of treatment strategies which can in turn reduce disease recurrence, but also to prevent over treatment of the patients which is very important in preventing unnecessary adverse affects. A better understanding of the molecular basis of PTC is important in improving both diagnostic and treatment strategies for PTC.

The major aim of the project is the identification and validation of novel targets and molecular mechanisms that underlies the pathogenesis of PTC by employing next generation genomics and proteomics approaches. In order to achieve this, we chose a patient sample that does not harbour any of the known PTC oncogenic alterations (BRAFV600E and NRAS). The workflow of the study is outlined below:

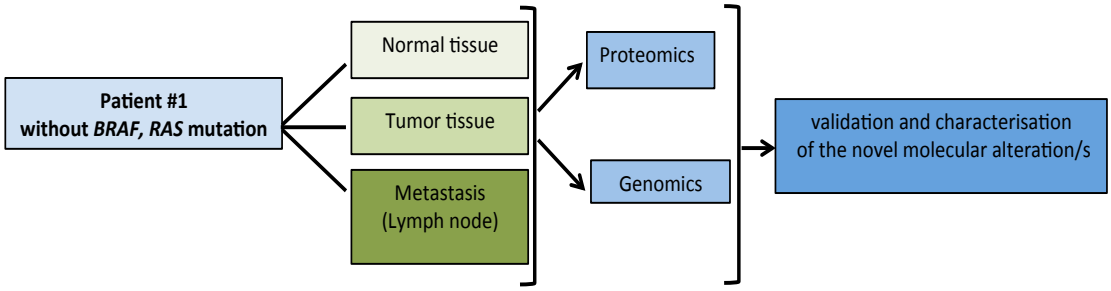

2 Materials and Methods

2.1 Patient tissue acquisition and omics analysis

2.1.1 Patient sample acquisition

Informed consent was obtained from the patients prior to surgery according to the recommendations of the institution's Ethics Committee. Tumor and normal tissue were harvested intraoperatively from a 35 years old male patient, and the patient is referred as the patient #1 in this study. The right thyroid lobe comprised mostly of tumor, while the left thyroid lobe consisted predominantly of normal tissue. Ultrasound examination revealed that the patient had multiple lateral lymph node metastases. The staging was: pT4b (5.3cm tumor), pN1b (17 metastases in 29 lymph nodes), M1 (pulmonary metastases), multifocal bilateral tumor, some with follicular pattern and also in the left lobe, capsular invasion but no invasion of adjacent structures. Routine Sanger sequencing was performed on the BRAF V600E, BRAF wild type and K, H, NRAS. Normal, tumor and metastasis (from lymph node) tissue were taken for further analysis.

2.1.2 Isolation of proteins, DNA and RNA from patient tissue

The tumor tissue was incubated in collagenase-D solution (1mg/ml) (11088866001, Roche) at 37˚C for 2 h and then transferred to a 6 well plate. The tissue was cut into smaller pieces with a scalpel and crushed using the thumb press of a syringe plunger. The tissue suspension was filtered by passing it through a 70 μm cell strainer (Easy Strainer 70 μm, 542070, VWR,), centrifuged at 1500 rpm for 5 min and subsequently washed with cold PBS. The cell pellet was re-suspended in lysing buffer (250 mM NaCl, 50 mM Tris-HCl pH 7.5, 10% Glycerine, 1% Triton X-100, 0.2 mM Na3VO4 and protease inhibitor cocktail (Calbiochem, cat.no.539131)) and kept on ice for 10 min. The cell suspension was sonicated (3 times 10 sec ,with 10 sec cooling intervals on ice between consecutive pulses, 50% amplitude), centrifuged at 13,000 rpm, 4˚C for 10

min and then the supernatant was subsequently used for mass spectrometric analysis. DNA and RNA was isolated using AllPrep DNA/RNA Mini Kit (80204, Qiagen) following manufacturer's protocol.

2.1.3 Sequencing

RNA-seq libraries were prepared using TruSeq RNA Sample Preparation v2 kit (Illumina). Exome capture was performed using the Agilent SureSelect Human All Exome kit (50 Mb). RNA-seq and Exome capture libraries were sequenced on HiSeq (Illumina) to generate 2 x 150 bp and 2 x 75 bp paired-end data respectively.

2.1.4 Exome data analysis

BWA software [161] set to default parameters was used to map sequencing short reads to UCSC human genome (GRCh37) using. Local realignment, duplicate removal and raw variant calling were performed as described previously [162] [161]. Strelka was used for somatic variant calling on tumor and its matched normal BAM file [163]. Known germline variants represented in the Exome Aggregation Consortium (ExAC) were filtered out [164].

2.1.5 RNA-seq data analysis

GSNAP was used to align RNA-seq reads to the human genome version NCBI GRCh37 [165]. Differential gene expression analysis performed using DESeq2 [166]. Fusions were identified using a computational pipeline called GSTRUCT-fusions [167].

2.1.6 Immunohistochemistry

H&E (Haemotoxylin and Eosin) staining of the patient tissue was performed on formalin fixed paraffin embedded sections using standard laboratory procedures. Antibodies were purchased from Dako (Thyroglobulin - M0781, calcitonin - A0576)

and immunohistochemistry was performed on paraffin sections by using the DAKO-EnVision FLEX-kit (Dako, Glostrup, Denmark). Staining was performed on an immunostainer (Autostainer +; Dako, Glostrup, Denkmark) according to the manufacturer´s instructions.

2.1.7 In-solution digestion

Four volumes of ice cold acetone was added to the protein lysates (prepared as mentioned in previous section (Isolation of proteins, DNA and RNA from patient tissue), vortexed and precipitated at -20°C overnight. Samples were centrifuged at 16,000 x g for 20 min at 4°C and the supernatant was discarded. Proteins were re-dissolved in 50 µl 6 M urea and 100 mM ammonium bicarbonate, pH 7.8. For reduction and alkylation of cysteines, 2.5 µl of 200 mM DTT in 100 mM Tris-HCl, pH 8 was added and the samples were incubated at 37°C for 1 h followed by addition of 7.5 µl 200 mM iodoacetamide for 1 h at room temperature in the dark. The alkylation reaction was quenched by adding 10 µl 200 mM DTT at 37°C for 1 h. Subsequently, the proteins were digested with 10 µg trypsin GOLD (Promega) for 16 h at 37°C. The digestion was stopped by adding 5 µl 50 % formic acid and the generated peptides were purified using OMIX C18, 10 µl (Agilent, Santa Clara), and dried using a Speed Vac concentrator (Concentrator Plus, Eppendorf).

2.1.8 Liquid chromatography-mass spectrometry (LC-MS)

The tryptic peptides were dissolved in 10 µl 0.1% formic acid/2% acetonitrile and 5 µl analyzed using an Ultimate 3000 RSLCnano-UHPLC system connected to a Q Exactive mass spectrometer (Thermo Fisher Scientific) equipped with a nano-electrospray ion source. For liquid chromatography separation, an Acclaim PepMap 100 column (C18, 2 µm beads, 100 Å, 75 µm inner diameter, 50 cm length) (Dionex, Sunnyvale CA, USA) was used. A flow rate of 300 nL/min was employed with a solvent gradient of 4-35% B in 180 min. Solvent A was 0.1% formic acid and solvent B was 0.1% formic acid/90% acetonitrile. The mass spectrometer was operated in the data-dependent mode to automatically switch between MS and MS/MS acquisition. Survey full scan MS spectra

(from m/z 400 to 2,000) were acquired with the resolution R = 70,000 at m/z 200, after accumulation to a target of 1e6. The maximum allowed ion accumulation times were 60 ms. The method used allowed sequential isolation of up to the ten most intense ions, depending on signal intensity (intensity threshold 1.7e4), for fragmentation using higher-energy collisional induced dissociation (HCD) at a target value of 1e5 charges, NCE 28, and a resolution R = 17,500. Target ions already selected for MS/MS were dynamically excluded for 30 sec. The isolation window was m/z = 2 without offset. For accurate mass measurements, the lock mass option was enabled in MS mode.

For label-free quantification analysis, raw data were imported into PEAKS v8.5 (Bioinfomatics Solutions Inc, Toronto, CA). Processed raw data were searched in PEAKS against the UniProt SwissProt database (Human, 20,279 proteins) assuming the digestion enzyme trypsin, at maximum two missed cleavage sites, parent ion tolerance of 10 ppm, fragment ion mass tolerance of 0.02 Da, carbamidomethylation of cysteines as fixed modification, and oxidation of methionines, deamidation of asparagine and glutamine residues as variable modifications. Label-free quantification was performed in the PEAKS software using a maximum mass difference of 15 ppm and a maximum retention time difference of 1.5 min for clustering and a 0.1% FDR threshold for peak annotation.

2.2 Molecular biology methods

2.2.1 Plasmids and constructs

pENTR221 TFG-RET, pENTR221 TFG-RETK14ER21ER22E and pENTR221 TFG-RETΔ97-124 were synthesized from Invitrogen and were cloned into expression plasmids pPHAGE C-TAP (FLAG and HA tagged), a kind gift from Prof. Dr. Christian Behrends, and Gateway™ pcDNA™-DEST40 Vector (His and V5 tagged) (12274015, ThermoFischer Scientific).

2.2.2 Quantitative RT-PCR

Total RNA was extracted using TRIzolTM reagent (15596018, Thermofisher scientific) according to manufacturer's protocol. Equal amounts of total RNA were used to

synthetize the corresponding cDNA using RevertAid reverse transcriptase cDNA Synthesis Kit (EP0441, Thermofisher scientific). To quantify gene expression levels, SYBR-Green (A25780, Thermofisher scientific) based qRT-PCR was performed using the StepOnePlus™ Real-Time PCR System (4376600). The normalized expression level of Huwe1, Usp7 and Usp9 was determined and three replicates were used for each determination.

2.2.3 Primer sequences:

Huwe1: Ref: NM_031407
for –TTGGACCGCTTCGATGGAATA, rev-TGAAGTTCAACACAGCCAAGAG
Usp9x: Ref: NM_001039590.2
for – GTGTCAGTTCGTCTTGCTCAGC, rev – GCTGTAACGACCCACATCCTGA
Usp7: Ref: NM_001286457.1
for – ACTTTGAGCCACAGCCCGGTAATA
rev - GCCTTGAACACACCAGCTTGGAAA
18s: Ref: NT_167214.1
for-AGAAACGGCTACCACATCCA, rev-CACCAGACTTGCCCTCCA
Rps13: Ref: NM_001017
for-CGAAAGCATCTTGAGAGGAACA, rev-TCGAGCCAAACGGTGAATC

2.3 Biochemical methods

2.3.1 SDS–PAGE and Western blot

For SDS–PAGE, cell lysates with equal amounts of total proteins were prepared in SDS-sample buffer (0.125 M Tris-HCl, pH 6.8, 4% SDS, 10% glycerol, 10 mM DTT and bromophenol blue) followed by boiling at 95˚C for 10 minutes. 20 µl of cell lysates from each sample were then loaded onto 4–15% mini-PROTEAN®TGX™ Precast protein gels (4561084, Biorad) or lab made polyacrylamide gels (comprising of 2 layers – resolving layer (7.5% or 12% gel, pH 8.8) and the stacking layer – (5% gel, pH 6.8). The proteins were then transferred to nitrocellulose blotting membranes (10600001, GE

Healthcare) by Western blotting. For immunoblot analysis, membranes were blocked with 5 % low-fat milk in phosphate-buffered saline for 30 min at room temperature and then incubated in primary antibodies (in 3% BSA, A7906, Sigma) overnight at 4°C. Subsequently, the membranes were washed in PBST, 3 times, 5 min per wash and incubated with horseradish peroxidase-coupled secondary antibodies for one hour at room temperature, followed by washes as previously stated. The antigen–antibody complexes were detected by enhanced chemiluminescence (Immobilon Western Chemiluminescent HRP Substrate, WBKLS0500, Millipore) using Biorad ChemiDoc™ Touch Imaging System (Biorad,). Quantification of Western blots was performed by densitometry using the quantification software provided by Biorad.

2.3.2 Antibodies

Anti-Phospho-Tyrosine (P-Tyr-1000) MultiMab™ (8954S,CST), anti- Myelin Basic Protein (MBP) (1344,CST), anti-V5 antibody (Invitrogen R960-25), anti-FLAG® M2-Peroxidase (A8592, Sigma), anti-phospho-RET (Y905) (3221S,CST), anti-RET (C31B4)(3223S, CST), anti-phospho-STAT3 (Ser727)(9134P,CST), anti-STAT3 (9129P, CST), anti-phospho-Akt (Thr308) (9275, CST), anti-Akt (C67E7) (4691, CST), anti-phospho MEK1/2 (9154, CST), anti-MEK1 antibody (2352,CST), anti-phospho-p44/42 MAPK (Thr202/Tyr204) (ERK1/2) (9101L, CST), anti- p44/42 MAPKinase (ERK1/2) (9102, CST), anti-M2-PK (S-1, Schebo Biotech), anti-histone H3 (4499S, CST) and Na-K ATPase (MA3-928, Thermo Scientific).

2.3.3 In vitro kinase assay

Two million HeLa cells were seeded in 10 cm cell culture plates and V5-tagged plasmids were transfected using PEI (as described in Cell culture and transient transfection) on the following day. Two days post transfection, cells were lysed in lysis buffer (250 mM NaCl, 50 mM Tris-HCl pH 7.5, 10% Glycerine, 1% Triton X-100 with protease inhibitor cocktail) and V5-tagged proteins were immunoprecipitated using V5 antibody immobilised to agarose-coupled protein A/G beads (Roche, cat. nos. 11-134-515-001 and 11-243-233-001) overnight. Protein bound beads were washed with the lysis buffer and used for in vitro kinase assay. Kinase assay was performed using

dephosphorylated myelin basic protein (MBP) (13-110, Merck) as substrate in 25 mM Tris (pH 7.5), 5 mM β-glycerophosphate, 2 mM DTT, 0.1 mM Na3VO4, 10 mM MgCl2 and 5mM ATP (Enzo, BML-EW9805-0100), 40µl final volume. The kinase assay mixture was incubated with the immunoprecipitated V5 tagged proteins for 30 min at 30˚C. The kinase reaction was terminated by adding 20 µl SDS-sample buffer (0.125 M Tris-HCl, pH 6.8, 4% SDS, 10% glycerol, 10 mM DTT and bromophenol blue) followed by boiling at 95˚C for 10 min. The samples were loaded onto 12% SDS-PAGE gel and subjected to immunoblotting analysis.

2.3.4 Protein Dimerisation experiments

RET Wild type, TFG-RET and TFG-RET mutant constructs in pPHAGE C-TAP (FLAG, HA tagged) and pcDNA3 Dest 40 (V5, His tagged) were co-transfected as indicated in the results in HeLa cells using PEI (see Cell culture and transient transfection). 48 h post transfection, cells were lysed in lysis buffer (250 mM NaCl, 50 mM Tris-HCl pH 7.5, 10% Glycerine, 1% Triton X-100 with protease inhibitor cocktail) and flag-tagged protein was immunoprecipitated using FLAG beads (ANTI-FLAG® M2 Affinity Gel, A2220-5ML, Sigma). The co-precipitation of V5-tagged proteins was tested by immunoblots.

Nthy-ori 3-1 cells stably expressing pPHAGE C-TAP RET wild type and pPHAGE C-TAP TFG-RET were seeded in 6 well cell culture plates. Upon becoming 70% confluent, cells were treated with DMSO (A3672.0250 Applichem) or Dithio-bismaleimidoethane (DTME) (0.2 mM, 1h), (22335,Thermo Scientific) or DTME followed by Dithiothreitol (DTT) (100 mM, 15 min). After thorough washes with PBS, cells were lysed in sample buffer (cells treated with only DTME were lysed in non-DTT containing sample buffer) and subjected to immunoblot analysis.

2.3.5 Gel filtration

HeLa cells were transiently transfected with TFG-RET, TFG-RET K14E.R22E.R23E and TFG-RET Δ97-124 in pcDNA3 Dest 40 (V5, His tagged). Cells (about 15 million cells per condition) were lysed 48 h post transfection in 500 µl lysis buffer (50 mM Tris

pH7.5, 150 mM NaCl, 10% Glycerol, protease inhibitor cocktail (539131, Calbiochem)) by sonication (50% Amplitude, five seconds, four cycles). Cell lysates were subjected to ultracentrifugation (30,000 x g for 1 h at 4 ˚C) and the supernatant (cytosolic fraction) was separated by size exclusion chromatography using an ÄKTA-Pure25 system equipped with two Superose-6 HR-10/30 columns (GE Healthcare, Freiburg, Germany) connected in series. The columns were pre-equilibrated with running buffer (50 mM Tris pH7.5, 150 mM NaCl buffer, filtered 0.22 µm). 500 µl of cytosolic fraction were injected and separated at a flow rate of 0.5 ml/min. Fractions of 500 µl were collected and subjected to immunoblot analysis. Molecular weight reference proteins (Gel Filtration Markers Kit (mwgf1000, Sigma-Aldrich) were separated under identical conditions and a calibration curve was obtained by plotting molecular weight (log scale) against elution volume.

2.3.6 Cellular fractionation assay

Nthy-ori 3-1 cells stably expressing pPHAGE C-TAP RET wild type and pPHAGE C-TAP TFG-RET were cultured in 10 cm dishes. 48 h post seeding, the growth media was removed from the culture dish and the cells were washed with cold PBS. Cells were subsequently lysed using buffers from ProteoExtract® Subcellular Proteome Extraction Kit (539790, Merck) according to manufacturer's protocol. Lysates collected were subjected to immunoblot analysis.

2.3.7 Cycloheximide-chase assay

NThy-ori-3-1 cells were transiently transfected using PEI (as described earlier) with different plasmids in 10 cm dishes. 24 h post transfection, cells were reseeded in 12-well plates. After 24 h, cycloheximide (100 µg/mL) was added to the cells and samples were collected in SDS-sample buffer at indicated time points and boiled at 95°C for 10 min. Cell lysates were subjected to immunoblot analysis.

2.3.8 Endogenous Ubiquitination experiments

Nthy-ori 3-1 cells stably expressing pPHAGE C-TAP TFG-RET (in 10 cm cell culture dishes, about 70% confluent) were treated with DMSO or with 20 μM BI-8622 or BI-8626 (synthesized by Syngene International limited) inhibitors for 2 h followed by treatment with 10 μM MG132 for 5 h at 37˚C. Following treatment, cells were lysed in lysis buffer and 250 μg protein was used to isolate ubiquitinated protein using UBIQAPTURE-Q® kit (BML-UW8995-0001, Enzo) according to manufacturer's protocol. Ubiquitination of proteins was determined by immunoblot analysis.

2.4 Cell biology methods

2.4.1 Cell culture

Nthy-ori 3-1 cells (90011609, Sigma) were cultured in RPMI-1640 medium supplemented with 10% heat inactivated FBS at 37°C in 5% carbon dioxide. HeLa (DSMZ) and 293T cells (a kind gift from Dr. Andreas Ernst) were cultured in DMEM supplemented with 10% heat inactivated FBS at 37°C in 5% carbon dioxide.

2.4.2 Transient transfections

Two million cells were seeded in 10 cm cell culture plates and the cells were transiently transfected on the following day. 5 μg plasmid and 27 μl of 10 mM polyethylenimine was mixed in 500 μl of PBS and incubated for 15 min at room temperature. After incubation, the transfection mixture was added drop-wise to cells cultured in 10 cm plates. Experiments were carried out 48 h post transfection.

2.4.3 Lentivirus production and stable cell line generation

For the production of lentiviruses, we adapted the protocol from Jiang W et al. [168]. 293T cells cultured in 10 cm culture dishes (4 dishes for each transfection) were transfected with pPHAGE C-TAP (empty vector) or pPHAGE_CMV_C_FLAG_HA_IRES_Puro (as well as the TFG-RET mutants) together with the pLenti package (HDM-VSV-G; HDM-tatlb; HDM-Hgprn2 (gag-pol); RC-CMV- Rev1b). Two days later, the virus-containing medium was collected and subsequently pre-cleaned by centrifugation for 5 minutes at 3000 g and a 0.45 µm filtration. The filtrate was overlaid on a sucrose buffer (50mM Tris HCl, pH 7.4, 100mM NaCl, 0.5mM ethylenediaminetetraacetic) at a 4:1 v/v ratio and centrifuged at 10,000 g for 4 h at 4°C. After centrifugation, the supernatant was carefully discarded and the pellet was re-suspended in 800 µl PBS for overnight recovery in 4°C.
For the generation of stable cell lines, 100 µl of the suspension was subsequently added to Nthy-ori 3-1 cells in presence of 8 µg/ml of polybrene. After 24 h, cells were subjected to puromycin selection by addition of puromycin to the cell culture media (2.5 µg/ml puromycin).

2.5 Phenotypic studies

2.5.1 MTT assay

MTT assay assay was performed by employing the Cell Proliferation Kit I, (11465007001, Roche). Nthy-ori 3-1 cells stably expressing pPHAGE C-TAP empty vector and pPHAGE C-TAP TFG-RET were seeded in 96-well cell culture plate in 100 µl of complete growth medium. (10,000 cells/well, triplicates per condition). 10 µl of MTT solution was added 2 h, 48 h and 72 h post seeding and incubated in CO_2 incubator for 2-4 h. After incubation, 100 µl of solubilisation buffer was added to each well and incubated overnight in CO_2 incubator. Absorbance of the solubilized MTT was measured by absorbance plate reader (O.D.570). Absorbance readings of 48 and 72 h time points were normalised to the respective absorbance measured at 2 h.

2.5.2 Soft agar colony formation assay

1.5 % agarose solution was mixed with 2X growth medium (with 20% FCS, 2X inhibitor) to get a final mixture with 0.75% agarose in 1X growth medium (bottom agar medium). 1.5ml of this bottom agar medium was added per well in a 6-well plate and incubated at room temperature for at least 10 min to solidify agarose. Nthy-ori 3-1 cells stably expressing pPHAGE C-TAP empty vector and pPHAGE C-TAP TFG-RET were diluted in 2X growth medium (with 20 % FCS, 2X inhibitors) and mixed with 0.9 % agarose solution to a final concentration of 0.45% agarose. 1.5 ml of this cell suspension was added to the bottom agarose layer (20,000 cells/condition). The cells seeded in soft agar were cultured for 2 to 4 weeks with addition of 100 µl of complete medium (with inhibitor) twice weekly. The colonies were stained with 0.02% crystal violet solution by gentle agitation at room temperature for about 30 minutes followed by washes with water. The images were taken with a ChemiDoc Touch (Bio-Rad) imaging System and the number of colonies was counted by image J software.

2.5.3 Imaging studies

NThy-ori-3-1 cells stably expressing flag tagged pPHAGE C-TAP TFG-RET or pPHAGE C-TAP RET were seeded onto glass coverslips (15 mm). The cells were transiently transfected with EGFP-C1 Lck-GFP (61099, addgene) using PEI (as described in Cell culture and transient transfection). 48 h later, the cells were fixed using 4 % PFA for 10 min after media removal and 2 PBS washes. The cells were permeabilised using 0.1% Triton X100 (3 min, room temperature). After 2 subsequent washes with PBS, the cells were blocked with 1% BSA for 30 mins at room temperature. The cells were then stained for TFG-RET/RET using anti-FLAG® M2-Peroxidase (A8592, Sigma, 1:500 dilution in 1 % BSA) for 1 h at room temperature. The cells were then washed with PBS and stained with anti –mouse Cy3 antibody (1:100 dilution in 1% BSA) along with Hoechst (2.5 µg/ml in 1% BSA) for 30 min (in dark, room temperature). The cells were washed with PBS and mounted on glass slides with Mowiol (+DABCO). Cells were imaged using a Leica SP8 confocal microscope (63X, oil immersion objective, Cy3 excitation at 552nm, GFP excitation 488nm).

3 Results

3.1 Identification of novel molecular alterations in PTC

3.1.1 Patient sample acquisition and immunohistochemical analysis

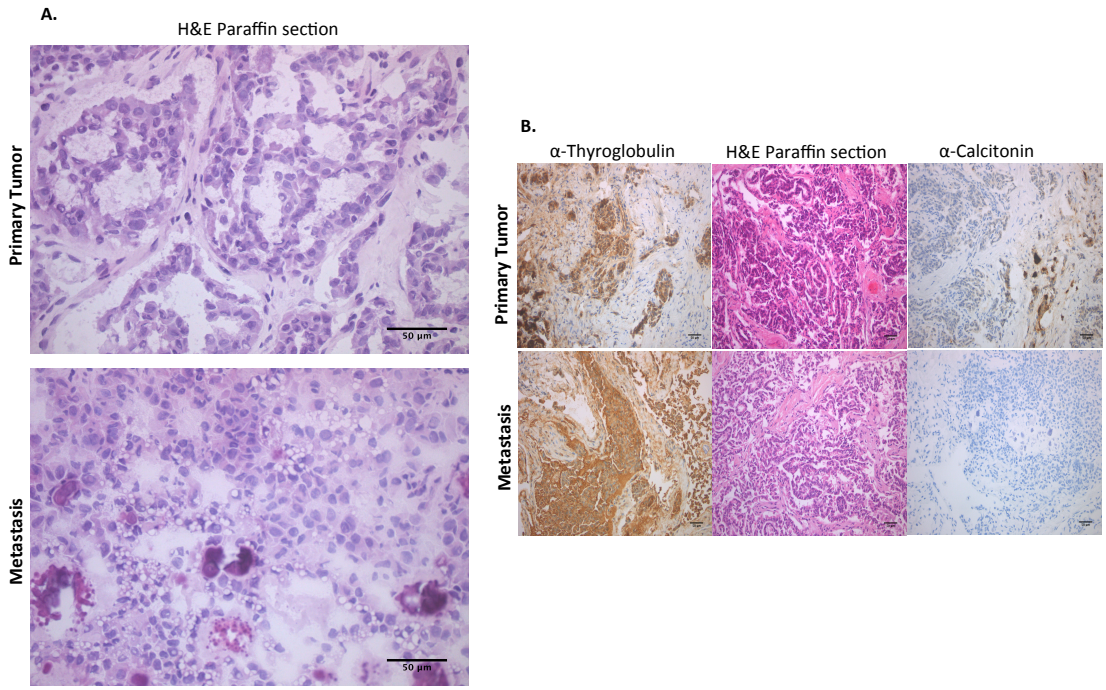

Figure 3.1: PTC with follicular growth - immunohistochemical analysis. (A) H&E staining of paraffin fixed primary tumor and metastatic tissue revealed distinct nuclear features characteristic of PTC (scale bar, 50 µm). **(B)** Primary and metastasis tissue were stained for thyroglobulin and calcitonin (scale bar, 50 µm).

With an aim to identify novel molecular events driving PTCs, we selected a small cohort of patients that have undergone partial thyroidectomy for genomics and proteomics analysis. A 35-year-old male patient (referred to as patient#1 in this study) was presented with a thyroid tumor, whose right thyroid lobe comprised mostly of tumor, while the left thyroid lobe predominantly was normal tissue. Ultrasound evaluation revealed the presence of multiple lateral lymph node metastases. The staging of the tumor was: pT4b (5.3 cm tumor), pN1b (17 metastases in 29 lymph nodes analyzed), M1 (pulmonary metastases), multifocal bilateral tumor, some with follicular pattern and also in the left lobe, capsular invasion but no invasion of adjacent structures.

Normal (thyroid), tumor (thyroid) and metastatic (lymph node) tissue were collected from the patient intra-operatively after obtaining informed consent from the patient prior to surgery. Routine Sanger sequencing for BRAF V600E, K-RAS, H-RAS and N-RAS (exon 2, 3 and 4) was carried out, which revealed the absence of any common BRAF and RAS mutations in the tumor. This observation was further confirmed by next-generation RNA sequencing of the patient sample (discussed later). Formalin fixed paraffin embedded sections of primary tumor and metastatic tissue was subjected to immunohistochemical analysis (Figure 3.1). Haemotoxylin and Eosin (H & E) staining revealed the distinct nuclear morphology of the cells indicative of PTC and it also showed the follicular nature of the tumor tissue. Both primary and metastatic tissue stained positive for thyroglobulin, implying the follicular cell origin of the tumor, as c-cells derived from the tumor would not be positive for thyroglobulin. The metastatic tissue was negative for calcitonin staining, a marker for c-cells, although few cells in the primary tumor were calcitonin positive. This may be indicative of c-cell hyperplasia. Also, the tumor tissue revealed calcitonin calcification, which is also typical of PTC. Together, these immunohistological observations suggest that the tumor is a PTC with follicular growth.

3.1.2 Identification of a novel RET fusion

Our next aim was the identification of genomic alterations in the patient-derived tissue. For this, we employed both exome sequencing and RNA-sequencing of normal, tumour and metastasis samples. We performed exome data analysis of normal vs tumor and tumor vs metastasis that revealed the occurrence of a total of 14 protein-altering mutations none of which were well-characterised oncogenic mutations (Figure 3.2A, 3.2B). 6 of these mutations were shared between the tumor and metastasis samples (Table 3.1). Further, we examined the RNA sequencing data to look for other genomic alterations. RNA sequencing did not identify any BRAF or RAS mutations, hence confirming the previous results obtained by Sanger sequencing.

RNA-sequencing based fusion analysis revealed the presence of a novel inter-chromosomal fusion between exon 4 of TFG located on chromosome 3 and exon 11 of RET located on chromosome 10 (Figure 3.2C). We also looked into the genes that exhibit significant differential expression in the tumor samples. Our analysis showed the

differential expression of 244 expressed genes, of which RET kinase was significantly overexpressed in the tumor sample, compared to the normal (Figure 3.2D). By comparing the Reads Per Kilobase Million (RPKM) values of RET, we found that it was significantly up regulated in metastatic (14.7) and tumor samples (10.2) as compared to adjacent normal tissue (0.3) (Figure 3.2E).

Table 3.1: List of mutations identified in tumor and metastasis tissue.

Gene_Name	# Samples	Samples	Polyphen2_pred	(COSMIC_ID)	Unique concatenate with count(HGVS_p)	Mean (PhyloP100way_vertebrate)	Kinase type	GPCR Family
ADRA1D	2	M, T	D		p.Arg282Cys(2)	2.866		Adrenoceptors
MAP2K2	1	M	B		p.Gln391His(1)	4.539	Protein Kinase	
ACCSL	1	T	D		p.Pro382Ser(1)	6.356		
ALCAM	2	M, T	B,B, D,D		p.Arg304Lys(2), p.Arg304Ser(2), p.Ser324Pro(2)	1.566333333		
ATP10A	1	T	B		p.Met1280Thr(1)	8.977		
MUC3A	1	T	?		p.Thr2064Asn(1)			
MYC	1	T	B		p.Ser21Asn(1)	1.778		
OR2L8	1	T	B	COSM226497	p.Leu132Pro(1)	-4.646		
OR5R1	2	M, T	D		p.Leu101Gln(2)	2.593		
PLEKHA5	2	M, T	?		p.Gln412fs(2)			
PPP1CC	1	T	B, D		p.Ile244Leu(1), p.Phe227Ser(1)	8.537		
RP1L1	1	T	B	COSM3762979	p.Glu1343Lys(1)	2.372		
TG	2	M, T	?		p.Thr1432_Ser1433del(2)			
ZFP42	2	M, T	D		p.Lys231Asn(2)	-0.012		

A

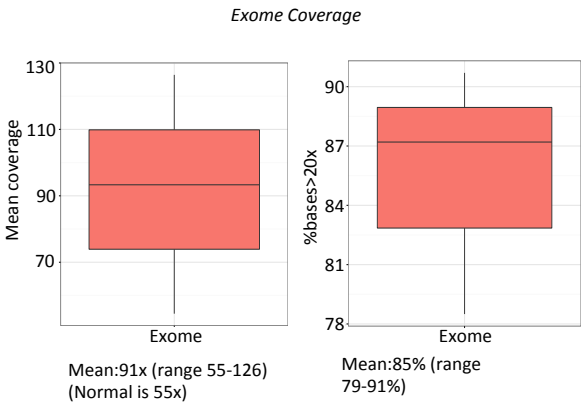

B

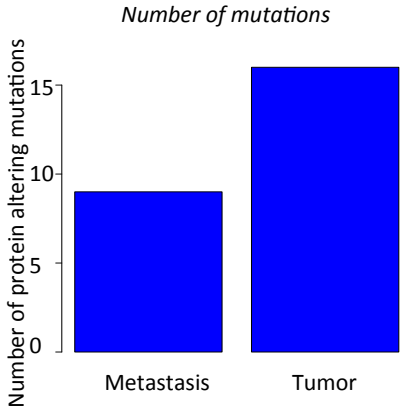

C

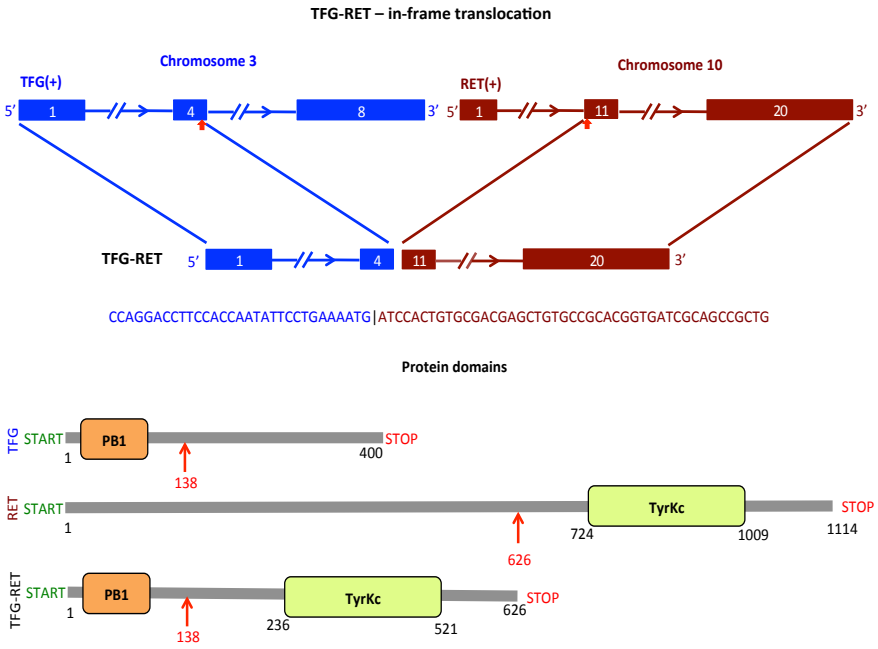

D

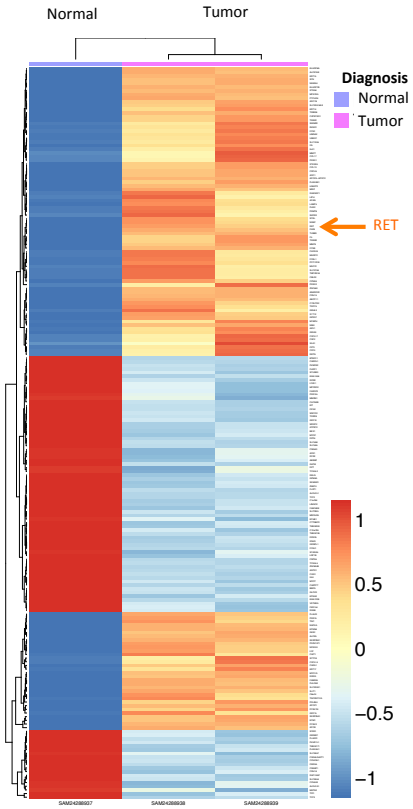

E

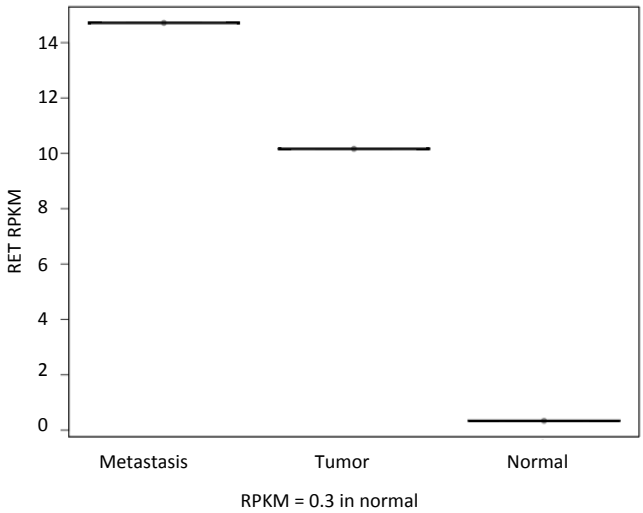

Figure 3.2: Exome analysis. (A) Exome analysis of patient#1 tissue. **(B)** Number of protein altering mutations detected in exome analysis of the patient. **(C)** Schematic representation of TFG-RET fusion protein. The N-terminal of TFG and C-terminal of RET forms a 626 amino acid containing fusion product. **(D)** Heat map of the exome analysis of patient tissue. **(E)** RPKM values for RET expression obtained from RNA-seq analysis of normal, tumor and metastasis patient tissue.

3.2 Functional and molecular characterisation of TFG-RET

3.2.1 TFG-RET expression upregulates oncogenic cell signalling and proliferation

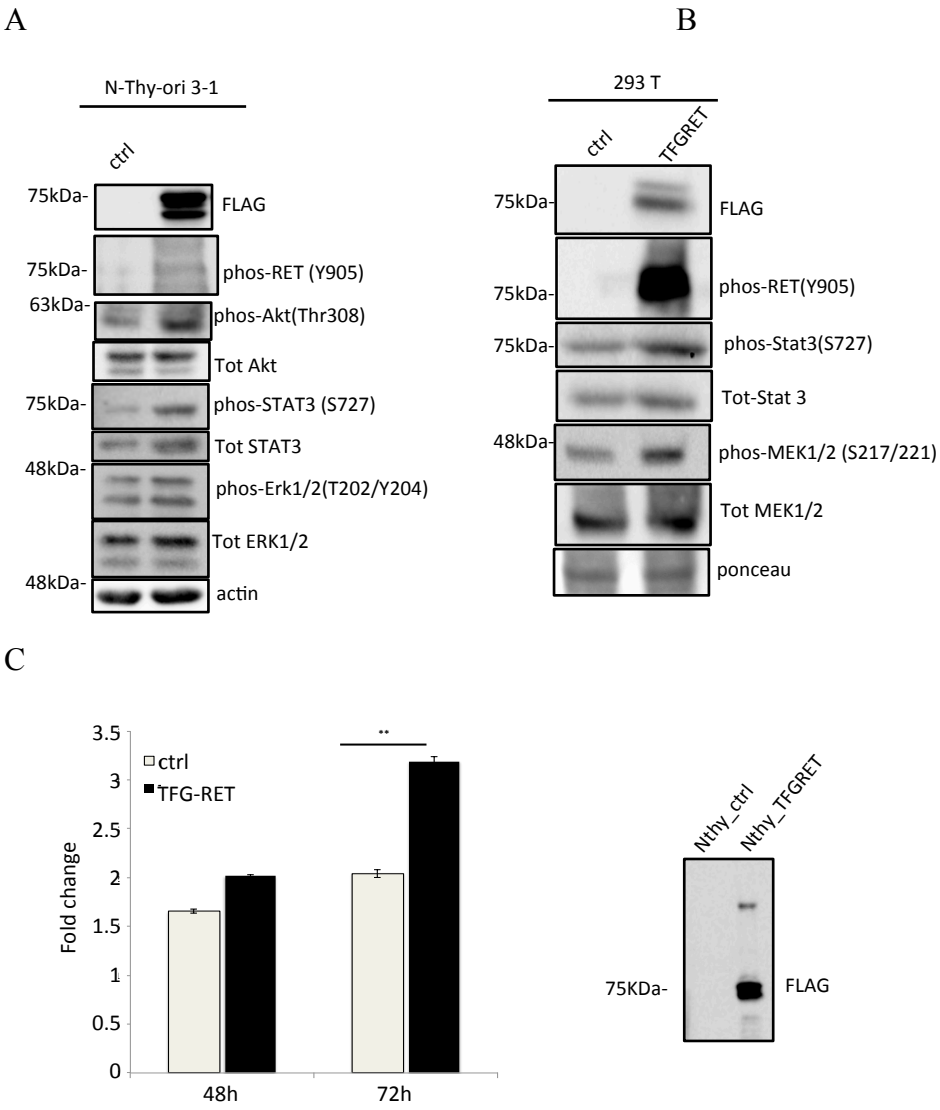

Figure 3.3: TFG-RET expression upregulates oncogenic cell signalling and proliferation. (A) Western blots for indicated proteins (phos, phosphorylated) from cell lysates obtained from N-Thy-Ori 3-1 cells stably transfected or 293T **(B)** cells transiently transfected with FLAG tagged TFG-RET fusion protein or with empty vector control (pHAGE C-TAP). **(C)** To analyze cellular proliferation, N-Thy-Ori 3-1 cells stably transfected with FLAG tagged TFG-RET (Nthy TFG-RET) or with empty vector control (Nthy ctrl) cells (expression shown on the right) were seeded in 96 well plates and subjected to an MTT assay. TFG-RET expression lead to an increase in cell proliferation after 72 hours (n = 3, error bars = standard error, p = 0.0003; paired t-test, two tailed distribution).

In order to functionally characterize the novel fusion protein, we first established stable expression of TFG-RET in the immortalised thyroid cell line, NThy-ori-3-1 (NThy TFG-RET cells), as well as NThy-ori-3-1 cells stably expressing the empty vector (NThy ctrl) as described in the methods. Immunoblot analysis showed that TFG-RET expression lead to the upregulation of various cancer-associated events like phosphorylation of Akt (T308), STAT3 (S727) and ERK1/2 (T202/Y204) (Figure 3.3A). Importantly, TFG-RET also exhibited phosphorylation of RET (Y905). The tyrosine residue 905 is an autophosphorylation site of RET which has been shown to be important for the transforming activity of RET [114, 169]. Further, immunoblot analysis also showed that transient expression of TFG-RET in 293T cells induced phosphorylation of RET (Y905) as well as up regulation of some cancer related phosphorylation events (Figure 3.3B). Next, we checked the effect of TFG-RET expression on cell proliferation. An MTT-based cell proliferation assay implied that NThy TFG-RET exhibited significantly higher cell proliferation (72 hours post cell seeding) as compared to empty vector carrying NThy-ori-3-1 cells (NThy ctrl) (Figure 3.3C).

3.2.2 TFG-RET localises in the cytoplasm

As RET fusion proteins exhibit cytoplasmic localisation following the loss of transmembrane domain of RET in its fusion product, we conducted subcellular localisation studies to check if this holds true for TFG-RET as well. The cytosolic, plasma membrane and nuclear fractions were collected using cell fractionation as described in materials and methods. We used specific cytosolic, plasma membrane and nuclear markers (M2-PK, Na-K ATPase and Histone, respectively) to confirm the proper fractionation of cell lysates by immunoblot analysis. The immunoblot analysis showed that unlike wild type RET (WT-RET) protein, which was present largely in the plasma membrane fraction, TFG-RET was present in the cytosolic fraction as well. Both RET and TFG-RET were detected in the nuclear fraction (Figure 3.4A). Further, we performed confocal imaging studies, which also revealed similar observations (Figure 3.4B)

A

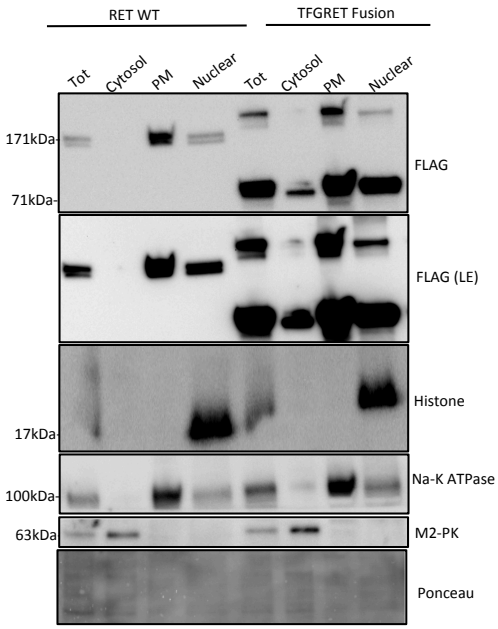

B

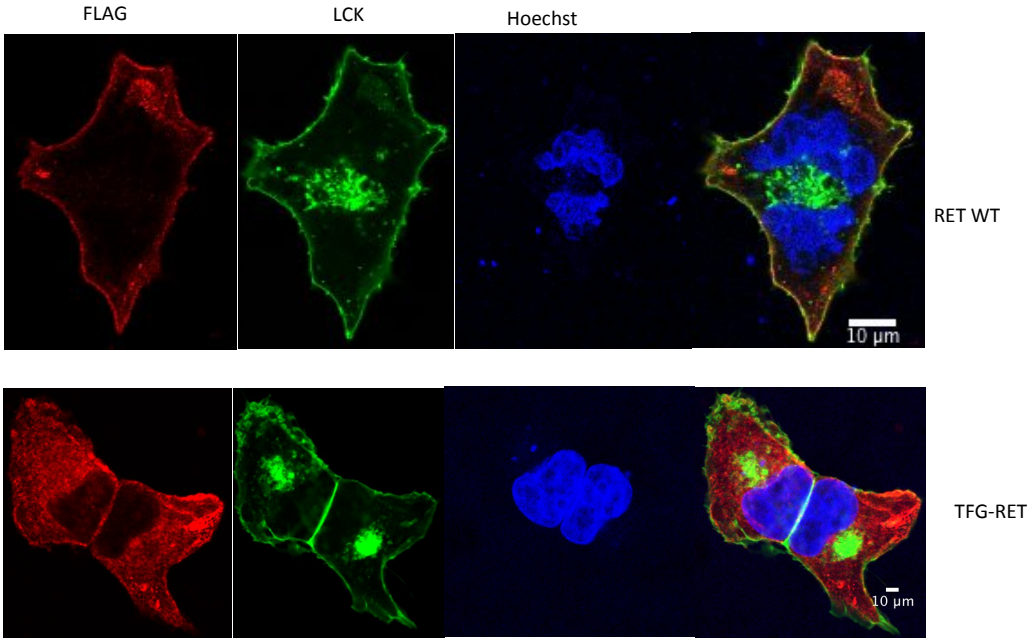

Figure 3.4: TFG-RET localizes in the cytoplasm. (A) Cellular fractions obtained from Nthy TFG-RET and Nthy RET WT cells were subjected to immunoblot analysis for TFG-RET (FLAG), RET WT (FLAG) and indicated markers for each of the cellular fractions. TFG-RET was detected in the cytosolic fraction. **(B)** Representative images of Nthy TFG-RET cells or Nthy RET WT grown on glass. While TFG-RET (FLAG tag, red) exhibited cytosolic distribution, RET (FLAG tag, red) expression was not seen in the cytoplasm. GFP-LCK (green) marks the plasma membrane (also, pericentrosome) Hoechst (nucleus).

3.2.3 TFG-RET can induce oncogenic transformation of Nthy-ori-3-1 cells

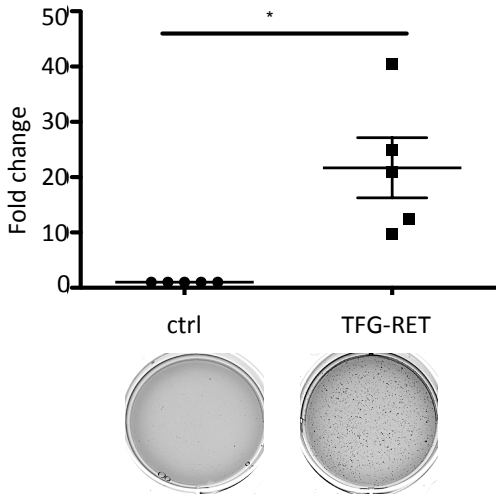

Figure 3.5: TFG-RET expression transforms Nthy-ori-3-1cells - Soft agar colony formation assay. Nthy TFG-RET cells and Nthy ctrl cells were cultured in soft agar. After 2 weeks, the colonies were stained with crystal violet. TFG-RET could transform Nthy-ori-3-1 cells. (Paired t test, two tailed, n=3, $P<0.05$.

We next investigated the transforming ability of TFG-RET by performing soft agar colony formation assays using NThy-ctrl and NThy-TFG-RET cells. Cells were seeded in soft agar media and were analysed for colony formation 14 days post seeding. We observed that stable expression of TFG-RET in the immortalised thyroid cell line induced colony formation, while NThy ctrl cells only formed very few colonies (Figure 3.5). Thus, expression of the TFG-RET fusion protein in the tested immortalized thyroid cancer cell line lead to anchorage independent growth (a classical marker of transformation) of these cells, indicating the ability of TFG-RET to induce oncogenic transformation.

Together, these data (section 1.2.1-1.2.3) show that expression of TFG-RET leads to the increased phosphorylation, hence activation of many cancer associated proteins. TFG-RET expression also resulted in the increased cell proliferation and transformation of NThy Ori-3 cells.

3.2.4 TFG-RET exhibits kinase activity

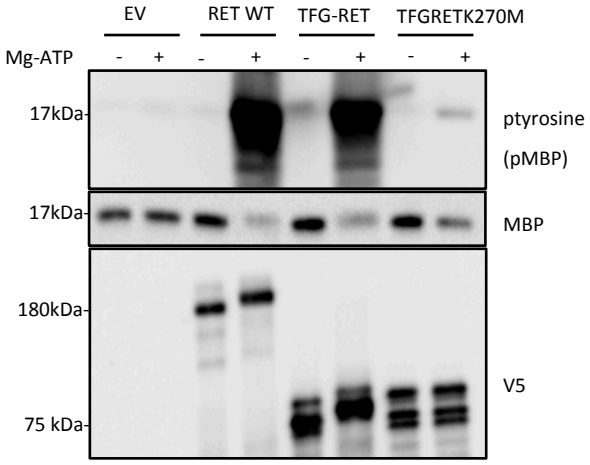

Figure 3.6: TFG-RET exhibits kinase activity (in vitro kinase assay). HeLa cells were transiently transfected with V5 tagged WT RET, TFG-RET, TFG-RET.K270M (kinase dead TFG-RET) along with empty vector (EV). Two days post transfection, cells were lysed and subjected to immunoprecipitation using anti-V5 antibody. After subsequent washes, the immunoprecipitated proteins were used for in vitro kinase assay, using MBP protein as substrate. TFG-RET phosphorylates MBP thus exhibiting kinase activity like RET kinase and this kinase activity was abrogated in the TFG-RET kinase dead mutant (phos, phosphorylated).

In order to investigate if the fusion protein exhibited enhanced kinase activity, which would in turn imply its probable role as a kinase in the phosphorylation and activation of other proteins, we conducted an in vitro kinase assay. Wild type RET and a kinase dead mutant of TFG-RET (TFG-RETK270M) were used as positive and negative controls, respectively. V5 tagged WT-RET, TFG-RET and TFG-RETK270M along with empty vector control were transiently expressed in HeLa cells and subsequently immunoprecipitated using V5 antibody and used for an in vitro kinase assay. The assay was performed using myelin-binding protein (MBP) as substrate, either in the presence or absence of Mg-ATP. The immunoblot observations using anti-phospho tyrosine antibody showed that in the presence of Mg-ATP, MBP was indeed phosphorylated by TFG-RET, while TFG-RETK270M lacked the ability to do so (Figure 3.6).

3.2.5 TFG-RET can form dimers

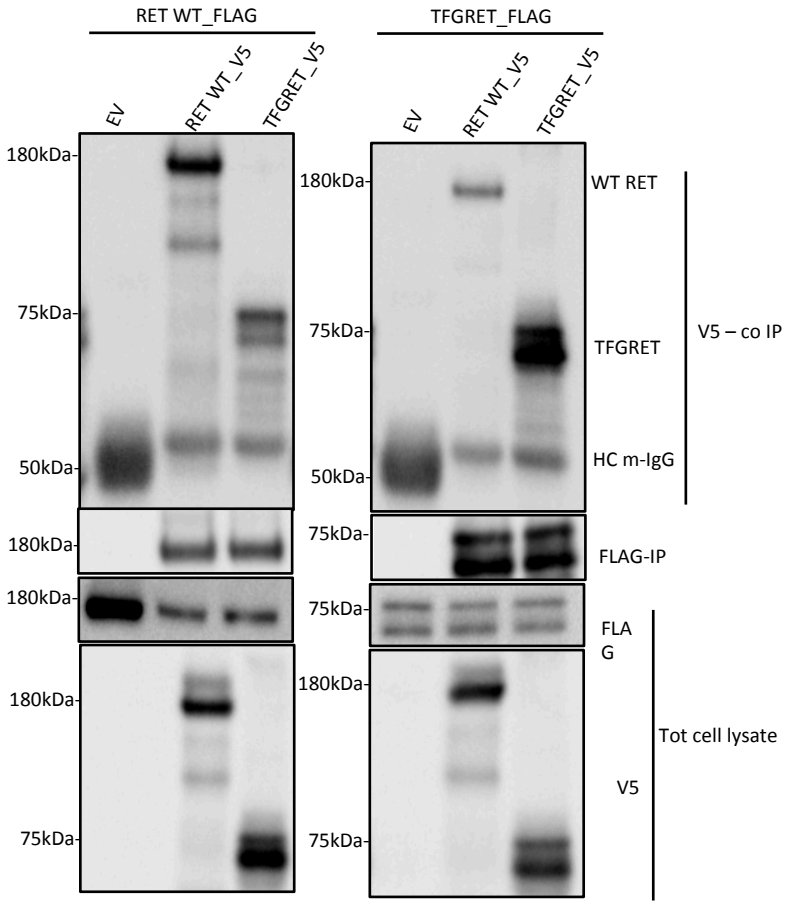

Figure 3.7: TFG-RET can form dimers – co-precipitation experiments. HeLa cells were co-transfected with FLAG-tagged and V5-tagged WT RET and TFG-RET as indicated. The cells were subjected to FLAG immunoprecipitation 48 hours post transfection. Lysates were analyzed by western blotting. WT RET co-immunoprecipitated with WT RET (V5) and also with TFG-RET (V5) (left panel), similarly, TFG-RET also co-immunoprecipitated with both RET WT (V5) and TFG-RET (V5), indicating that TFG-RET can form dimers with themselves, as well as with RET WT. Cells transfected with the empty vector (EV) were included as controls.

Since dimerisation is an important event in the activation of protein kinases, we next investigated the ability of TFG-RET to form dimers with themselves (homodimers) as well as with RET WT (heterodimers). For this, HeLa cells were transiently transfected with RET WT and TFG-RET with FLAG or V5 tags, viz., FLAG-RET WT + V5-RET WT, FLAG-RET WT + V5-TFG-RET, FLAG-TFG-RET + V5-RET WT, FLAG-TFG-RET + V5-TFG-RET. FLAG-tagged RET WT and TFG-RET were immunoprecipitated and were checked for co-precipitating V5-tagged proteins (Figure 3.7A). As expected,

we saw that V5-RET WT co-precipitated with FLAG-RET WT. We also detected the co-precipitation of V5-TFG-RET with FLAG-RET WT. Similarly, we also observed that both V5-RET and V5-TFG-RET co-precipitated with FLAG-RET WT and FLAG-TFG-RET. Together, these data suggest that TFG-RET has the ability to interact with TFG-RET, as well as RET-WT to form homo-dimers and heterodimers.

3.2.6 TFG-RET can form oligomeric complexes in vivo

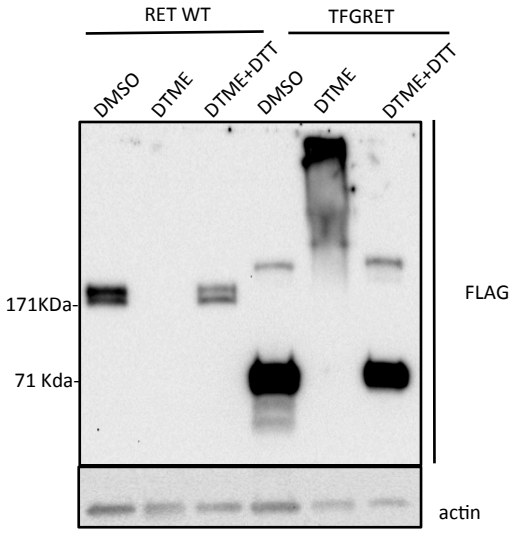

Figure 3.8: TFG-RET can form heteromers – DTME cross-linking studies. Nthy TFG-RET and Nthy-RET WT cells were treated with i) DTME (0.2 mM, 1 hour) or ii) DTME followed by (DTT) (100 mM, 15 minutes) along with DMSO control. After thorough washes with PBS, cells were lysed in sample buffer (cells treated with only DTME were lysed in non-DTT containing sample buffer) and subjected to immunoblot analysis. Upon chemical crosslinking with DTME, similar to WT RET, TFG-RET also formed high molecular weight heteromeric complexes (lane 2 (band not seen due to high molecular weight of the complex) and lane 5, respectively) and these complexes were disrupted upon reduction with DTT (lane 3 and 6).

Although dimerisation is an important event in the activation of kinases, it is not the only requirement in the activation of these proteins. Formation of heteromeric complexes with other proteins is also important in the functional regulation of kinases. In order to investigate the ability of TFG-RET to form heteromeric complexes, we carried out crosslinking experiments using the maleimide cross-linker dithio-bis-maleimidoethane (DTME). NThy TFG-RET cells were treated with DMSO, DTME or DTME followed by DTT (reducing agent). NThy RET WT cells were also included, as RET WT is known to form heteromeric complexes. Immunoblot analysis revealed that

DTME crosslinking resulted in the formation of high molecular weight complexes: The TFG-RET band around 75kDa was no longer visible, since it was cross-linked with interacting proteins, leading to the formation of a high molecular weight complex (the cross-linked TFG-RET was not detected due to the limitation in the detection of larger oligomers with the employed gels). Addition of DTT disrupted these complexes, as seen by the re-emergence of TFG-RET around 75kDa. As expected, complex formation upon cross-linking was also observed in RET WT (Figure 3.8).

3.3 Characterisation of the role of functional domains of TFG in TFG-RET

3.3.1 The PB1 domain and coiled-coil domain of TFG play a role in RET phosphorylation

The N-terminus of TFG has two putative functional domains – the Phox and Bem 1p (PB1) domain (position 10-91) and a coiled-coil domain (CC domain) (position 97-124) (Figure 3.9A). We next focused our investigation on the characterisation of the role of these domains of the TFG in regulating the kinase activity of TFG-RET. A structural comparison of TFG and PB1 domain containing p62 protein is shown in Figure 3.9B. We generated point mutations in the PB1 domain by replacing the positively charged lysine in position 14, and arginine in positions 22 and 23 with the negatively charged glutamic acid, as indicated in Figure 3.9C. HeLa cells were transiently transfected with TFG-RET.K14E, TFG-RET.R22E, TFG-RET.R23E as well as a triple mutant TFG-RET.K14E.R22E.R23E (in pcDNA3 Dest 40 (V5, His tagged)) and immunoblot analysis was performed to investigate the effect of these mutations in the phosphorylation of RET. The results indicated that expression of the triple mutant construct (TFG-RET.K14E.R22E.R23E) resulted in the decreased phosphorylation of RET (Y905), indicating that this may possibly have functional consequences (Figure 3.9D).

A

B

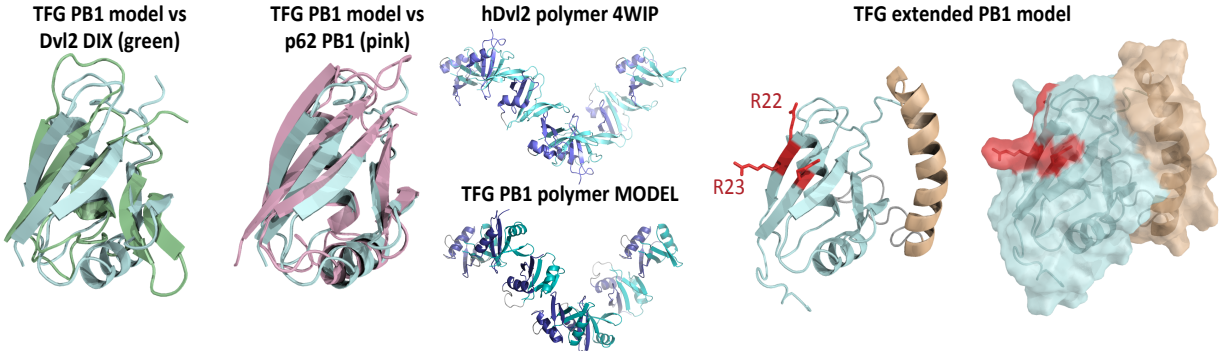

C

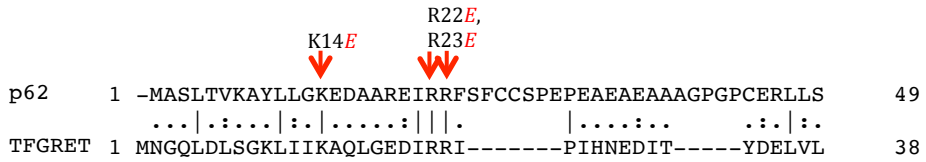

D

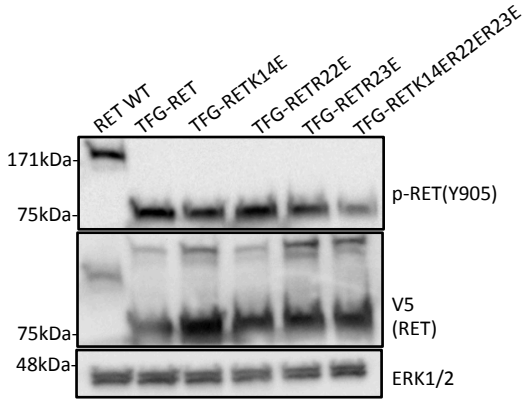

Figure 3.9: Mutations in PB1 domain reduces RET phosphorylation. (A) Schematic representation of human TFG protein (from [170]). **(B)**. Structural comparison of TFG PB1 with PB1 domains of p62, Dvl2 DIX. **(C)** Point mutations to create PB1 domain mutant TFG-RET. HeLa cells were transiently transfected with RET WT, TFG-RET, and indicated point mutations (in pcDNA DEST40 Vector (His and V5 tagged)). **(D)** 48 hours post transfection, cells were lysed and the cell lysates were subjected to immunoblot analysis, which suggested that the TFG-RET. K14E.R22E.R23E mutant showed lesser phosphorylation of RET (Y905).

Further, in order to investigate the role of the CC domain of TFG-RET, we created mutant TFG-RET, wherein the CC domain was deleted (TFG-RETΔ97-124) (Figure 3.10 A). We then transiently transfected NThy ori-3-1 cells with TFG-RET and TFG-RETΔ97-124 construct (in pcDNA3 Dest 40 (V5, His tagged)) and checked the status of RET (Y905) phosphorylation. Immunoblot analysis revealed that TFG-RETΔ97-124 exhibited lesser phosphorylation when compared to TFG-RET, thus implying that deletion of the CC domain also may have functional consequences (Figure 3.10 B).

A

1 MNGQLDLSGK LIIKAQLGED IRRIPIHNED ITYDELVLMM QRVFRGKLLS NDEVTIKYKD EDGDLITIFD SSDLSFAIQC
81 SRILKLTLFV NGQPRP*LESS QVKYLRRELI ELRNKVNRLL DSLE*PPGEPG PSTNIPENDP LCDELCRTVI AAAVLFSFIV
161 SVLLSAFCIH CYHKFAHKPP ISSAEMTFRR PAQAFPVSYS SSGARRPSLD SMENQVSVDA FKILEDPKWE FPRKNLVLGK
241 TLGEGEFGKV VKATAFHLKG RAGYTTVAVK MLKENASPSE LRDLLSEFNV LKQVNHPHVI KLYGACSQDG PLLLIVEYAK
321 YGSLRGFLRE SRKVGPGYLG SGGSRNSSSL DHPDERALTM GDLISFAWQI SQGMQYLAEM KLVHRDLAAR NILVAEGRKM
401 KISDFGLSRD VYEEDSYVKR SQGRIPVKWM AIESLFDHIY TTQSDVWSFG VLLWEIVTLG GNPYPGIPPE RLFNLLKTGH
481 RMERPDNCSE EMYRLMLQCW KQEPDKRPVF ADISKDLEKM MVKRRDYLDL AASTPSDSLI YDDGLSEEET PLVDCNNAPL
561 PRALPSTWIE NKLYGMSDPN WPGESPVPLT RADGTNTGFP RYPNDSVYAN WMLSPSAAKL MDTFDS

B

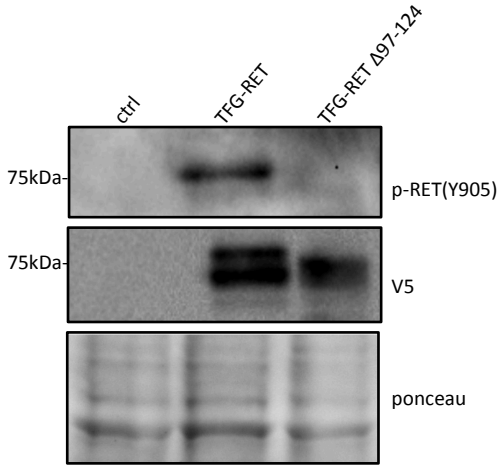

Figure 3.10: Deletion of the CC domain of TFG reduces RET phosphorylation. The CC domain (L97 to E124) of TFG-RET was deleted to create the TFG-RET Δ97-124 ((A)- deleted amino acids in red). Nthy-ori-3-1 cells were transiently transfected with TFG-RET and TFG-RET Δ97-124 in pcDNA DEST40 Vector (His and V5 tagged) along with empty vector control. 48 hours post transfection, cells were lysed and the cell lysates were subject to immunoblot analysis, which suggested that the TFG-RET Δ97-124 mutant showed lesser phosphorylation of RET (Y905) (B).

3.3.2 PB1 domain and CC domain are important for TFG-RET oligomerisation.

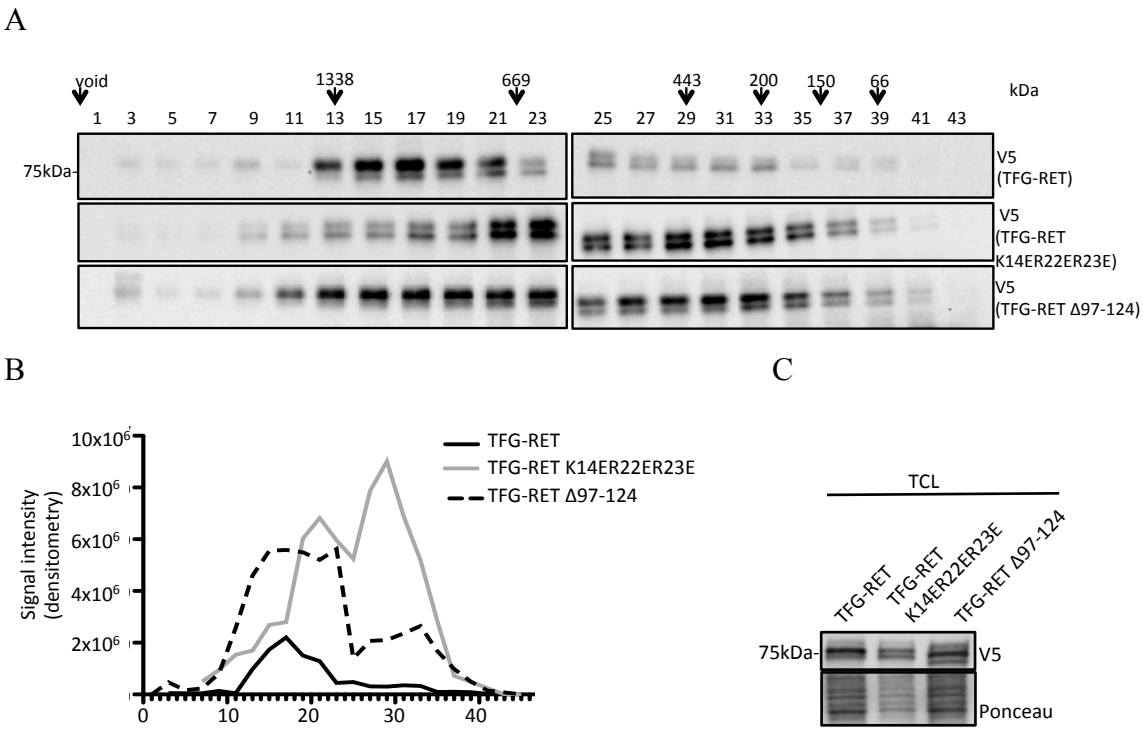

Figure 3.11: Functional domains of TFG contribute to TFG-RET heteromerisation - Gel filtration studies. HeLa cells were transiently transfected with TFG-RET, TFG-RET K14E.R22E.R23E and TFG-RET Δ97-124 in pcDNA3 Dest 40 (V5, His tagged). 48 hours post transfection, cells were lysed in 500 µl lysis buffer by sonication. Subsequently, the cell lysates were ultracentrifuged and the supernatant (cytosolic fraction) was separated by size exclusion chromatography. **(C)** Protein expression of TFG-RET K14E.R22E.R23E, TFG-RET Δ97-124 (in pcDNA DEST V5.His vector) in HeLa cells were verified by immunoblot analysis of the cell lysates. **(A)** Collected fractions (every second fraction) were subjected to western blotting and TFG-RET, TFG-RET K14E.R22E.R23E and TFG-RET Δ97-124 were detected using V5 tag. **(A, B)** Most of TFG-RET was detected in high molecular weight fractions, while TFG-RET K14E.R22E.R23E shifted towards the later, lower molecular weight fractions. TFG-RET Δ97-124 was distributed among higher and lower molecular weight fractions.

Our next step was to investigate if the PB1 domain and CC domain of TFG played any role in the regulation of TFG-RET heteromeric complex formation. To check this, cytosolic fractions from cell lysates collected from HeLa cells transiently expressing TFG-RET, TFG-RET K14E.R22E.R23E and TFG-RET Δ97-124 (Figure 3.11C) were loaded on Superose6 gel filtration columns. Every second fraction collected after gel filtration was used for immunoblot analysis. As expected, most of TFG-RET was detected in the higher molecular weight fractions, indicating TFG-RET being present in

high molecular weight protein complexes, while in the case of TFG-RET K14E.R22E.R23E, most of the protein was detected in relatively lower molecular weight fractions. On the other hand, TFG-RET Δ97-124 was distributed among higher and lower molecular weight fractions, which looked like a combined pattern of TFG-RET and TFG-RET K14E.R22.R23E. (Figure 3.11A, 11B). These data suggested that both PB1 domain and the CC domain have a role in the heteromeric complex formation of TFG-RET.

3.3.3 PB1 domain is important for the stability of TFG-RET

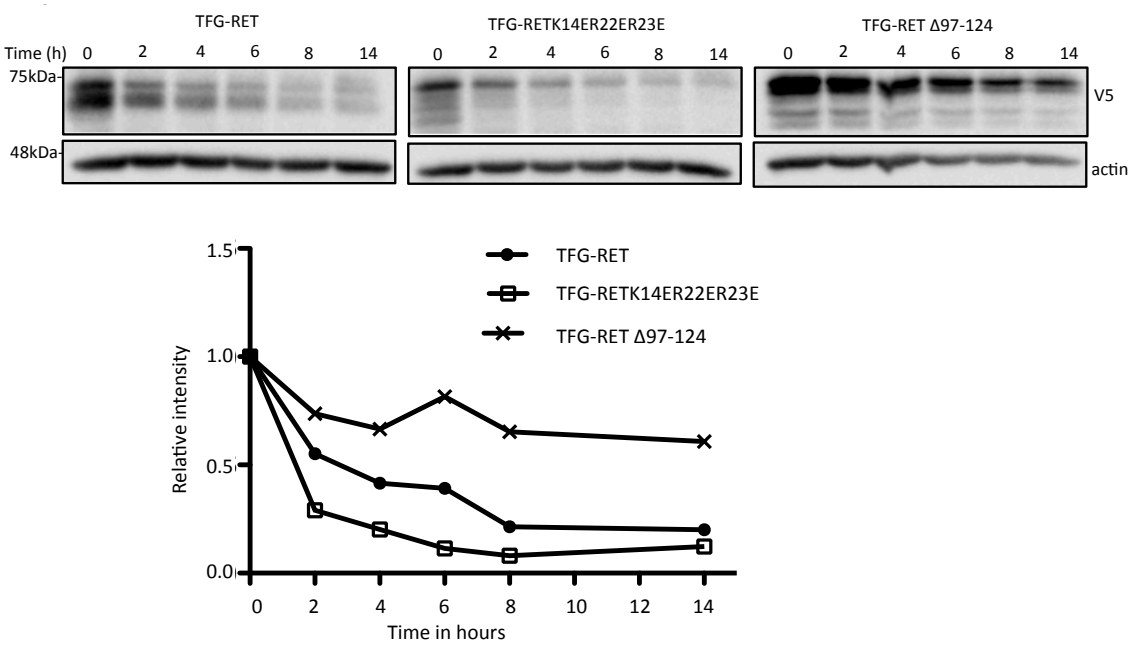

Figure 3.12: Functional domains of TFG influences TFG-RET stability (Cycloheximide chase assay). Nthy-ori-3-1cells were transiently transfected with TFG-RET, TFG-RET K14E.R22E.R23E and TFG-RET Δ97-124. 48 hours post transfection, cycloheximide (100ug/mL) was added to the cells and cell lysates were collected in SDS-sample buffer at indicated time points. The samples were subjected to immunoblot analysis. The results suggest that TFG-RET K14ER22.R23E exhibits lesser protein stability relative to TFG-RET, while, TFG-RET Δ97-124exhibits higher protein stability relative to TFG-RET.

We next checked if either of these two putative functional domains of TFG played a role in maintaining the stability of TFG-RET. For this, transiently transfected NThy-ori-3-1 cells with TFG-RET, TFG-RET K14ER22,23E and TFG-RET Δ97-124and performed a cycloheximide chase assay. Immunoblot analysis of the cell lysates showed

that the mutations on the PB1 domain resulted in a faster degradation of TFG-RET, while the deletion of CC domain resulted in a higher stability of TFG-RET (Figure 3.12). This data implies that both the PB1 domain and CCdomain of TFG has a role in the regulation of stability of TFG-RET.

3.3.4 Deletion of CC domain of TFG results in the reduction of TFG-RET induced transformation

In order to investigate any possible role of the PB1 domain and CC domain in the transformation ability of TFG-RET, we conducted soft agar colony formation assay as described earlier. For this, we first established TFG-RET K14E.R22E.R23E and TFG-RET Δ97-124 expressing stable NThy-ori-3-1 cell lines. The results indicated that the deletion of CC domain significantly reduced the colony formation ability of NThy-TFG-RET cells (i.e, TFG-RET Δ97-124 cells). Though a similar observation was seen in the NThy-TFG-RET K14E.R22E.R23E cells, the result remain inconclusive due to the lower expression of TFG-RET K14E.R22E.R23E in these stable cell lines (Figure 3.13).

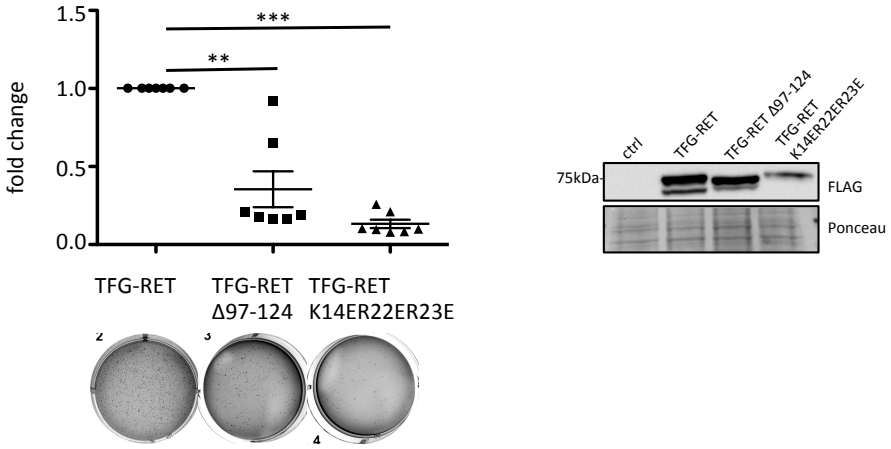

Figure 3.13: Mutation in the PB1 domain of TFG affects the transformation ability of TFG-RET – soft agar colony formation assay. Nthy TFG-RET, Nthy TFG-RET Δ97-124 and Nthy TFG-RET K14E.R22E.R23E along with Nthy ctrl cells were cultured in soft agar for 2 weeks followed by staining with crystal violet. Nthy TFG-RET Δ97-124 cells exhibited reduced transformation ability compared to Nthy TFG-RET cells. TFG-RET K14E.R22E.R23E also might affect the transformation ability of TFG-RET, but the results are inconclusive due to lower expression level of this mutant (Paired t test, two tailed, n = 3, $P<0.05$).

3.4 Mass spectrometric analysis of patient normal, tumor and metastatic tissue

3.4.1 Differential expression of proteins in cancer tissue

With the aim to investigate any differential expression of proteins between normal and cancer tissue, we conducted liquid chromatography-mass spectrometric (LC-MS) analysis of protein lysates prepared from normal, tumor and metastatic tissue of the same patient (three technical repeats of each sample). A total of 1,734 proteins were detected and the average signal intensities for every protein in each sample were determined and compared between the three samples. Label-free quantitative analysis of the mass spectrometry data implied differential expression of proteins among the three samples, with 184 proteins being expressed only in the tumor and metastatic samples (Figure 3.14A, C). The number of proteins with differential regulation between tumor and metastatic samples is shown in Figure 3.14 B. Table 2 and 3 enlists the proteins that were detected in the tumor and metastatic lesions only, respectively.

A

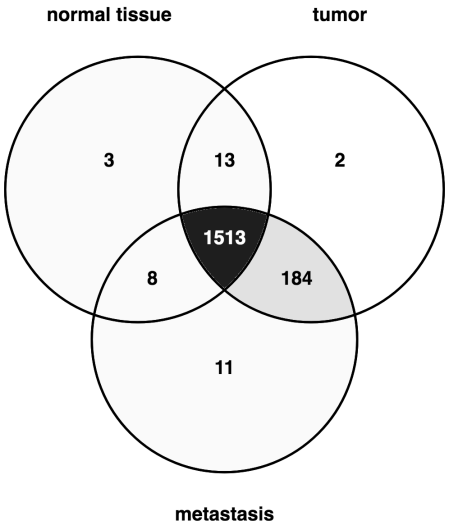

B

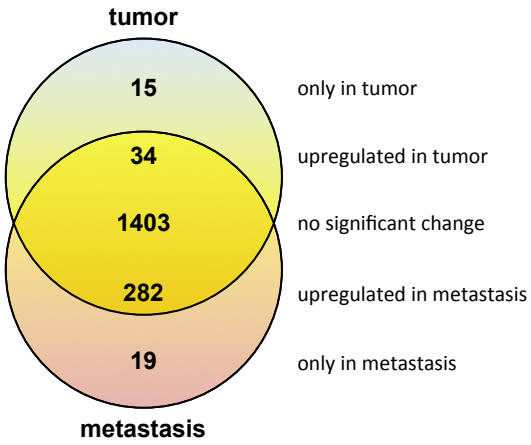

C

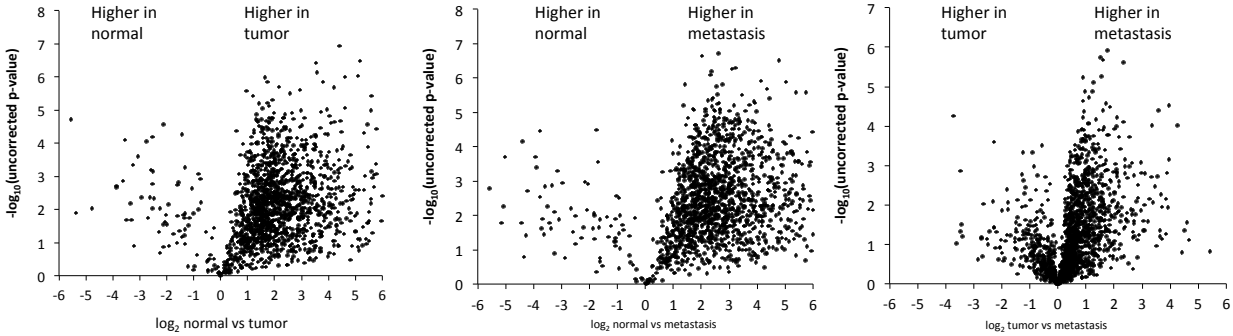

Figure 3.14: Differential regulation of protein expression in tumor and metastatic tissue. (A, B) Venn diagrams representing the differential regulation of proteins in normal, tumor and metastasis tissue from the patient tissue. **(C)** Scatter plots showing differential expression of proteins between various sets of tissues.

Table 2: List of proteins that were detected only in tumor lesions in the mass spectrometric analysis.

Protein List Tumor only			
	Accession	Entry	Description
1	P01258	CALC_HUMAN	Calcitonin OS=Homo sapiens GN=CALCA PE=1 SV=2
2	P22748	CAH4_HUMAN	Carbonic anhydrase 4 OS=Homo sapiens GN=CA4 PE=1 SV=2
3	P16671	CD36_HUMAN	Platelet glycoprotein 4 OS=Homo sapiens GN=CD36 PE=1 SV=2
4	P35908	K22E_HUMAN	Keratin type II cytoskeletal 2 epidermal OS=Homo sapiens GN=KRT2 PE=1 SV=2
5	Q16647	PTGIS_HUMAN	Prostacyclin synthase OS=Homo sapiens GN=PTGIS PE=1 SV=1
6	P63267	ACTH_HUMAN	Actin gamma-enteric smooth muscle OS=Homo sapiens GN=ACTG2 PE=1 SV=1
7	Q15326	ZMY11_HUMAN	Zinc finger MYND domain-containing protein 11 OS=Homo sapiens GN=ZMYND11 PE=1 SV=2
8	P55058	PLTP_HUMAN	Phospholipid transfer protein OS=Homo sapiens GN=PLTP PE=1 SV=1
9	P50440	GATM_HUMAN	Glycine amidinotransferase mitochondrial OS=Homo sapiens GN=GATM PE=1 SV=1
10	Q8IWL1	SFPA2_HUMAN	Pulmonary surfactant-associated protein A2 OS=Homo sapiens GN=SFTPA2 PE=1 SV=1
11	O00422	SAP18_HUMAN	Histone deacetylase complex subunit SAP18 OS=Homo sapiens GN=SAP18 PE=1 SV=1
12	Q86XX4	FRAS1_HUMAN	Extracellular matrix protein FRAS1 OS=Homo sapiens GN=FRAS1 PE=1 SV=2
13	P30566	PUR8_HUMAN	Adenylosuccinate lyase OS=Homo sapiens GN=ADSL PE=1 SV=2
14	P17661	DESM_HUMAN	Desmin OS=Homo sapiens GN=DES PE=1 SV=3
15	Q06828	FMOD_HUMAN	Fibromodulin OS=Homo sapiens GN=FMOD PE=1 SV=2

Table 3: List of proteins that were detected only in metastatic lesions in the mass spectrometric analysis.

Protein List – Metastasis Only			
	Accession	Entry	Description
1	Q04446	GLGB_HUMAN	1 4-alpha-glucan-branching enzyme OS=Homo sapiens GN=GBE1 PE=1 SV=3
2	Q96C23	GALM_HUMAN	Aldose 1-epimerase OS=Homo sapiens GN=GALM PE=1 SV=1
3	Q96CN7	ISOC1_HUMAN	Isochorismatase domain-containing protein 1 OS=Homo sapiens GN=ISOC1 PE=1 SV=3
4	Q06124	PTN11_HUMAN	Tyrosine-protein phosphatase non-receptor type 11 OS=Homo sapiens GN=PTPN11 PE=1 SV=2
5	P32456	GBP2_HUMAN	Guanylate-binding protein 2 OS=Homo sapiens GN=GBP2 PE=1 SV=3
6	Q9NVE7	PANK4_HUMAN	Pantothenate kinase 4 OS=Homo sapiens GN=PANK4 PE=1 SV=1
7	Q53RD9	FBLN7_HUMAN	Fibulin-7 OS=Homo sapiens GN=FBLN7 PE=2 SV=1
8	Q9UDY2	ZO2_HUMAN	Tight junction protein ZO-2 OS=Homo sapiens GN=TJP2 PE=1 SV=2
9	P35237	SPB6_HUMAN	Serpin B6 OS=Homo sapiens GN=SERPINB6 PE=1 SV=3
10	P07358	CO8B_HUMAN	Complement component C8 beta chain OS=Homo sapiens GN=C8B PE=1 SV=3
11	Q6RW13	ATRAP_HUMAN	Type-1 angiotensin II receptor-associated protein OS=Homo sapiens GN=AGTRAP PE=1 SV=1
12	Q8WXX5	DNJC9_HUMAN	DnaJ homolog subfamily C member 9 OS=Homo sapiens GN=DNAJC9 PE=1 SV=1
13	Q16625	OCLN_HUMAN	Occludin OS=Homo sapiens GN=OCLN PE=1 SV=1
14	Q6P2P2	ANM9_HUMAN	Putative protein arginine N-methyltransferase 9 OS=Homo sapiens GN=PRMT9 PE=2 SV=1
15	P27361	MK03_HUMAN	Mitogen-activated protein kinase 3 OS=Homo sapiens GN=MAPK3 PE=1 SV=4
16	Q9UKG1	DP13A_HUMAN	DCC-interacting protein 13-alpha OS=Homo sapiens GN=APPL1 PE=1 SV=1
17	P17301	ITA2_HUMAN	Integrin alpha-2 OS=Homo sapiens GN=ITGA2 PE=1 SV=1
18	Q49A26	GLYR1_HUMAN	Putative oxidoreductase GLYR1 OS=Homo sapiens GN=GLYR1 PE=1 SV=3
19	Q9BXR6	FHR5_HUMAN	Complement factor H-related protein 5 OS=Homo sapiens GN=CFHR5 PE=1 SV=1

3.4.2 Ubiquitination pathway-related proteins are up regulated in patient cancer tissue

As we are interested in the ubiquitination machinery, we then looked into the regulation of ubiquitination-associated proteins in the patient's tissue. The mass spectrometric data suggested that the ubiquitination pathway associated proteins HUWE1, USP9X and UBP7 were upregulated in the tumor and metastatic tissue of the patient (Figure 3.15A). Our next step was to investigate if the upregulation of these ubiquitination pathway associated proteins could also be detected in NThy TFG-RET cells. We carried out RT-PCR studies as well as immunoblot analysis to compare the expression of these ubiquitination-associated molecules both at the mRNA and protein level in NThy-TFG-RET cells and NThy-ctrl cells. Immunoblot analysis implied an upregulation of HUWE1, USP9X and USP7 proteins in NThy TFG-RET cells compared to NThy ctrl cells (Figure 3.15 B). The RT-PCR data indicated higher levels of Huwe1, Usp9x and Usp7 at mRNA levels, although not significant in all cases (Figure 3.15 C).

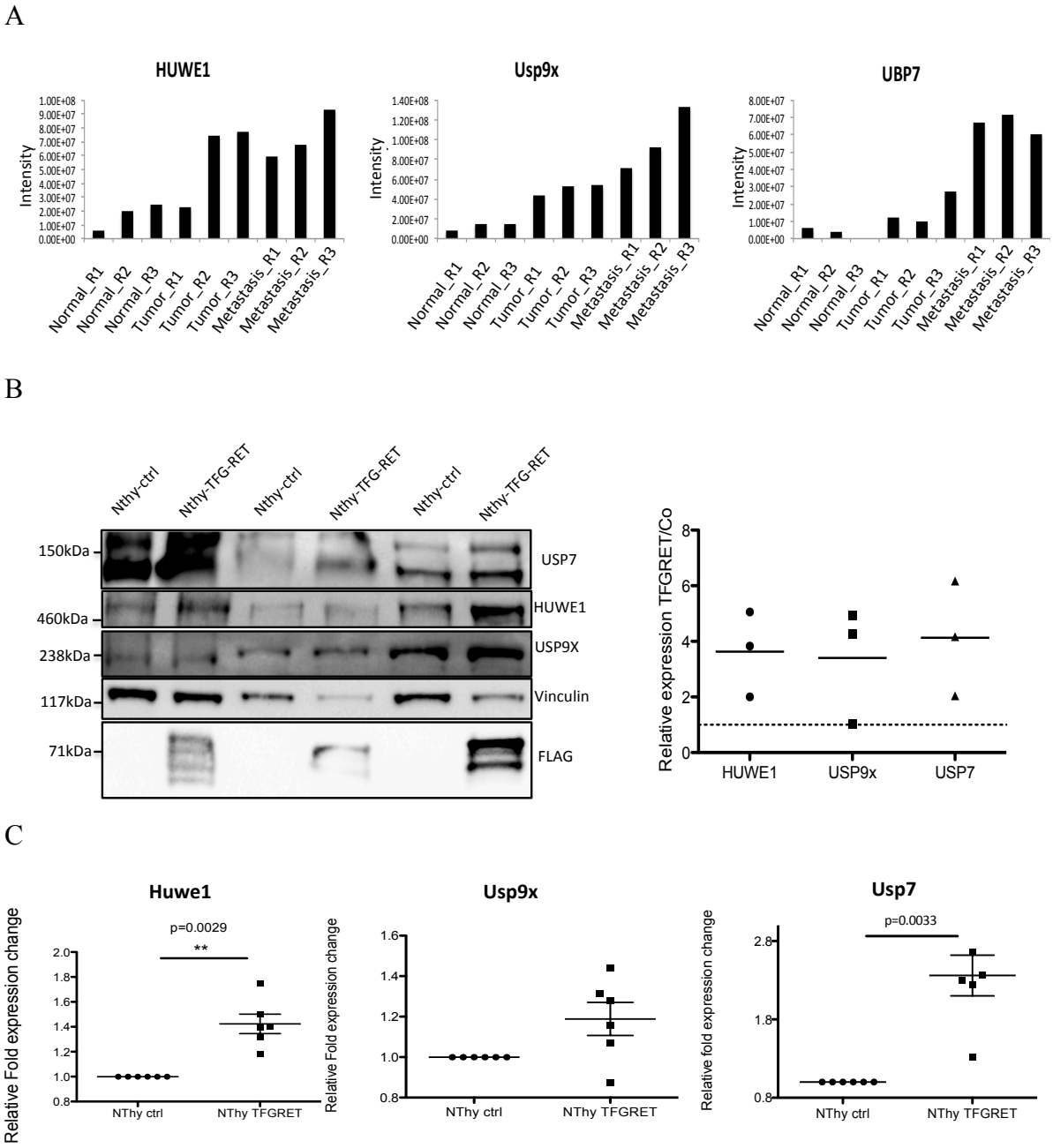

Figure 3.15: Ubiquitination associated proteins are up regulated in TFG-RET expressing cells. (A) Mass spectrometric analysis showing up regulation of ubiquitination associated proteins in patient tumor samples. **(B)** Cell lysates of Nthy ctrl and Nthy TFG-RET cells were subjected to western blot analysis of the indicated proteins. **(C)** Total RNA extraction followed by cDNA synthesis from Nthy ctrl and Nthy TFG-RET cells was performed to determine the relative gene expression levels based on qRT-PCR studies (n = 3, paired t test, Two-tailed) (internal control – 18S, RPS13). Ubiquitination associated proteins were upregulated, not only at the protein level, but also at the mRNA level.

3.4.3 Inhibition of RET and ubiquitin-associated protein reduces colony formation of NThy TFG-RET cells

Since our data suggested that HUWE1, USP9X and USP7 were up regulated in NThy TFG-RET cells, we next examined if inhibition of these proteins using chemical inhibitors would affect the transformation ability of NThy TFG-RET cells. We also checked the effect of inhibition of RET kinase using FDA approved tyrosine kinase inhibitors. Table 4 shows a list and short description about the inhibitors used in our experiments. Briefly, WP1130 is a cell-permeable chemical that has been demonstrated to directly inhibit the activity of DUBs including USP9X, USP5 and USP14 [171]. A study showed that WP1130 mediated DUB inhibition lead to tumor cell apoptosis as a result of formation of aggresomes due to induced accumulation of protein-ubiquitin conjugates [171]. XL184 (Cabozantinib), is a multiple receptor tyrosine kinase inhibitor that has the potential to produce synergistic antitumor effects [172]. Since it can bind to and inhibit many RTKs overexpressed in tumors including RET, VEGFR1/2/3, it can contribute to tumor regression by inhibiting tumor growth as well as angiogenesis [172]. Vandatenib is an orally available multiple kinase inhibitor that has the potential to inhibit VEGF signalling and oncogenic RET at nanomolar concentrations, and EGFR tyrosine kinase at submicromolar concentrations [173]. Hence, vandatenib also can act as both an anti-angiogenic as well as an anti-neoplastic drug. It has been demonstrated that Vandatenib can block phosphorylation and activity of RET oncoproteins (both RET activating mutants and RET fusions) in cells as well as inhibit the transforming effects of RET/PTC in cells and RET/PTC3-induced tumors in mice [174]. BI8622 and BI8626 are small molecule inhibitors of HUWE1 that were identified using high-throughput screening in an attempt to repress MYC-activated genes by promoting stabilisation of MIZ1, a negative regulator of MYC, which in turn is degraded by E3 ligase HUWE1 [175]. Since HUWE1 can autoubiquitinate its HECT-domain, the high throughput approach screened for the reduction in HUWE1 autoubiquitination activity [176]. We synthesised BI8622 and BI8626 (Syngene International Limited, India) and checked for the auto-ubiquitination of HUWE1 upon treatment with the inhibitors. NThy TFG-RET cells were treated with 20 μM BI-8622 or BI-8626 for 2 hours followed by treatment with proteasome inhibitor MG132 (10 μM) for 5 hours in order to capture the ubiquitin-conjugated proteins. Ubiquitinated proteins were isolated using UBIQAPTURE-Q kit

followed by western blot analysis. Immunoblots showed that treatment of NThy TFG-RET cells with BI-8622 and BI-8626 did indeed reduce ubiquitination of HUWE1 (Figure 3.16).

We investigated the effect of these inhibitors on the transformation of NThy-ori-3-1 cells. Soft agar colony formation assay in the presence of inhibitors was conducted. The DUB inhibitor WP1130 and kinase inhibitor XL-184 significantly reduced the transforming ability of NThy-TFG-RET as seen by the reduction in the number of colonies formed (Figure 3.17). Both inhibitors of HUWE1 also reduced the transformation ability of NThy TFG-RET cells, although BI-8622 seem to inhibit transformation of NThy TFG-RET cells to a much greater extent (Figure 3.17).

Table 4: List of inhibitors and targets/functions

Compound	IC50	Description
WP1130	1.25 – 5 μM (Usp9x)	Deubiquitinase inhibitor
XL184 (Cabozantinib)	4 nM (Ret)	RTK inhibitor, Used in the treatment of MTC, RCC
Vandatenib	40 nM (VEGFR2) 110 nM (VEGFR3) 500 nM (EGFR)	TK inhibitor, used in the treatment of MTC
BI8622	3.1 μM (HUWE1)	HUWE1 inhibitor
BI8626 2.5 μM	2.5 μM (HUWE1)	HUWE1 inhibitor

RTK-Receptor Tyrosine Kinase, TK-Tyrosine Kinase
MTC-Medullary Thyroid Cancer, RCC-Renal Cell Carcinoma

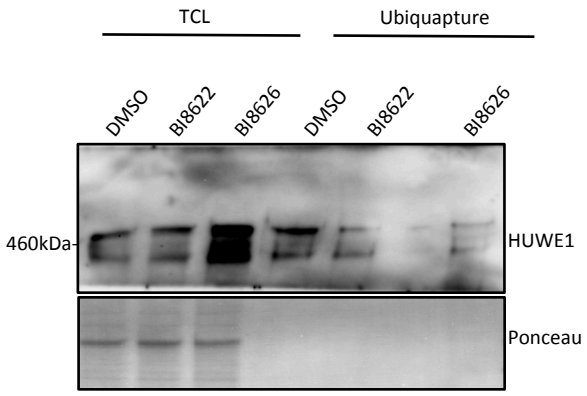

Figure 3.16: Immunoblot analysis showing reduced HUWE1 ubiquitination up on treatment with BI-8622 (20 μM) and BI-8626 (20 μM).

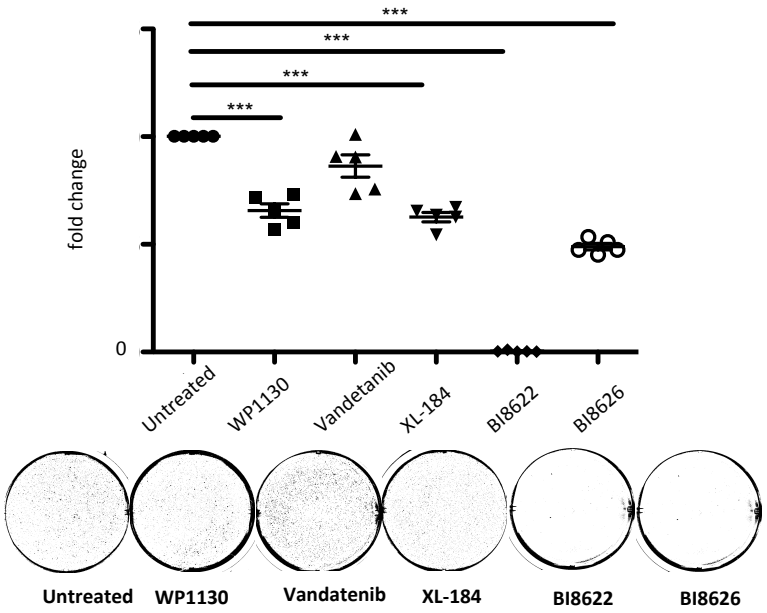

Figure 3.17: Tyrosine Kinase, DUB and HUWE1 inhibitors reduce oncogenic growth in TFG-RET expressing cells - soft agar colony formation assay. Nthy TFG-RET cells were cultured in soft agar colonies along with the indicated inhibitors for 2 weeks followed by staining with crystal violet. Inhibitor treatment resulted in the reduction in the relative number of colonies (Paired t test, two tailed, n=3, $P<0.05$).

4 Discussion

BCR-ABL fusion (philadelphia chromosome), an inter-chromosomal translocation between ABL gene from chromosome 9 and BCR gene on chromosome 22, in patients with chronic myeloid leukaemia (CML) was the first ever described oncogenic gene fusion [177]. This discovery had lead to the development of targeted molecular therapies including imatinib, nilotinib and dasatinib for the treatment of CML patients harbouring BCR-ABL fusion [178, 179]. Since then, the list of oncogenic gene fusions identified has increased, although they seem to have a much higher frequency in haematological malignancies as compared to solid tumors. However, this discrepancy might be in part mostly due to the higher karyotypic complexity of heterogeneous solid tumors, which posed technical difficulties in employing cytogenetic tools to identify chromosomal rearrangements like chromosome banding and fluorescence in situ hybridisation [180]. Many shortcomings of these techniques including culturing tumor cells in vitro and poor banding resolutions were overcome to a good extent with the development of high throughput global genetic analysis tools which allowed genome wide gene expression and copy number profiling. This approach made it possible to identify genes that showed outlier expression values or copy number shifts, which were further investigated for involvement in fusion events. However, it was the development of next generation sequencing (NGS) technologies in the 2000s that contributed dramatically to the current list of identified gene fusions [181]. NGS enables an unbiased approach for massive and in depth sequencing of the genome, exome or transcriptome which thereby allows identification of molecular alterations. This, along with the tremendous advancements in bioinformatics and computational biology has drastically changed our understanding of the landscape of genomic fusions, particularly with respect to solid tumors. The discovery of the presence of recurrent fusions of TMPRSS2 with ETS transcription genes (ERG or ETV) in over 50% of prostate cancer patients on the basis of outlier gene expression studies and phosphoproteomic studies for the identification of known and novel tyrosine kinase fusions in non-small cell lung cancers revealed the so far unknown prevalence of oncogenic fusions in epithelial cancers [182, 183]. The Cancer Genome Atlas (TCGA), which was set up in an effort to unveil the spectra of oncogenic genetic alterations using high-end genomic analysis technologies, now serves as an immense resource of identified genetic alterations across

33 cancer types [184]. Tumor-Fusions, a data portal that catalogues tumor fusions detected from 9966 well-characterised cancer samples from TCGA now enlists 20,731 fusion events [185]. The very high sensitivity offered by the recent high-end sequencing tools and the fact that gene fusions are also detected in non-malignant cells, emphasises the importance of characterising the functionality of the identified fusion products in order to distinguish nonspecific passenger fusions from recurrent oncogenic driver fusions.

A recent study by Gao et al. estimates that 16.5% of cancers harbour oncogenic driver fusions and these fusions function as sole driver in more than 1% of these cancers [186]. The same study also identified druggable fusions in 6% of the total cancers investigated and suggested that fusions involving oncogenes exhibited a higher likelihood for overexpression, while those involving tumor suppressor genes showed underexpression tendencies. Certain types of cancers including sarcoma, stomach cancer and breast cancer show higher prevalence of fusion events and many fusions exhibit lineage specific occurrence as in the cases of TMPRSS2-ERG in prostate cancer, CCDC6-RET in thyroid cancer, and PML-RARA and CBFB-MYH1 in acute leukemia [185]. Fusions involving kinases, which result in the increased activity of the kinase involved are important oncogenic events that could be relevant in terms of targeted therapy. Kinase fusions involving tyrosine kinases (RET, NTRK1/3, ROS, ALK) and serine threonine kinases (A/B/CRAF, MAST1/2) have been reported in various types of cancers [107]. Kinase fusions can be either 5’ or 3’ kinase fusions with the kinase at the 5’ or 3’ end of the fusion gene, respectively. Gao et al.’s study suggests that while most of the 5’ kinase fusions showed lower expression with the partner gene in comparison with the kinase, most of the 3’ kinase fusions showed higher expression with the partner gene, probably as a consequence of higher promoter activity of the 5’ partner gene [186].

Various studies have established the prevalence of NTRK fusions and RET fusions in PTCs and they form the underlying genetic alteration in about 5-13% and 13-43% of PTCs, respectively [187]. In this study, we identified a novel RET fusion in a PTC patient and functionally characterised its function and its role in oncogenesis. Further, we compared the genetic and proteomic expression profiles of normal and tumor tissues with the aim of identifying possible new therapeutic targets in PTCs.

4.1 Identification of a novel RET fusion in PTC

Since BRAFV600E and NRAS mutations are the most common genetic alterations in PTC, we selected a patient who did not harbour these mutations with the aim of identifying novel molecular alterations in PTC. We conducted immunohistochemical staining that implied that the tumor was a PTC with follicular growth (Figure 1). RNA and protein samples were obtained from normal, tumor and metastatic tissues for subsequent genomics and proteomics analysis. RNA sequencing analysis identified a novel 3' kinase fusion gene involving the N-terminal of TRK fused gene (TFG) and C-terminal RET kinase, which would give rise to the 626 amino acid containing fusion product TFG-RET, and translating to an approximately 68 kDa size fusion protein. TFG-RET results from an inter-chromosomal translocation involving exons 1-4 of the TFG gene located on chromosome 3 and exons 11-20 of the RET proto-oncogene located on chromosome 10 (Figure 3.2.C). Chromosome fragile sites are regions in the chromosome that are known to be involved in the formation of DNA breaks and generation of cancer specific rearrangements in human cells [188]. Similar to all the oncogenic RET fusions reported in PTC to date, the breakpoint of RET in TFG-RET lies within the fragile site containing the 1.8 kb intron 11 of RET. The resulting fusion retains the entire kinase domain of RET intact, while it leads to the deletion of its the negative regulatory elements. RET itself is not expressed in the follicular cells of the thyroid, although it is expressed in the parafollicular C cells. TFG is a ubiquitously expressed protein containing 400 amino acids, which is conserved among many species including *Caenorhabditis elegans*. TFG has been identified to interact with and negatively regulate the tyrosine phosphatase protein SHP-1 that is involved in the down regulation of various signalling pathways [189]. Studies also suggest that TFG plays a role in the induction of NF-kB pathway through its interaction with NEMO and TANK, which are known regulators of NF-kB pathway [190]. TFG was initially reported as the fusion partner of NTRK1 gene, named TRK-T3, in human PTC [191]. Subsequently, TFG was also reported the fusion partner of NOR1 in extra skeletal myxoid chondrosarcoma as well as to form fusion with ALK gene in anaplastic large cell lymphoma as well as the fusion partner of NOR1 in extra skeletal myxoid chondrosarcoma [192-194]. Upon TFG-RET fusion, expression of the novel protein is regulated by the TFG promoter which eventually results in the unscheduled expression

of RET in the thyroid follicular cells. A study by Witte et al. showed that TFG localises at the endoplasmic reticulum (ER) and is involved in protein secretion [195]. The study also suggests that fusion of NTRK1 with TFG recruits NTRK1 to the ER exit sites which leads to an increased kinase activity of the TFG fused NTRK1 at the ER exit sites resulting in the premature stimulation of multiple effectors including ERK1/2 signalling as a possible mechanism by which TFG fusion results in oncogenicity. The N-terminus and other functional domains (discussed in detail later) contained within the TFG portion have been shown to play crucial roles in various steps involved in the activation of the oncogenic TRK-T3 [114, 196], [197].

Apart from the TFG-RET fusion, our exome sequencing data also revealed the presence of other mutations that have not been yet well characterised (Figure 3.2 A,B and Table 1). Among others, our data revealed a mutation in the protein kinase MAP2K2 (MEK2), which was detected only in metastatic lesions. MAP2K2 is an important member of the RAS-RAF-MEK-ERK pathway, which in turn regulates various cellular processes including cell proliferation, differentiation and migration [60]. No studies so far have reported any MAP2K2Q391H mutation in any pathologic conditions. MAP2K2Q391 lies outside the kinase domain of MAP2K2, hence this mutation is less likely to directly affect the kinase activity of MAP2K2 [198]. Whether this mutation affects any other aspects of MAP2K2 like protein stability or protein-protein interactions remains to be investigated. A mutation in Myc (MycS21N), which also has not been reported so far, was detected in the exome analysis. MYC is a transcription factor that undergoes oncogenic activation in about 30% of human cancers [199]. Oncogenic activation of Myc usually occurs through chromosomal translocation, gene amplification or retroviral insertional mutagenesis [200]. MycS21 lies within the transactivation domain of Myc that plays a role in the regulation of gene transcription [200]. It may be interesting to check if the MycS21N mutation affects gene transcription that may in turn have oncogenic consequences.

4.2 TFG-RET is an oncogenic chromosomal rearrangement

Not all fusion genes result in the formation of an oncogene, the fusions can also be mere ‘passenger’ chromosomal translocations, which may not have any oncogenic or even functional consequence. So, we next aimed at investigating if the novel fusion gene we

identified was indeed oncogenic. For this we synthesised a plasmid construct in the pENTR221 gateway vector containing the TFG-RET sequence (from Invitrogen), which was subsequently cloned into various mammalian expression vector systems (pHAGE C-TAP (FLAG and HA tagged)) and Gateway™ pcDNA™-DEST40 Vector (His and V5 tagged). We established stable cell lines that constitutively expressed TFG-RET. NThy-ori-3-1 cells, which are immortalised normal human primary thyroid follicular epithelial cells, were stably transfected with pHAGE C-TAP TFG-RET constructs along with empty vector controls. Firstly, we checked if TFG-RET was phosphorylated at RET Y905, as Y905 has been identified as an auto-phosphorylation site of RET and it has been shown that impairing Y905 phosphorylation resulted in the impairment of kinase activity and transformation ability of RET [114, 169]. We observed that TFG-RET was indeed phosphorylated at Y905 and further, we saw the activation of several pro-survival signalling proteins including phosphorylation of ERK1/2, AKT and STAT3, all of which are implied to play a role in RET mediated tumorogenicity (Figure 3.3) [201-203]. We also observed the upregulation of oncogenic signalling pathways in 293T cells that were transiently transfected with TFG-RET. Not surprisingly, we also observed that stable expression of TFG-RET increased cell proliferation in NThy-ori-3-1 cells (Figure 3.3). While RET is located at the cell membrane, the novel fusion protein TFG-RET is mainly found in the cytosol (Figure 3.4). Within the fusion protein various domains including the transmembrane domain are deleted. This has also been observed for other RET fusions. We also detected TFG-RET at the plasma membrane. This could be explained by relocation due to interaction of RET fusion proteins with other docking and signal adaptor proteins like FRS2, SHC and Enigma and for subsequent propagation of signalling cascades [204, 205].

We next investigated the ability of TFG-RET to induce malignant transformation in NThy-ori-3-1 cells. Soft agar colony formation assay is a technique used to evaluate the ability of cells to grow and divide in an anchorage-independent manner, which is a characteristic of transformed cells. We clearly observed that TFG-RET expression transformed NThy-ori-3-1 cells as it led to colony formation (Figure 3.5). To our knowledge this is the first study that demonstrates the transformation ability of a RET fusion in immortalised human thyroid cells. Phosphorylation of STAT3, ERK1/2 and Akt in TFG-RET expressing cells implied that TFG-RET exhibits kinase activity. We wanted to confirm that TFG-RET indeed possesses kinase activity and for this we performed in vitro kinase assay using MBP as the phosphorylation substrate. As the

mutation of lysine 758 which is present with in in the activation loop of full length RET abolishes the kinase activity of RET, we generated a kinase dead variant of TFG-RET by introducing a point mutation corresponding to K758M of RET (TFG-RETK270M). We used TFG-RETK270M as a negative control and wild type RET as a positive control in our kinase assay. Not surprisingly, TFG-RET phosphorylated MBP in vitro, which was also true for wild type RET, although the kinase activity was of TFG-RET was indeed abolished in the kinase dead mutant (Figure 3.6).

4.3 TFG-RET forms dimers and heteromers

Ligand-induced dimerisation and oligomerisation is a crucial step in receptor tyrosine kinases mediated cell signal transduction [206]. Structural studies suggest that autophosphorylation of receptor kinases occurs by a trans mechanism, i.e. between two kinase domains of distinct dimers rather than within the same dimer. Thus, oligomerisation is a crucial event in the autophosphorylation dependent activation of receptor kinases [207]. Previous studies showed that constitutive dimerisation and oligomerisation of RET fusion protein are mechanisms that are required for the transforming activity and activation of receptor tyrosine kinase oncogenes [208]. Greco et al. demonstrated that TFG containing NTRK fusion (termed as TRK-T3) required formation of oligomeric complexes for its transforming activity [196]. So, we next investigated if TFG-RET was capable of dimerisation. As RET is known to form dimers, we included wild type RET as well in our experiments along with TFG-RET. We checked the ability of TFG-RET to form homodimers as well as heterodimers with wild type RET. Our data (Figure 3.7) implied that TFG-RET exhibited both homomeric and heteromeric interactions with TFG-RET and WT-RET, respectively. We were then curious to check if TFG-RET also formed oligomeric complexes. For this, we conducted cross-linking assays using DTME. DTME is a cell membrane permeable cross-linker, which can conjugate sulfhydryl groups of proteins via maleimide group cross-linking. It contains a reducible disulphide bond, which enables the reversal of protein cross-linking using reducing agents like DTT. Our data (Figure 3.8) showed that upon crosslinking with DTME, TFG-RET formed high molecular weight protein complexes that were indicated by the shift in size of TFG-RET detection. RET WT also

formed high molecular weight complexes, which were not seen in gel analyses, most likely because of the very large size of the complex. Further, upon addition of the reducing agent DTT, the cross-linking was disrupted leading to the disassembly of the protein complex and subsequently, TFG-RET was detected as monomer. Together, these data suggest that TFG-RET can indeed form oligomers, which demonstrates to an extent, the mechanism behind TFG-RET oncogenicity as oligomerisation is a crucial requirement for kinase mediated signalling.

4.4 TFG domains are crucial for oligomerisation and oncogenicity of TFG-RET

Our next aim in the study was the characterisation of the role of TFG in the functionality of TFG-RET. The TFG segment in TFG-RET retained two of its distinct functional domains namely the Phox and Bem 1p (PB1) domain and the coiled-coil (CC) domain (Figure 3.9). The PB1 domains are protein modules comprising about 80 amino acid residues, which are conserved across amoebas, fungi, plants and animals [209]. Interaction of PB1 containing proteins with other PB1 domain proteins mediates the formation of homomeric and heteromeric complexes, which in turn is crucial for various cellular signalling cascades. So far, PB1 domains are reported in 13 different human proteins including some scaffold and adaptor proteins like p62 and Nbr1, as well as kinases including the MAPK signalling proteins like MEK5, MEKK2 and MEKK3 [210]. A study by Roccato et al. demonstrated that a K14A point mutation in the PB1 domain of TFG in the TRK-T3 fusion completely abrogated the transforming ability of TRK-T3 oncogene [197]. However, it was also demonstrated that the self-association of TRK-T3 proteins was not dependent on the PB1 domain of TFG, but rather the CC domain [196]. This could imply that the role of the PB1 domain in inducing transformation of TRK-T3 is rather because of its role in interaction with other proteins leading to transformation associated cellular signalling. Further, they investigated the interaction between PB1 containing proteins and reported that TFG exhibited a weak self-interaction and was the only protein that did not interact with other PB1 domain containing proteins. Although not much is known about the possible domains with which the TFG PB1 domain might interact, these data suggest the probable PB1 mediated interaction of TFG with other protein domains that might shed light about role of TFG in protein signalling [210].

CC domains are super helical structures characterised by repetitive heptad peptide motifs that consist of 2 to 5 helices that are arranged either in parallel or anti-parallel to each other. They are important in the facilitation of oligomerisation of proteins and thus crucial for various signaling mechanisms. They are thought to act as molecular spacers separating functional domains and scaffold multimeric protein complexes [211]. Proteins known and predicted to contain CC domains comprise a wide spectrum including kinases, kinesins, kinetochore and centriole proteins as well the family of the structural maintenance of chromosome (SMC) proteins [211]. Various studies have implied the role of CC domain in cellular functions including accurate chromosome segregation [212], [213], vesicle tethering [214], DNA recognition and cleavage [211]. Gel filtration studies have demonstrated the ability of CC domain containing proteins to form molecular complexes [215]. The role of CC domains in regulating various signalling pathways has also been illustrated. The CC domain of Ras-GRF has been shown to be important for the calcium-mediated activation of Ras-GRF, which in turn is required for Ras activation [216]. A study by Zhang et al. demonstrated that the CC domain of the transcription factor STAT3 is important for its tyrosine phosphorylation and its subsequent translocation to the nucleus, recruitment to the cytokine receptor IL-6 and subsequent tyrosine phosphorylation [217]. CC domain mediated dimerisation has been demonstrated to be crucial for the oncogenic activity of various tyrosine kinase fusions including TPR-MET and BCR-ABL [218, 219]. All NTRK and RET fusion proteins are predicted to contain one or multiple CC domains. These domains promote the dimerisation of the of the fusions proteins, that now lack the ligand binding domains due to their location upstream of the breakpoint [220, 221]. Monaco et al. demonstrated that the RET-PTC3 in which NcoA (also called RFG) is the fusion partner whose N-terminal CC domain was important in the oligomerisation, activation and transformation ability of RET-PTC3 [222]. Similar observations emphasizing on the indispensible role of CC domains has been reported in the cases of RET-PTC1 as well [223]. A study aimed at the characterisation of TFG protein predicted the presence of a trimeric CC domain at the N-terminus of TFG [224]. The role of TFG CC domain in the oligomerisation and oncogenicity of TRK-T3 was demonstrated by Greco et al.[196]. The study clearly demonstrated that deletion of the CC domain abolished the ability of TRK-T3 to form complexes as well as affected focus formation in NIH3T3 cells.

Our studies indicated that three point mutations (K14E.R22E.R23E) in the PB1 domain of TFG as well as the deletion of the CC domain reduced the autophosphorylation of

RET at Y905 (Figure 3.9 and 10). This effect was not seen in any of the single point mutants. This could be probably due to the fact that single point mutations are not sufficient to dampen the protein-protein interactions that are crucial for phosphorylation of RET Y905. It remains to be investigated whether each of these single point mutations affect other autophosphorylation sites of RET. Our gel filtration studies confirmed our previous observation that TFG-RET formed high molecular protein complexes and importantly, also suggested a role for both PB1 domain and CC domain in the oligomerisation of TFG-RET (Figure 3.11). This was in agreement with many other studies that were mentioned earlier which implied a role of both these domains in oligomerisation and activity of fusion proteins [196, 197]. Further, deletion of CC domain increased the stability of TFG-RET protein as seen in the cycloheximide chase assay, which might be probably because of the inability of CC domain deficient TFG-RET to undergo proper protein folding and attain its normal conformation and/or interact with other proteins that would allow its proper regulation (Figure 3.12). We then checked the functional significance that these domains might have in terms of oncogenicity of TFG-RET. We used stable cells where we achieved comparable expression of TFG-RET and TFG-RETΔ97-124, while the TFG-RETK14E.R22E.R23E mutant expression was greatly reduced. This could be because of the reduced stability of the triple mutant, as was also implied in the cycloheximide chase assay. In agreement with previous studies, CC domain indeed seemed to play a role in the transforming ability of TFG-RET (Figure 3.13). As the expression of PB1 mutant was incomparable with TFG-RET, we were unable to comment on the role PB1 domain in the oncogenicity of TFG-RET.

4.5 Ubiquitination-associated proteins are upregulated in TFG-RET expressing PTC

Our proteomics studies implied differential expression of proteins among normal, tumor and metastasis patient tissue (Figure 3.14). Our data implied the up regulation of HUWE1 E3 ligase, USP9X and USP7 in the cancer samples and our data from studies in NThy-TFG-RET further strengthened our observations (Figure 3.15). HUWE1 (the HECT, UBA, and WWE domain-containing protein 1) is an E3 ligase whose role in cancer propagation is controversial, which can be probably attributed to the complexity

in HUWE1 mediated molecular regulation whose targets include MCL-1, c-MYC, p53, and histones that are involved in various tumorigenisis-associated cellular processes. Studies report the upregulation of HUWE1 at both transcriptomic and protein levels in lung, breast and colorectal carcinomas [225-227]. Adhikary et al. showed that HUWE1 mediated lysine 63-linked polyubiquitination of MYC (which is not a degradation signal rather a regulatory modification) is required for the transactivation of multiple MYC targets, hence playing a crucial role in the tumor propagation [225]. Peter et al. showed that HUWE1 inhibition stabilised MIZ1, which in turn turned off the transcriptional activation of MYC activated target genes, hence inhibiting the oncogenic function of MYC in colorectal cancer [175]. The same work used high-throughput screening to develop HUWE1 inhibitors, which was also validated using functional assays. We used these inhibitors in our study too, and the results suggested that HUWE1 inhibition reduced TFG-RET-dependent transformation (Figure 3.16). Zhong et al. demonstrated that inhibition of HUWE1 stabilised MCL-1 which in turn attenuated the induction of apoptosis, as elimination of MCL-1 is an important step for DNA-damage-induced apoptosis [228]. Chen et al. showed that inhibition of HUWE1 stabilises p53 and induces p53-dependent apoptosis, hence implying the tumor suppressive role of HUWE1 through p53 regulation [229]. These studies link HUWE1-mediated degradation to divergent phenotypic effects – increased survival and increased apoptosis. Studies also suggest a role of HUWE1 as a tumor suppressor in colorectal cancer and thyroid cancer [230, 231]. Ma et al. reported the down regulation of HUWE1 in thyroid cancer tissues compared to normal tissues and demonstrated that HUWE1 knockdown lead to increased cell proliferation, cell migration and invasion in thyroid cancer cell lines (WRO, FTC133, BCPAP) [230]. The role that HUWE1 plays in oncogenicity might be determined by various factors like the type of tumor, the driver mutations involved and probably other factors, which clearly needs to be further investigated. It would be interesting to check if HUWE1 upregulation is seen in other RET fusion tumors as well as in PTCs in general. We also checked for any differential gene expression of the known HUWE1 targets in our PTC patient sample and could not detect any deregulation, which might be indicative of other substrates through which HUWE1 mediates cellular processes.

Further, our studies also shows that inhibition of USP9X and USP7 using small molecule inhibitors also reduced the transformation ability of TFG-RET expressing immortalised thyroid cells. A study by Ritorto et al. demonstrated that WP1130 showed

lower activity and lesser selectivity towards DUBs when compared to other DUB inhibitors (like BAY 11-7082, NSC 697923, SJB3-019A, PR-619, HBX 41,108) included in the study [232]. So, these studies can be further confirmed by using other inhibitors like GNE-6640 and GNE-6776 that have been demonstrated to be more specific against USP7 [233]. USP7 has been shown to be associated with various cancers including prostate, lung, breast, leukaemia and colon cancers where it displays context-specific tumor suppressive and oncogenic roles [234]. A study by Cheng et al. showed that USP7 expression levels were increased from grade I to grade IV in the tumors of glioma patients and that expression of USP7 was associated with lower survival rates [235]. Another study that investigated the mechanism underlying cancer progression associated with nuclear exclusion of the PTEN tumour suppressor links deubiquitination of PTEN by USP7 to its nuclear localisation [236]. Further, they saw an overexpression of USP7 in prostate cancer. Apart from its role in stabilising p53, in a deubiquitination enzyme-activity independent manner, USP7 is also required for the regulation of sequence-specific DNA binding of p53 [237]. USP7 plays important roles in the regulation of genomic integrity, cell growth, apoptosis and various other important cellular processes, since it is activated by several substrates including HIF-1 α, Ki-67, β-catenin, FOXO1, CCD6 and TRAF6 [234]. Increased USP9X expression in multiple myeloma patients has been associated with poor prognosis [238]. USP9X has been shown to stabilize the anti-apoptotic protein MCL1, which in turn promotes tumor survival. Further, USP9X overexpression correlated with MCL1 overexpression in human follicular lymphomas and diffuses large B-cell lymphomas [238]. Kushwaha et al.'s investigation to identify molecular targets that can promote radiation-induced apoptosis showed that USP9X inhibition using the small molecule inhibitor WP1130 could synergise radiation-induced cytotoxicity in NSCLC cells with mid-to-high MCL1 expression [239]. As in the case of E3 ligases, deciphering the roles of DUBs in cancer progression is a complex task mostly because of the large number of substrates and the consequential diversity in the mechanisms they regulate. However, as illustrated by some of the above-mentioned examples, we now understand these mechanisms better and can hopefully employ this knowledge to successful novel therapeutic interventions in the future. Since E3 ligases and DUBs are abundant in occurrence, they could serve as excellent diagnostic and prognostic markers as soon as we can establish reliable correlation between its expression and cancer – a rather easier and quicker exploitation than therapeutic intervention. It would be worth to investigate if these ubiquitination

associated proteins show similar expression patterns in other PTCs mediated by RET fusions or PTCs in general. The identification of unique expression patterns might serve as an excellent diagnostic tool that can aid the precise stratification of thyroid tumors – a long-standing problem in this area.

5 Outlook and perspective

5.1 Precision medicine and personalised therapeutics

Cancer is a disorder of the genome and the biggest challenge in the management of cancer is the inter- and intra-tumor diversity of the highly unstable genome that constantly undergoes changes. Every patient has a distinct set of molecular alterations that defines the tumor, and hence the 'one-size-fits-all' treatment approach for patients with similar clinical presentations might not be the most effective treatment strategy in many cases. Precision medicine, on the other hand is the approach where patient samples are investigated at the genomic and proteomic levels that can help better understand the disease, in order to conduct a distinct 'personalised' or 'individualised' treatment strategy that can be more effective than a general treatment approach [240]. The use of the tyrosine kinase inhibitor imatinib for the targeted interference of BCR-ABL fusion in CML patients with this fusion and the use of vemurafenib for the treatment of melanoma patients with BRAFV600E mutation are excellent examples of how molecular information-driven clinical approaches can improve cancer treatment [241-243]. With the improvements made in the fields of genomic sequencing, proteomics and data analysis, we are now better equipped to implement personalised targeted therapeutics.

Understanding the underlying genomic and proteomic alterations of PTC is important for the treatment and prognosis of PTC. A recent study by Musholt et al. revealed that RET/PTC1 arrangements were identified in 16% of PTC patients who did not harbour any BRAFV600E mutation [244]. Patients with the RET fusions were at a significantly higher risk of developing iodine refractory condition as well as lymph node metastasis. Another study using targeted NGS analysis of PTC patient samples with wild type BRAF identified two RET transformations (RUFY2-RET and KIAA1468-RET) which were previously not reported in PTC [245]. Conducting more studies like these can help reveal a more realistic spectrum of distribution of RET fusions in PTC and other tumors. Such studies will also help better correlate the association between RET fusions and disease prognosis, which can in turn contribute to better disease management through precision medicine. Subbiah et al.'s recent work reported that BLU-667 as a

highly potent and selective inhibitor of RET which could inhibit RET mutant and RET fusion harbouring NSCLC and thyroid xenografts [139]. These studies may pave the way for targeted therapeutics in tumors with RET fusion. Our studies establishes TFG-RET as an oncogenic fusion and it would be interesting to conduct more targeted NGS analysis to investigate the presence of this alteration in other PTC and non-PTC tumors. The findings of these studies could then help tailor targeted therapeutics against RET fusion harbouring tumors.

5.2 Proteomics and phospho-proteomics in cancer therapy

The past few decades have seen tremendous development in the area of genomic analysis centred approach of understanding cancer, which has resulted in unprecedented improvement in the management of the disease. Nevertheless, in order to fully understand the molecular profile of tumors, it is also important to investigate what the genetic material finally translates to – i.e., the proteins, which are the ultimate effector molecules, their abundance, the post translational modifications they undergo, particularly phosphorylation and protein-protein interactions [246]. Large-scale proteome and transcriptome profiling experiments indicate only a partial correlation between mRNA abundances and protein abundances [246]. The human genome estimated to be comprised of only about 20,000 protein-coding genes gives rise to about an estimated 500,000 protein isoforms largely achieved by alternative splicing and post-translational modifications [247], [248]. Advances in the field of mass spectrometry based proteomic studies along with bioinformatics not only improved our understanding of the protein expression profiles of cells and tissues, but have also helped develop complementary pathway analysis tools, which can give a better idea of the cellular regulation at a molecular level [248]. A very recent study by Tong et al. used a global phosphoproteomics data analysis workflow to analyse high-grade serous ovarian cancer to classify the cancer into distinct molecular subtypes based on phosphorylation-based markers, which could then predict clinically actionable kinases as drug targets [249]. Another study by Zhang et al. integrated mass spectrometry based proteomic characterisation of ovarian tumors with the TCGA genomic data identified protein

modulations including phosphorylation and acetylation, which could be associated with tumor stratification and patient outcomes [250].

Our studies have identified the upregulation of ubiquitination-associated proteins in PTC. It would be interesting to exploit proteomics analysis to investigate the expression of these proteins in a larger cohort of PTC patients and to check if the upregulation of these proteins has any correlation with RET fusions. These studies could also be extended to other solid tumors including lung and breast cancers where RET fusions are being reported. Such studies can help explore the potential of targeting the ubiquitome in addition to the kinases that might result in synergistic outcomes, or in cases where patients develop resistance to kinase inhibitors.

6 References

1. Fulda, S., K. Rajalingam, and I. Dikic, *Ubiquitylation in immune disorders and cancer: from molecular mechanisms to therapeutic implications.* EMBO Mol Med, 2012. **4**(7): p. 545-56.
2. Muhammad A Shahid, S.S., *Physiology, Thyroid, Hormone*. NCBI Bookshelf: StatPearls [Internet]. Treasure Island (FL): StatPearls Publishing; 2018 Jan-.
3. Felsenfeld, A.J. and B.S. Levine, *Calcitonin, the forgotten hormone: does it deserve to be forgotten?* Clin Kidney J, 2015. **8**(2): p. 180-7.
4. Bernard Rousset, C.D., Françoise Miot, Jacques Dumont, *Chapter 2 Thyroid Hormone Synthesis And Secretion*, in *Thyroid Hormone Synthesis And Secretion*, C.G. De Groot LJ, Dungan K, et al., Editor.: NCBI Bookshelf.
5. Clermont oncology center. *Thyroid Cancer*. 2014; Available from: http://clermontoncology.com/cancer-education/thyroid-cancer/.
6. Vissenberg, R., et al., *Pathophysiological aspects of thyroid hormone disorders/thyroid peroxidase autoantibodies and reproduction.* Hum Reprod Update, 2015. **21**(3): p. 378-87.
7. Taylor, P.N., et al., *Global epidemiology of hyperthyroidism and hypothyroidism.* Nat Rev Endocrinol, 2018. **14**(5): p. 301-316.
8. Kilfoy, B.A., et al., *Gender is an age-specific effect modifier for papillary cancers of the thyroid gland.* Cancer Epidemiol Biomarkers Prev, 2009. **18**(4): p. 1092-100.
9. Gilliland, F.D., et al., *Prognostic factors for thyroid carcinoma. A population-based study of 15,698 cases from the Surveillance, Epidemiology and End Results (SEER) program 1973-1991.* Cancer, 1997. **79**(3): p. 564-73.
10. Pellegriti, G., et al., *Worldwide increasing incidence of thyroid cancer: update on epidemiology and risk factors.* J Cancer Epidemiol, 2013. **2013**: p. 965212.
11. society, A.c. *Key statistics for thyroid cancer*. Available from: https://http://www.cancer.org/cancer/thyroid-cancer/about/key-statistics.html.
12. Lim, H., et al., *Trends in Thyroid Cancer Incidence and Mortality in the United States, 1974-2013.* JAMA, 2017. **317**(13): p. 1338-1348.
13. Rahib, L., et al., *Projecting cancer incidence and deaths to 2030: the unexpected burden of thyroid, liver, and pancreas cancers in the United States.* Cancer Res, 2014. **74**(11): p. 2913-21.
14. Davies, L. and H.G. Welch, *Current thyroid cancer trends in the United States.* JAMA Otolaryngol Head Neck Surg, 2014. **140**(4): p. 317-22.
15. American cancer society. *Thyroid cancer survival rates, by type and stage*. Available from: https://http://www.cancer.org/cancer/thyroid-cancer/detection-diagnosis-staging/survival-rates.html.
16. Siegel, R., et al., *Cancer statistics, 2014.* CA Cancer J Clin, 2014. **64**(1): p. 9-29.
17. Hall, P., *Radiation-induced thyroid cancer.* Med Oncol Tumor Pharmacother, 1992. **9**(4): p. 183-9.

18. Imaizumi, M., et al., *Radiation dose-response relationships for thyroid nodules and autoimmune thyroid diseases in Hiroshima and Nagasaki atomic bomb survivors 55-58 years after radiation exposure.* JAMA, 2006. **295**(9): p. 1011-22.
19. Kazakov, V.S., E.P. Demidchik, and L.N. Astakhova, *Thyroid cancer after Chernobyl.* Nature, 1992. **359**(6390): p. 21.
20. Hannibal, C.G., et al., *Risk of thyroid cancer after exposure to fertility drugs: results from a large Danish cohort study.* Hum Reprod, 2008. **23**(2): p. 451-6.
21. Guignard, R., et al., *Alcohol drinking, tobacco smoking, and anthropometric characteristics as risk factors for thyroid cancer: a countrywide case-control study in New Caledonia.* Am J Epidemiol, 2007. **166**(10): p. 1140-9.
22. Brindel, P., et al., *Menstrual and reproductive factors in the risk of differentiated thyroid carcinoma in native women in French Polynesia: a population-based case-control study.* Am J Epidemiol, 2008. **167**(2): p. 219-29.
23. Ezzat, S., et al., *Thyroid incidentalomas. Prevalence by palpation and ultrasonography.* Arch Intern Med, 1994. **154**(16): p. 1838-40.
24. Smith, J.J., et al., *Cancer after thyroidectomy: a multi-institutional experience with 1,523 patients.* J Am Coll Surg, 2013. **216**(4): p. 571-7; discussion 577-9.
25. Raparia, K., et al., *Clinical outcomes for "suspicious" category in thyroid fine-needle aspiration biopsy: Patient's sex and nodule size are possible predictors of malignancy.* Arch Pathol Lab Med, 2009. **133**(5): p. 787-90.
26. Kamran, S.C., et al., *Thyroid nodule size and prediction of cancer.* J Clin Endocrinol Metab, 2013. **98**(2): p. 564-70.
27. Haymart, M.R., et al., *Higher serum thyroid stimulating hormone level in thyroid nodule patients is associated with greater risks of differentiated thyroid cancer and advanced tumor stage.* J Clin Endocrinol Metab, 2008. **93**(3): p. 809-14.
28. Danese, D., et al., *Diagnostic accuracy of conventional versus sonography-guided fine-needle aspiration biopsy of thyroid nodules.* Thyroid, 1998. **8**(1): p. 15-21.
29. Hambleton, C. and E. Kandil, *Appropriate and accurate diagnosis of thyroid nodules: a review of thyroid fine-needle aspiration.* Int J Clin Exp Med, 2013. **6**(6): p. 413-22.
30. Pinchot, S.N., et al., *Accuracy of fine-needle aspiration biopsy for predicting neoplasm or carcinoma in thyroid nodules 4 cm or larger.* Arch Surg, 2009. **144**(7): p. 649-55.
31. Yoon, J.H., et al., *The diagnostic accuracy of ultrasound-guided fine-needle aspiration biopsy and the sonographic differences between benign and malignant thyroid nodules 3 cm or larger.* Thyroid, 2011. **21**(9): p. 993-1000.
32. Mazzaferri, E.L. and J. Sipos, *Should all patients with subcentimeter thyroid nodules undergo fine-needle aspiration biopsy and preoperative neck ultrasonography to define the extent of tumor invasion?* Thyroid, 2008. **18**(6): p. 597-602.
33. Cibas, E.S. and S.Z. Ali, *The 2017 Bethesda System for Reporting Thyroid Cytopathology.* Thyroid, 2017. **27**(11): p. 1341-1346.
34. Hauch, A., et al., *Total thyroidectomy is associated with increased risk of complications for low- and high-volume surgeons.* Ann Surg Oncol, 2014. **21**(12): p. 3844-52.

35. Gartland, R.M. and C.C. Lubitz, *Impact of Extent of Surgery on Tumor Recurrence and Survival for Papillary Thyroid Cancer Patients.* Ann Surg Oncol, 2018.
36. Schlumberger, M., et al., *Defects in iodide metabolism in thyroid cancer and implications for the follow-up and treatment of patients.* Nat Clin Pract Endocrinol Metab, 2007. **3**(3): p. 260-9.
37. Schlumberger, M., et al., *Definition and management of radioactive iodine-refractory differentiated thyroid cancer.* Lancet Diabetes Endocrinol, 2014. **2**(5): p. 356-8.
38. Ho, A.L., et al., *Selumetinib-enhanced radioiodine uptake in advanced thyroid cancer.* N Engl J Med, 2013. **368**(7): p. 623-32.
39. Rothenberg, S.M., et al., *Redifferentiation of iodine-refractory BRAF V600E-mutant metastatic papillary thyroid cancer with dabrafenib.* Clin Cancer Res, 2015. **21**(5): p. 1028-35.
40. Xing, M., *Molecular pathogenesis and mechanisms of thyroid cancer.* Nat Rev Cancer, 2013. **13**(3): p. 184-99.
41. Ahmadi, S., et al., *Hurthle cell carcinoma: current perspectives.* Onco Targets Ther, 2016. **9**: p. 6873-6884.
42. Cheng, D.T., et al., *Memorial Sloan Kettering-Integrated Mutation Profiling of Actionable Cancer Targets (MSK-IMPACT): A Hybridization Capture-Based Next-Generation Sequencing Clinical Assay for Solid Tumor Molecular Oncology.* J Mol Diagn, 2015. **17**(3): p. 251-64.
43. Tiedje, V., et al., *Anaplastic thyroid carcinoma: review of treatment protocols.* Endocr Relat Cancer, 2018. **25**(3): p. R153-R161.
44. Greene, F.L., American Joint Committee on Cancer., and American Cancer Society., *AJCC cancer staging manual*. 6th ed. 2002, New York: Springer-Verlag. xiv, 421 p.
45. Smallridge, R.C. and J.A. Copland, *Anaplastic thyroid carcinoma: pathogenesis and emerging therapies.* Clin Oncol (R Coll Radiol), 2010. **22**(6): p. 486-97.
46. Ranganath, R., M.A. Shah, and A.R. Shah, *Anaplastic thyroid cancer.* Curr Opin Endocrinol Diabetes Obes, 2015. **22**(5): p. 387-91.
47. FDA. *FDA approves new uses for two drugs administered together for the treatment of BRAF-positive anaplastic thyroid cancer*. Available from: https://http://www.fda.gov/news-events/press-announcements/fda-approves-new-uses-two-drugs-administered-together-treatment-braf-positive-anaplastic-thyroid.
48. Sanders, E.M., Jr., et al., *An evidence-based review of poorly differentiated thyroid cancer.* World J Surg, 2007. **31**(5): p. 934-45.
49. Ibrahimpasic, T., et al., *Outcomes in patients with poorly differentiated thyroid carcinoma.* J Clin Endocrinol Metab, 2014. **99**(4): p. 1245-52.
50. Samip R.Master, B.B., *Cancer, Thyroid, Medullary*. NCBI Bookshelf. : StatPearls Publishing LLC .
51. Priya, S.R., et al., *Targeted Therapy for Medullary Thyroid Cancer: A Review.* Front Oncol, 2017. **7**: p. 238.
52. Call, J.A., et al., *A role for radiotherapy in the management of advanced medullary thyroid carcinoma: the mayo clinic experience.* Rare Tumors, 2013. **5**(3): p. e37.

53. Berber, E., N. Flesher, and A.E. Siperstein, *Laparoscopic radiofrequency ablation of neuroendocrine liver metastases.* World J Surg, 2002. **26**(8): p. 985-90.
54. Wells, S.A., Jr., et al., *Vandetanib in patients with locally advanced or metastatic medullary thyroid cancer: a randomized, double-blind phase III trial.* J Clin Oncol, 2012. **30**(2): p. 134-41.
55. Elisei, R., et al., *Cabozantinib in progressive medullary thyroid cancer.* J Clin Oncol, 2013. **31**(29): p. 3639-46.
56. Thornton, K., et al., *Vandetanib for the treatment of symptomatic or progressive medullary thyroid cancer in patients with unresectable locally advanced or metastatic disease: U.S. Food and Drug Administration drug approval summary.* Clin Cancer Res, 2012. **18**(14): p. 3722-30.
57. *FDA Approves Cabozantinib for Thyroid Cancer*.
58. E. Cohen, R.E., M.J. Schlumberger, S.P. Müller, P. Schöffski, M. Brose, M. Shah, D.R. Miles, L.T. Nguyen, S. Sherman. *445PD - Clinical activity and pharmacokinetics (PK) of cabozantinib (XL184) in patients with progressive medullary thyroid carcinoma (MTC)*. in *ESMO Congress 2012*. 2012.
59. Raue, F. and K. Frank-Raue, *Thyroid Cancer: Risk-Stratified Management and Individualized Therapy.* Clin Cancer Res, 2016. **22**(20): p. 5012-5021.
60. Matallanas, D., et al., *Raf family kinases: old dogs have learned new tricks.* Genes Cancer, 2011. **2**(3): p. 232-60.
61. Papin, C., et al., *Identification of signalling proteins interacting with B-Raf in the yeast two-hybrid system.* Oncogene, 1996. **12**(10): p. 2213-21.
62. Marais, R., et al., *Differential regulation of Raf-1, A-Raf, and B-Raf by oncogenic ras and tyrosine kinases.* J Biol Chem, 1997. **272**(7): p. 4378-83.
63. Wan, P.T., et al., *Mechanism of activation of the RAF-ERK signaling pathway by oncogenic mutations of B-RAF.* Cell, 2004. **116**(6): p. 855-67.
64. Davies, H., et al., *Mutations of the BRAF gene in human cancer.* Nature, 2002. **417**(6892): p. 949-54.
65. Tavares, C., et al., *ENDOCRINE TUMOURS: Genetic predictors of thyroid cancer outcome.* Eur J Endocrinol, 2016. **174**(4): p. R117-26.
66. Trovisco, V., et al., *Type and prevalence of BRAF mutations are closely associated with papillary thyroid carcinoma histotype and patients' age but not with tumour aggressiveness.* Virchows Arch, 2005. **446**(6): p. 589-95.
67. Kim, T.H., et al., *The association of the BRAF(V600E) mutation with prognostic factors and poor clinical outcome in papillary thyroid cancer: a meta-analysis.* Cancer, 2012. **118**(7): p. 1764-73.
68. Xing, M., et al., *Association between BRAF V600E mutation and recurrence of papillary thyroid cancer.* J Clin Oncol, 2015. **33**(1): p. 42-50.
69. Henke, L.E., et al., *BRAF mutation is not predictive of long-term outcome in papillary thyroid carcinoma.* Cancer Med, 2015. **4**(6): p. 791-9.
70. Gouveia, C., et al., *Lack of association of BRAF mutation with negative prognostic indicators in papillary thyroid carcinoma: the University of California, San Francisco, experience.* JAMA Otolaryngol Head Neck Surg, 2013. **139**(11): p. 1164-70.
71. McFadden, D.G., et al., *p53 constrains progression to anaplastic thyroid carcinoma in a Braf-mutant mouse model of papillary thyroid cancer.* Proc Natl Acad Sci U S A, 2014. **111**(16): p. E1600-9.

72. Subbiah, V., et al., *Dabrafenib and Trametinib Treatment in Patients With Locally Advanced or Metastatic BRAF V600-Mutant Anaplastic Thyroid Cancer.* J Clin Oncol, 2018. **36**(1): p. 7-13.
73. Kim, K.B., et al., *Clinical responses to vemurafenib in patients with metastatic papillary thyroid cancer harboring BRAF(V600E) mutation.* Thyroid, 2013. **23**(10): p. 1277-83.
74. Brose, M.S., et al., *Vemurafenib in patients with BRAF(V600E)-positive metastatic or unresectable papillary thyroid cancer refractory to radioactive iodine: a non-randomised, multicentre, open-label, phase 2 trial.* Lancet Oncol, 2016. **17**(9): p. 1272-82.
75. Cox, A.D. and C.J. Der, *Ras history: The saga continues.* Small GTPases, 2010. **1**(1): p. 2-27.
76. Malumbres, M. and M. Barbacid, *RAS oncogenes: the first 30 years.* Nat Rev Cancer, 2003. **3**(6): p. 459-65.
77. Saxena, N., et al., *RAS: target for cancer therapy.* Cancer Invest, 2008. **26**(9): p. 948-55.
78. Cox, A.D., et al., *Drugging the undruggable RAS: Mission possible?* Nat Rev Drug Discov, 2014. **13**(11): p. 828-51.
79. Howell, G.M., S.P. Hodak, and L. Yip, *RAS mutations in thyroid cancer.* Oncologist, 2013. **18**(8): p. 926-32.
80. Lemoine, N.R., et al., *High frequency of ras oncogene activation in all stages of human thyroid tumorigenesis.* Oncogene, 1989. **4**(2): p. 159-64.
81. Jang, E.K., et al., *NRAS codon 61 mutation is associated with distant metastasis in patients with follicular thyroid carcinoma.* Thyroid, 2014. **24**(8): p. 1275-81.
82. Liu, R.T., et al., *Selective occurrence of ras mutations in benign and malignant thyroid follicular neoplasms in Taiwan.* Thyroid, 2004. **14**(8): p. 616-21.
83. Olovnikov, A.M., *A theory of marginotomy. The incomplete copying of template margin in enzymic synthesis of polynucleotides and biological significance of the phenomenon.* J Theor Biol, 1973. **41**(1): p. 181-90.
84. Blasco, M.A., *Telomeres and human disease: ageing, cancer and beyond.* Nat Rev Genet, 2005. **6**(8): p. 611-22.
85. Hanahan, D. and R.A. Weinberg, *The hallmarks of cancer.* Cell, 2000. **100**(1): p. 57-70.
86. Kim, N.W., et al., *Specific association of human telomerase activity with immortal cells and cancer.* Science, 1994. **266**(5193): p. 2011-5.
87. Greider, C.W., *Telomerase activity, cell proliferation, and cancer.* Proc Natl Acad Sci U S A, 1998. **95**(1): p. 90-2.
88. Stewart, S.A. and R.A. Weinberg, *Telomeres: cancer to human aging.* Annu Rev Cell Dev Biol, 2006. **22**: p. 531-57.
89. Ghosh, A., et al., *Telomerase directly regulates NF-kappaB-dependent transcription.* Nat Cell Biol, 2012. **14**(12): p. 1270-81.
90. Smith, L.L., H.A. Coller, and J.M. Roberts, *Telomerase modulates expression of growth-controlling genes and enhances cell proliferation.* Nat Cell Biol, 2003. **5**(5): p. 474-9.
91. Koh, C.M., et al., *Telomerase regulates MYC-driven oncogenesis independent of its reverse transcriptase activity.* J Clin Invest, 2015. **125**(5): p. 2109-22.
92. Preto, A., et al., *Telomerase expression and proliferative activity suggest a stem cell role for thyroid solid cell nests.* Mod Pathol, 2004. **17**(7): p. 819-26.
93. Soares, P., et al., *Genetic alterations in poorly differentiated and undifferentiated thyroid carcinomas.* Curr Genomics, 2011. **12**(8): p. 609-17.

94. Liu, X., et al., *Highly prevalent TERT promoter mutations in aggressive thyroid cancers.* Endocr Relat Cancer, 2013. **20**(4): p. 603-10.
95. Huang, F.W., et al., *Highly recurrent TERT promoter mutations in human melanoma.* Science, 2013. **339**(6122): p. 957-9.
96. Liu, R. and M. Xing, *TERT promoter mutations in thyroid cancer.* Endocr Relat Cancer, 2016. **23**(3): p. R143-55.
97. Rusinek, D., et al., *Current Advances in Thyroid Cancer Management. Are We Ready for the Epidemic Rise of Diagnoses?* Int J Mol Sci, 2017. **18**(8).
98. Nikiforova, M.N., et al., *Targeted next-generation sequencing panel (ThyroSeq) for detection of mutations in thyroid cancer.* J Clin Endocrinol Metab, 2013. **98**(11): p. E1852-60.
99. Xing, M., *Genetic alterations in the phosphatidylinositol-3 kinase/Akt pathway in thyroid cancer.* Thyroid, 2010. **20**(7): p. 697-706.
100. Karakas, B., K.E. Bachman, and B.H. Park, *Mutation of the PIK3CA oncogene in human cancers.* Br J Cancer, 2006. **94**(4): p. 455-9.
101. Garcia-Rostan, G., et al., *Mutation of the PIK3CA gene in anaplastic thyroid cancer.* Cancer Res, 2005. **65**(22): p. 10199-207.
102. Wu, G., et al., *Uncommon mutation, but common amplifications, of the PIK3CA gene in thyroid tumors.* J Clin Endocrinol Metab, 2005. **90**(8): p. 4688-93.
103. Liu, D., et al., *Letter re: uncommon mutation but common amplifications of the PIK3CA gene in thyroid tumors.* J Clin Endocrinol Metab, 2005. **90**(9): p. 5509.
104. Halachmi, N., et al., *Somatic mutations of the PTEN tumor suppressor gene in sporadic follicular thyroid tumors.* Genes Chromosomes Cancer, 1998. **23**(3): p. 239-43.
105. Beg, S., et al., *PTEN loss is associated with follicular variant of Middle Eastern papillary thyroid carcinoma.* Br J Cancer, 2015. **112**(12): p. 1938-43.
106. Xing, M., B.R. Haugen, and M. Schlumberger, *Progress in molecular-based management of differentiated thyroid cancer.* Lancet, 2013. **381**(9871): p. 1058-69.
107. Kumar-Sinha, C., S. Kalyana-Sundaram, and A.M. Chinnaiyan, *Landscape of gene fusions in epithelial cancers: seq and ye shall find.* Genome Med, 2015. **7**: p. 129.
108. Takahashi, M., J. Ritz, and G.M. Cooper, *Activation of a novel human transforming gene, ret, by DNA rearrangement.* Cell, 1985. **42**(2): p. 581-8.
109. Takahashi, M., et al., *Developmentally regulated expression of a human "finger"-containing gene encoded by the 5' half of the ret transforming gene.* Mol Cell Biol, 1988. **8**(4): p. 1853-6.
110. Takahashi, M. and G.M. Cooper, *ret transforming gene encodes a fusion protein homologous to tyrosine kinases.* Mol Cell Biol, 1987. **7**(4): p. 1378-85.
111. Myers, S.M., et al., *Characterization of RET proto-oncogene 3' splicing variants and polyadenylation sites: a novel C-terminus for RET.* Oncogene, 1995. **11**(10): p. 2039-45.
112. Pachnis, V., B. Mankoo, and F. Costantini, *Expression of the c-ret proto-oncogene during mouse embryogenesis.* Development, 1993. **119**(4): p. 1005-17.
113. de Groot, J.W., et al., *RET as a diagnostic and therapeutic target in sporadic and hereditary endocrine tumors.* Endocr Rev, 2006. **27**(5): p. 535-60.
114. Kawamoto, Y., et al., *Identification of RET autophosphorylation sites by mass spectrometry.* J Biol Chem, 2004. **279**(14): p. 14213-24.

115. Williams, D., *Cancer after nuclear fallout: lessons from the Chernobyl accident.* Nat Rev Cancer, 2002. **2**(7): p. 543-9.
116. Collins, B.J., et al., *RET expression in papillary thyroid cancer from patients irradiated in childhood for benign conditions.* J Clin Endocrinol Metab, 2002. **87**(8): p. 3941-6.
117. Nikiforova, M.N., et al., *Proximity of chromosomal loci that participate in radiation-induced rearrangements in human cells.* Science, 2000. **290**(5489): p. 138-41.
118. Smanik, P.A., et al., *Breakpoint characterization of the ret/PTC oncogene in human papillary thyroid carcinoma.* Hum Mol Genet, 1995. **4**(12): p. 2313-8.
119. Santoro, M., R.M. Melillo, and A. Fusco, *RET/PTC activation in papillary thyroid carcinoma: European Journal of Endocrinology Prize Lecture.* Eur J Endocrinol, 2006. **155**(5): p. 645-53.
120. Henderson, Y.C., M.J. Fredrick, and G.L. Clayman, *Differential responses of human papillary thyroid cancer cell lines carrying the RET/PTC1 rearrangement or a BRAF mutation to MEK1/2 inhibitors.* Arch Otolaryngol Head Neck Surg, 2007. **133**(8): p. 810-5.
121. Lodyga, M., et al., *XB130, a tissue-specific adaptor protein that couples the RET/PTC oncogenic kinase to PI 3-kinase pathway.* Oncogene, 2009. **28**(7): p. 937-49.
122. Neely, R.J., et al., *The RET/PTC3 oncogene activates classical NF-kappaB by stabilizing NIK.* Oncogene, 2011. **30**(1): p. 87-96.
123. Hwang, E.S., et al., *Regulation of signal transducer and activator of transcription 1 (STAT1) and STAT1-dependent genes by RET/PTC (rearranged in transformation/papillary thyroid carcinoma) oncogenic tyrosine kinases.* Mol Endocrinol, 2004. **18**(11): p. 2672-84.
124. Plaza-Menacho, I., L. Mologni, and N.Q. McDonald, *Mechanisms of RET signaling in cancer: current and future implications for targeted therapy.* Cell Signal, 2014. **26**(8): p. 1743-52.
125. Carling, T. and R. Udelsman, *Thyroid cancer.* Annu Rev Med, 2014. **65**: p. 125-37.
126. Menicali, E., et al., *Intracellular signal transduction and modification of the tumor microenvironment induced by RET/PTCs in papillary thyroid carcinoma.* Front Endocrinol (Lausanne), 2012. **3**: p. 67.
127. Powell, D.J., Jr., et al., *The RET/PTC3 oncogene: metastatic solid-type papillary carcinomas in murine thyroids.* Cancer Res, 1998. **58**(23): p. 5523-8.
128. Santoro, M., et al., *Development of thyroid papillary carcinomas secondary to tissue-specific expression of the RET/PTC1 oncogene in transgenic mice.* Oncogene, 1996. **12**(8): p. 1821-6.
129. Jhiang, S.M., et al., *Targeted expression of the ret/PTC1 oncogene induces papillary thyroid carcinomas.* Endocrinology, 1996. **137**(1): p. 375-8.
130. Santoro, M., et al., *The TRK and RET tyrosine kinase oncogenes cooperate with ras in the neoplastic transformation of a rat thyroid epithelial cell line.* Cell Growth Differ, 1993. **4**(2): p. 77-84.
131. Penna, G.C., et al., *Molecular Markers Involved in Tumorigenesis of Thyroid Carcinoma: Focus on Aggressive Histotypes.* Cytogenet Genome Res, 2016. **150**(3-4): p. 194-207.
132. Takeuchi, K., et al., *RET, ROS1 and ALK fusions in lung cancer.* Nat Med, 2012. **18**(3): p. 378-81.

133. Wang, R., et al., *RET fusions define a unique molecular and clinicopathologic subtype of non-small-cell lung cancer.* J Clin Oncol, 2012. **30**(35): p. 4352-9.
134. Stransky, N., et al., *The landscape of kinase fusions in cancer.* Nat Commun, 2014. **5**: p. 4846.
135. Kato, S., et al., *RET Aberrations in Diverse Cancers: Next-Generation Sequencing of 4,871 Patients.* Clin Cancer Res, 2017. **23**(8): p. 1988-1997.
136. Romei, C., R. Ciampi, and R. Elisei, *A comprehensive overview of the role of the RET proto-oncogene in thyroid carcinoma.* Nat Rev Endocrinol, 2016. **12**(4): p. 192-202.
137. Ball, D.W., *Management of medullary thyroid cancer.* Minerva Endocrinol, 2011. **36**(1): p. 87-98.
138. Subbiah, V., et al., *Selective RET kinase inhibition for patients with RET-altered cancers.* Ann Oncol, 2018. **29**(8): p. 1869-1876.
139. Subbiah, V., et al., *Precision Targeted Therapy with BLU-667 for RET-Driven Cancers.* Cancer Discov, 2018. **8**(7): p. 836-849.
140. Farago, A.F. and C.G. Azzoli, *Beyond ALK and ROS1: RET, NTRK, EGFR and BRAF gene rearrangements in non-small cell lung cancer.* Transl Lung Cancer Res, 2017. **6**(5): p. 550-559.
141. FDA. *FDA approves larotrectinib for solid tumors with NTRK gene fusions*. 12/14/2018:[Available from: https://http://www.fda.gov/drugs/fda-approves-larotrectinib-solid-tumors-ntrk-gene-fusions-0.
142. Di Fiore, P.P., S. Polo, and K. Hofmann, *When ubiquitin meets ubiquitin receptors: a signalling connection.* Nat Rev Mol Cell Biol, 2003. **4**(6): p. 491-7.
143. Clague, M.J., J.M. Coulson, and S. Urbe, *Cellular functions of the DUBs.* J Cell Sci, 2012. **125**(Pt 2): p. 277-86.
144. Haglund, K. and I. Dikic, *Ubiquitylation and cell signaling.* EMBO J, 2005. **24**(19): p. 3353-9.
145. Ikeda, F. and I. Dikic, *Atypical ubiquitin chains: new molecular signals. 'Protein Modifications: Beyond the Usual Suspects' review series.* EMBO Rep, 2008. **9**(6): p. 536-42.
146. Roccaro, A.M., A. Vacca, and D. Ribatti, *Bortezomib in the treatment of cancer.* Recent Pat Anticancer Drug Discov, 2006. **1**(3): p. 397-403.
147. Mitsiades, N., et al., *Molecular sequelae of proteasome inhibition in human multiple myeloma cells.* Proc Natl Acad Sci U S A, 2002. **99**(22): p. 14374-9.
148. Miliani de Marval, P.L. and Y. Zhang, *The RP-Mdm2-p53 pathway and tumorigenesis.* Oncotarget, 2011. **2**(3): p. 234-8.
149. Lind, H., et al., *Association of a functional polymorphism in the promoter of the MDM2 gene with risk of nonsmall cell lung cancer.* Int J Cancer, 2006. **119**(3): p. 718-21.
150. Yoshida, A., et al., *MDM2 and CDK4 immunohistochemical coexpression in high-grade osteosarcoma: correlation with a dedifferentiated subtype.* Am J Surg Pathol, 2012. **36**(3): p. 423-31.
151. Halatsch, M.E., et al., *Uniform MDM2 overexpression in a panel of glioblastoma multiforme cell lines with divergent EGFR and p53 expression status.* Anticancer Res, 2006. **26**(6B): p. 4191-4.
152. Rayburn, E., et al., *MDM2 and human malignancies: expression, clinical pathology, prognostic markers, and implications for chemotherapy.* Curr Cancer Drug Targets, 2005. **5**(1): p. 27-41.
153. de Rozieres, S., et al., *The loss of mdm2 induces p53-mediated apoptosis.* Oncogene, 2000. **19**(13): p. 1691-7.

154. Yang, Y., et al., *Small molecule inhibitors of HDM2 ubiquitin ligase activity stabilize and activate p53 in cells.* Cancer Cell, 2005. **7**(6): p. 547-59.
155. Masuya, D., et al., *The HAUSP gene plays an important role in non-small cell lung carcinogenesis through p53-dependent pathways.* J Pathol, 2006. **208**(5): p. 724-32.
156. Li, M., et al., *A dynamic role of HAUSP in the p53-Mdm2 pathway.* Mol Cell, 2004. **13**(6): p. 879-86.
157. Yuan, J., et al., *USP10 regulates p53 localization and stability by deubiquitinating p53.* Cell, 2010. **140**(3): p. 384-96.
158. Hoeller, D. and I. Dikic, *Targeting the ubiquitin system in cancer therapy.* Nature, 2009. **458**(7237): p. 438-44.
159. Popov, N., et al., *The ubiquitin-specific protease USP28 is required for MYC stability.* Nat Cell Biol, 2007. **9**(7): p. 765-74.
160. Kato, M., et al., *Frequent inactivation of A20 in B-cell lymphomas.* Nature, 2009. **459**(7247): p. 712-6.
161. Li, H. and R. Durbin, *Fast and accurate short read alignment with Burrows-Wheeler transform.* Bioinformatics, 2009. **25**(14): p. 1754-60.
162. DePristo, M.A., et al., *A framework for variation discovery and genotyping using next-generation DNA sequencing data.* Nat Genet, 2011. **43**(5): p. 491-8.
163. Saunders, C.T., et al., *Strelka: accurate somatic small-variant calling from sequenced tumor-normal sample pairs.* Bioinformatics, 2012. **28**(14): p. 1811-7.
164. Lek, M., et al., *Analysis of protein-coding genetic variation in 60,706 humans.* Nature, 2016. **536**(7616): p. 285-91.
165. Wu, T.D. and S. Nacu, *Fast and SNP-tolerant detection of complex variants and splicing in short reads.* Bioinformatics, 2010. **26**(7): p. 873-81.
166. Anders, S. and W. Huber, *Differential expression analysis for sequence count data.* Genome Biol, 2010. **11**(10): p. R106.
167. Seshagiri, S., et al., *Recurrent R-spondin fusions in colon cancer.* Nature, 2012. **488**(7413): p. 660-4.
168. Jiang, W., et al., *An optimized method for high-titer lentivirus preparations without ultracentrifugation.* Sci Rep, 2015. **5**: p. 13875.
169. Iwashita, T., et al., *Identification of tyrosine residues that are essential for transforming activity of the ret proto-oncogene with MEN2A or MEN2B mutation.* Oncogene, 1996. **12**(3): p. 481-7.
170. Yagi, T., D. Ito, and N. Suzuki, *TFG-Related Neurologic Disorders: New Insights Into Relationships Between Endoplasmic Reticulum and Neurodegeneration.* J Neuropathol Exp Neurol, 2016. **75**(4): p. 299-305.
171. Kapuria, V., et al., *Deubiquitinase inhibition by small-molecule WP1130 triggers aggresome formation and tumor cell apoptosis.* Cancer Res, 2010. **70**(22): p. 9265-76.
172. Durante, C., et al., *XL184 (cabozantinib) for medullary thyroid carcinoma.* Expert Opin Investig Drugs, 2011. **20**(3): p. 407-413.
173. Wedge, S.R., et al., *ZD6474 inhibits vascular endothelial growth factor signaling, angiogenesis, and tumor growth following oral administration.* Cancer Res, 2002. **62**(16): p. 4645-55.
174. Carlomagno, F., et al., *ZD6474, an orally available inhibitor of KDR tyrosine kinase activity, efficiently blocks oncogenic RET kinases.* Cancer Res, 2002. **62**(24): p. 7284-90.

175. Peter, S., et al., *Tumor cell-specific inhibition of MYC function using small molecule inhibitors of the HUWE1 ubiquitin ligase.* EMBO Mol Med, 2014. **6**(12): p. 1525-41.
176. Pandya, R.K., et al., *A structural element within the HUWE1 HECT domain modulates self-ubiquitination and substrate ubiquitination activities.* J Biol Chem, 2010. **285**(8): p. 5664-73.
177. Nowell, P.C., *The minute chromosome (Phl) in chronic granulocytic leukemia.* Blut, 1962. **8**: p. 65-6.
178. Wong, S. and O.N. Witte, *The BCR-ABL story: bench to bedside and back.* Annu Rev Immunol, 2004. **22**: p. 247-306.
179. Desogus, A., et al., *Bcr-Abl tyrosine kinase inhibitors: a patent review.* Expert Opin Ther Pat, 2015. **25**(4): p. 397-412.
180. Mertens, F., et al., *The emerging complexity of gene fusions in cancer.* Nat Rev Cancer, 2015. **15**(6): p. 371-81.
181. Latysheva, N.S. and M.M. Babu, *Discovering and understanding oncogenic gene fusions through data intensive computational approaches.* Nucleic Acids Res, 2016. **44**(10): p. 4487-503.
182. Rikova, K., et al., *Global survey of phosphotyrosine signaling identifies oncogenic kinases in lung cancer.* Cell, 2007. **131**(6): p. 1190-203.
183. Tomlins, S.A., et al., *Recurrent fusion of TMPRSS2 and ETS transcription factor genes in prostate cancer.* Science, 2005. **310**(5748): p. 644-8.
184. National Cancer Institute, N.H.G.R.I. *The Cancer Genome Atlas*. July 2nd, 2018 Available from: https://tcga-data.nci.nih.gov/docs/publications/tcga/?
185. Hu, X., et al., *TumorFusions: an integrative resource for cancer-associated transcript fusions.* Nucleic Acids Res, 2018. **46**(D1): p. D1144-D1149.
186. Gao, Q., et al., *Driver Fusions and Their Implications in the Development and Treatment of Human Cancers.* Cell Rep, 2018. **23**(1): p. 227-238 e3.
187. Kondo, T., S. Ezzat, and S.L. Asa, *Pathogenetic mechanisms in thyroid follicular-cell neoplasia.* Nat Rev Cancer, 2006. **6**(4): p. 292-306.
188. Gandhi, M., et al., *DNA breaks at fragile sites generate oncogenic RET/PTC rearrangements in human thyroid cells.* Oncogene, 2010. **29**(15): p. 2272-80.
189. Roccato, E., et al., *Analysis of SHP-1-mediated down-regulation of the TRK-T3 oncoprotein identifies Trk-fused gene (TFG) as a novel SHP-1-interacting protein.* J Biol Chem, 2005. **280**(5): p. 3382-9.
190. Miranda, C., et al., *The TFG protein, involved in oncogenic rearrangements, interacts with TANK and NEMO, two proteins involved in the NF-kappaB pathway.* J Cell Physiol, 2006. **208**(1): p. 154-60.
191. Greco, A., et al., *The DNA rearrangement that generates the TRK-T3 oncogene involves a novel gene on chromosome 3 whose product has a potential coiled-coil domain.* Mol Cell Biol, 1995. **15**(11): p. 6118-27.
192. Hisaoka, M., et al., *TFG is a novel fusion partner of NOR1 in extraskeletal myxoid chondrosarcoma.* Genes Chromosomes Cancer, 2004. **40**(4): p. 325-8.
193. Lamant, L., et al., *A new fusion gene TPM3-ALK in anaplastic large cell lymphoma created by a (1;2)(q25;p23) translocation.* Blood, 1999. **93**(9): p. 3088-95.
194. Hernandez, L., et al., *TRK-fused gene (TFG) is a new partner of ALK in anaplastic large cell lymphoma producing two structurally different TFG-ALK translocations.* Blood, 1999. **94**(9): p. 3265-8.
195. Witte, K., et al., *TFG-1 function in protein secretion and oncogenesis.* Nat Cell Biol, 2011. **13**(5): p. 550-8.

196. Greco, A., et al., *Role of the TFG N-terminus and coiled-coil domain in the transforming activity of the thyroid TRK-T3 oncogene.* Oncogene, 1998. **16**(6): p. 809-16.
197. Roccato, E., et al., *Role of TFG sequences outside the coiled-coil domain in TRK-T3 oncogenic activation.* Oncogene, 2003. **22**(6): p. 807-18.
198. Roskoski, R., Jr., *MEK1/2 dual-specificity protein kinases: structure and regulation.* Biochem Biophys Res Commun, 2012. **417**(1): p. 5-10.
199. Schaub, F.X., et al., *Pan-cancer Alterations of the MYC Oncogene and Its Proximal Network across the Cancer Genome Atlas.* Cell Syst, 2018. **6**(3): p. 282-300 e2.
200. Meyer, N. and L.Z. Penn, *Reflecting on 25 years with MYC.* Nat Rev Cancer, 2008. **8**(12): p. 976-90.
201. Knauf, J.A., et al., *RET/PTC-induced dedifferentiation of thyroid cells is mediated through Y1062 signaling through SHC-RAS-MAP kinase.* Oncogene, 2003. **22**(28): p. 4406-12.
202. Vasko, V., et al., *Akt activation and localisation correlate with tumour invasion and oncogene expression in thyroid cancer.* J Med Genet, 2004. **41**(3): p. 161-70.
203. Schuringa, J.J., et al., *MEN2A-RET-induced cellular transformation by activation of STAT3.* Oncogene, 2001. **20**(38): p. 5350-8.
204. Durick, K., G.N. Gill, and S.S. Taylor, *Shc and Enigma are both required for mitogenic signaling by Ret/ptc2.* Mol Cell Biol, 1998. **18**(4): p. 2298-308.
205. Melillo, R.M., et al., *Docking protein FRS2 links the protein tyrosine kinase RET and its oncogenic forms with the mitogen-activated protein kinase signaling cascade.* Mol Cell Biol, 2001. **21**(13): p. 4177-87.
206. Ullrich, A. and J. Schlessinger, *Signal transduction by receptors with tyrosine kinase activity.* Cell, 1990. **61**(2): p. 203-12.
207. Mohammadi, M., J. Schlessinger, and S.R. Hubbard, *Structure of the FGF receptor tyrosine kinase domain reveals a novel autoinhibitory mechanism.* Cell, 1996. **86**(4): p. 577-87.
208. Tong, Q., et al., *Characterization of the promoter region and oligomerization domain of H4 (D10S170), a gene frequently rearranged with the ret proto-oncogene.* Oncogene, 1995. **10**(9): p. 1781-7.
209. Sumimoto, H., S. Kamakura, and T. Ito, *Structure and function of the PB1 domain, a protein interaction module conserved in animals, fungi, amoebas, and plants.* Sci STKE, 2007. **2007**(401): p. re6.
210. Lamark, T., et al., *Interaction codes within the family of mammalian Phox and Bem1p domain-containing proteins.* J Biol Chem, 2003. **278**(36): p. 34568-81.
211. Truebestein, L. and T.A. Leonard, *Coiled-coils: The long and short of it.* Bioessays, 2016. **38**(9): p. 903-16.
212. Wang, Y., et al., *Coiled-coil networking shapes cell molecular machinery.* Mol Biol Cell, 2012. **23**(19): p. 3911-22.
213. Jeyaprakash, A.A., et al., *Structural and functional organization of the Ska complex, a key component of the kinetochore-microtubule interface.* Mol Cell, 2012. **46**(3): p. 274-86.
214. Cheung, P.Y. and S.R. Pfeffer, *Transport Vesicle Tethering at the Trans Golgi Network: Coiled Coil Proteins in Action.* Front Cell Dev Biol, 2016. **4**: p. 18.
215. Matthews, J.M., et al., *The core of the respiratory syncytial virus fusion protein is a trimeric coiled coil.* J Virol, 2000. **74**(13): p. 5911-20.

216. Buchsbaum, R., et al., *The N-terminal pleckstrin, coiled-coil, and IQ domains of the exchange factor Ras-GRF act cooperatively to facilitate activation by calcium.* Mol Cell Biol, 1996. **16**(9): p. 4888-96.
217. Zhang, T., et al., *The coiled-coil domain of Stat3 is essential for its SH2 domain-mediated receptor binding and subsequent activation induced by epidermal growth factor and interleukin-6.* Mol Cell Biol, 2000. **20**(19): p. 7132-9.
218. Rodrigues, G.A. and M. Park, *Dimerization mediated through a leucine zipper activates the oncogenic potential of the met receptor tyrosine kinase.* Mol Cell Biol, 1993. **13**(11): p. 6711-22.
219. McWhirter, J.R., D.L. Galasso, and J.Y. Wang, *A coiled-coil oligomerization domain of Bcr is essential for the transforming function of Bcr-Abl oncoproteins.* Mol Cell Biol, 1993. **13**(12): p. 7587-95.
220. Greco, A., C. Miranda, and M.A. Pierotti, *Rearrangements of NTRK1 gene in papillary thyroid carcinoma.* Mol Cell Endocrinol, 2010. **321**(1): p. 44-9.
221. Jhiang, S.M., *The RET proto-oncogene in human cancers.* Oncogene, 2000. **19**(49): p. 5590-7.
222. Monaco, C., et al., *The RFG oligomerization domain mediates kinase activation and re-localization of the RET/PTC3 oncoprotein to the plasma membrane.* Oncogene, 2001. **20**(5): p. 599-608.
223. Tong, Q., S. Xing, and S.M. Jhiang, *Leucine zipper-mediated dimerization is essential for the PTC1 oncogenic activity.* J Biol Chem, 1997. **272**(14): p. 9043-7.
224. Mencinger, M. and P. Aman, *Characterization of TFG in mus musculus and Caenorhabditis elegans.* Biochem Biophys Res Commun, 1999. **257**(1): p. 67-73.
225. Adhikary, S., et al., *The ubiquitin ligase HectH9 regulates transcriptional activation by Myc and is essential for tumor cell proliferation.* Cell, 2005. **123**(3): p. 409-21.
226. Chen, C., et al., *A possible tumor suppressor role of the KLF5 transcription factor in human breast cancer.* Oncogene, 2002. **21**(43): p. 6567-72.
227. Yoon, S.Y., et al., *Over-expression of human UREB1 in colorectal cancer: HECT domain of human UREB1 inhibits the activity of tumor suppressor p53 protein.* Biochem Biophys Res Commun, 2005. **326**(1): p. 7-17.
228. Zhong, Q., et al., *Mule/ARF-BP1, a BH3-only E3 ubiquitin ligase, catalyzes the polyubiquitination of Mcl-1 and regulates apoptosis.* Cell, 2005. **121**(7): p. 1085-95.
229. Chen, D., et al., *ARF-BP1/Mule is a critical mediator of the ARF tumor suppressor.* Cell, 2005. **121**(7): p. 1071-83.
230. Ma, W., et al., *Tumour suppressive function of HUWE1 in thyroid cancer.* J Biosci, 2016. **41**(3): p. 395-405.
231. Zhang, L., et al., *Identification of novel driver tumor suppressors through functional interrogation of putative passenger mutations in colorectal cancer.* Int J Cancer, 2013. **132**(3): p. 732-7.
232. Ritorto, M.S., et al., *Screening of DUB activity and specificity by MALDI-TOF mass spectrometry.* Nat Commun, 2014. **5**: p. 4763.
233. Kategaya, L., et al., *USP7 small-molecule inhibitors interfere with ubiquitin binding.* Nature, 2017. **550**(7677): p. 534-538.
234. Bhattacharya, S., et al., *Emerging insights into HAUSP (USP7) in physiology, cancer and other diseases.* Signal Transduct Target Ther, 2018. **3**: p. 17.

235. Cheng, C., et al., *Expression of HAUSP in gliomas correlates with disease progression and survival of patients.* Oncol Rep, 2013. **29**(5): p. 1730-6.
236. Song, M.S., et al., *The deubiquitinylation and localization of PTEN are regulated by a HAUSP-PML network.* Nature, 2008. **455**(7214): p. 813-7.
237. Sarkari, F., Y. Sheng, and L. Frappier, *USP7/HAUSP promotes the sequence-specific DNA binding activity of p53.* PLoS One, 2010. **5**(9): p. e13040.
238. Schwickart, M., et al., *Deubiquitinase USP9X stabilizes MCL1 and promotes tumour cell survival.* Nature, 2010. **463**(7277): p. 103-7.
239. Kushwaha, D., et al., *USP9X inhibition promotes radiation-induced apoptosis in non-small cell lung cancer cells expressing mid-to-high MCL1.* Cancer Biol Ther, 2015. **16**(3): p. 392-401.
240. Garraway, L.A., J. Verweij, and K.V. Ballman, *Precision oncology: an overview.* J Clin Oncol, 2013. **31**(15): p. 1803-5.
241. Branford, S., et al., *Imatinib produces significantly superior molecular responses compared to interferon alfa plus cytarabine in patients with newly diagnosed chronic myeloid leukemia in chronic phase.* Leukemia, 2003. **17**(12): p. 2401-9.
242. Hughes, T.P., et al., *Frequency of major molecular responses to imatinib or interferon alfa plus cytarabine in newly diagnosed chronic myeloid leukemia.* N Engl J Med, 2003. **349**(15): p. 1423-32.
243. Flaherty, K.T., et al., *Inhibition of mutated, activated BRAF in metastatic melanoma.* N Engl J Med, 2010. **363**(9): p. 809-19.
244. Musholt, T.J., et al., *Detection of RET rearrangements in papillary thyroid carcinoma using RT-PCR and FISH techniques - A molecular and clinical analysis.* Eur J Surg Oncol, 2018.
245. Staubitz, J.I., et al., *Novel rearrangements involving the RET gene in papillary thyroid carcinoma.* Cancer Genet, 2019. **230**: p. 13-20.
246. Vogel, C. and E.M. Marcotte, *Insights into the regulation of protein abundance from proteomic and transcriptomic analyses.* Nat Rev Genet, 2012. **13**(4): p. 227-32.
247. Ezkurdia, I., et al., *Multiple evidence strands suggest that there may be as few as 19,000 human protein-coding genes.* Hum Mol Genet, 2014. **23**(22): p. 5866-78.
248. Maes, E., et al., *Proteomics in cancer research: Are we ready for clinical practice?* Crit Rev Oncol Hematol, 2015. **96**(3): p. 437-48.
249. Tong, M., et al., *Molecular subtyping of cancer and nomination of kinase candidates for inhibition with phosphoproteomics: Reanalysis of CPTAC ovarian cancer.* EBioMedicine, 2019. **40**: p. 305-317.
250. Zhang, H., et al., *Integrated Proteogenomic Characterization of Human High-Grade Serous Ovarian Cancer.* Cell, 2016. **166**(3): p. 755-765.